Dimer models and Calabi-Yau algebras

submitted by

Nathan Broomhead

for the degree of Doctor of Philosophy

of the

University of Bath

November 2008

Contents

Summary

In this thesis we use techniques from algebraic geometry and homological algebra, together with ideas from string theory to construct a class of 3-dimensional Calabi-Yau algebras. The Calabi-Yau property appears throughout geometry and string theory and is increasingly being studied in algebra.

Dimer models, first studied in theoretical physics, give a way of writing down a class of non-commutative algebras, as the path algebra of a quiver with relations obtained from a 'superpotential'. Some examples are Calabi-Yau and some are not. We consider two types of 'consistency' condition on dimer models, and show that a 'geometrically consistent' dimer model is 'algebraically consistent'. Finally we prove that the algebra obtained from an algebraically consistent dimer model is a 3-dimensional Calabi-Yau algebra.

Chapter 1

Introduction

1.1 Overview

In this thesis we use techniques from algebraic geometry and homological algebra, together with ideas from string theory to construct a class of 3-dimensional Calabi-Yau algebras. The Calabi-Yau property appears throughout geometry and string theory where, for example, 3-dimensional Calabi-Yau manifolds play an important role in mirror symmetry. A characteristic property of an n-dimensional Calabi-Yau manifold X, is that the nth power of the shift functor on $D(X) := D^b(coh(X))$, the bounded derived category of coherent sheaves on X, is a Serre functor. That is, there exists a natural isomorphism

$$\mathrm{Hom}_{D(X)}(A, B) \cong \mathrm{Hom}_{D(X)}(B, A[n])^* \qquad \forall A, B \in D(X)$$

This property is not restricted to categories of the form $D(X)$. The idea behind Calabi-Yau algebras is to write down conditions on the algebra A such that $D(A) := D^b(mod(A))$, the bounded derived category of modules over A, has the same property. In this form the Calabi-Yau property is increasingly being studied in algebra.

Calabi-Yau algebras also appear in the context of non-commutative resolutions of singularities. One way of studying resolutions of singularities is by considering their derived categories. Of particular interest are crepant (i.e. suitably minimal) resolutions of toric Gorenstein singularities. Crepant resolutions do not always exist and if they do, they are not in general unique. However it is conjectured (Bondal and Orlov) that if $f_1 : Y_1 \to X$ and $f_2 : Y_2 \to X$ are crepant resolutions then there is a derived equivalence $D(Y_1) \cong D(Y_2)$. Thus the derived category of a crepant resolution is an invariant of the singularity.

One way to try to understand the derived category of a toric crepant resolution Y,

is to look for a tilting bundle T, i.e. a bundle which determines a derived equivalence $D(Y) \cong D(A)$, where $A = \mathrm{End}(T)$. If an equivalence of this form exists, then one could consider the algebra A as a type of non-commutative crepant resolution (NCCR) of the singularity. Van den Bergh [31] formalised this idea with a definition of an NCCR which depends only on the singularity. Given an NCCR A, a (commutative) crepant resolution Y such that $D(Y) \cong D(A)$ can be constructed as a moduli space of certain stable A-representations (Van den Bergh [31]). This is a generalisation of the approach to the McKay correspondence in [5].

If $X = \mathrm{Spec}(R)$ is a Gorenstein singularity, then any crepant resolution is a Calabi-Yau variety. Therefore if A is an NCCR it must be a Calabi-Yau algebra. The center of A must also be the coordinate ring R of the singularity. Thus any 3-dimensional Calabi-Yau algebra whose center R is the coordinate ring of toric Gorenstein 3-fold, is potentially an NCCR of $X = \mathrm{Spec}(R)$.

In [4], Bocklandt proved that every graded Calabi-Yau algebra of global dimension 3 is isomorphic to a superpotential algebra. A superpotential algebra $A = \mathbb{C}Q/(dW)$ is the quotient of the path algebra of a quiver Q by an ideal of relations (dW), where the relations are generated by taking (formal) partial derivatives of a single element W called the 'superpotential'. The superpotential not only gives a very concise way of writing down the relations in a non-commutative algebra, it also encodes some information about the syzygies, i.e. relations between the relations. The Calabi-Yau condition is actually equivalent to saying that all the syzygies can be obtained from the superpotential. Not all superpotential algebras are Calabi-Yau, and it is a open question to understand which ones are.

1.2 Structure of the thesis and main results

Chapter 2 acts as a general introduction to dimer models. A dimer model is finite bipartite tiling of a compact (oriented) Riemann surface Y. The examples that will be of particular interest are tilings of the 2-torus, and in this case, we can consider the dimer model as a doubly periodic tiling of the plane. Given a dimer model we also consider its dual tiling, where faces are dual to vertices and edges dual to edges. The edges of this dual tiling inherit an orientation from the bipartiteness of the dimer model. This is usually chosen so that the arrows go clockwise around a face dual to a white vertex. Therefore the dual tiling is actually a quiver Q, with faces. In the example below we draw the dimer model and the quiver together, with the dimer model highlighted in the left hand diagram. The dotted lines show a fundamental domain.

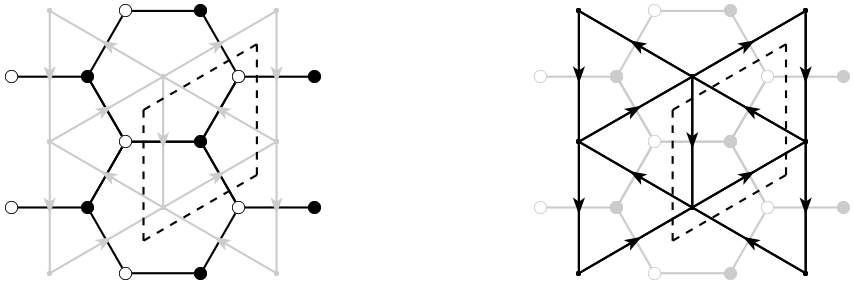

The faces of the quiver encode a superpotential W, and so there is a superpotential algebra $A = \mathbb{C}Q/(dW)$ associated to every dimer model.

In [16] Hanany *et al* describe a way of using 'perfect matchings' to construct a commutative ring R from a dimer model. A perfect matching is subset of the edges of a dimer model with the property that every vertex of the dimer model is the end point of precisely one of these edges. For example the following diagram shows the three perfect matchings of the hexagonal tiling, where the edges in the perfect matchings are shown as thick grey lines.

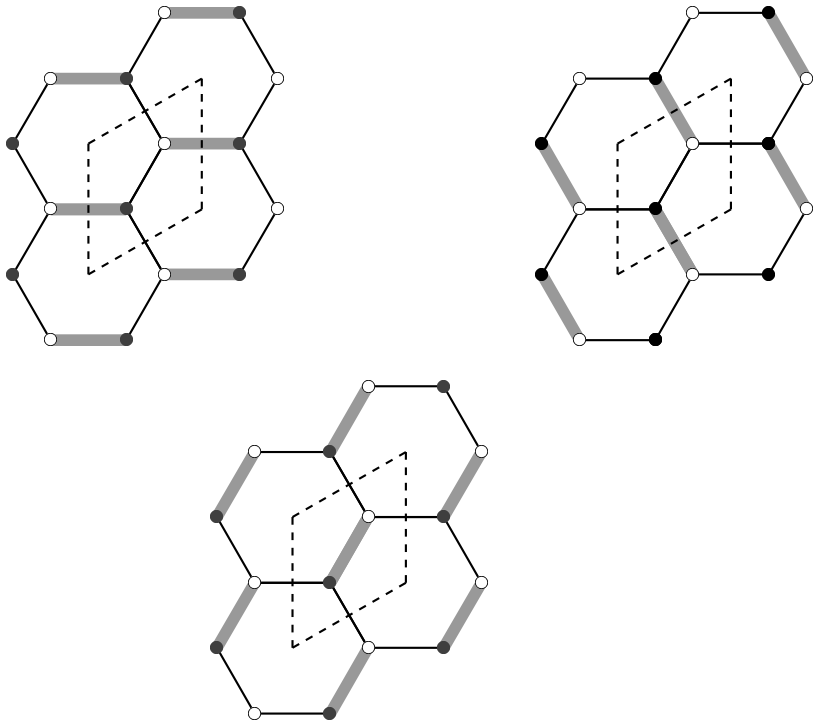

The difference of two perfect matchings defines a homology class of the 2-torus and so, by choosing a fixed 'reference matching' to subtract from each perfect matching, we obtain a set of points in the integer homology lattice of the 2-torus $H_1(T) \cong \mathbb{Z}^2$. The convex hull of these points is a lattice polygon. Taking the cone on the polygon and using the machinery of toric geometry, this defines $R = \mathbb{C}[X]$, the coordinate ring of an affine toric Gorenstein 3-fold X. Given a lattice point in the polygon, its multiplicity is defined to be the number of perfect matchings corresponding to that point. A perfect matching is said to be extremal if it corresponds to a vertex of the polygon. Looking at the example above we see that the polygon is a triangle, with each of the three perfect matching corresponding to a vertex, and no other lattice points. The ring R is the polynomial ring in three variables.

Since we have a superpotential algebra associated to every dimer model, it is natural to ask if these algebras are Calabi-Yau. In fact there are some examples which are Calabi-Yau and some which are not. Therefore we ask what conditions can be placed on a dimer model so that its superpotential algebra is Calabi-Yau. In Chapter 3 we discuss the two ideas of 'consistency' first understood by Hanany and Vegh [17]. Consistency conditions are a strong type of non-degeneracy condition. Following Kenyon and Schlenker [24], we give necessary and sufficient conditions for a dimer model to be 'geometrically consistent' in terms of the intersection properties of special paths called zig-zag flows on the universal cover $\widetilde{Q}$ of the quiver Q. Geometric consistency amounts to saying that zig-zag flows behave effectively like straight lines.

In Chapter 4 we introduce the concept of (non-commutative, affine, normal) toric algebras. These are non-commutative algebras which have an underlying combinatoric structure. They are defined by knowledge of a lattice containing a strongly convex rational polyhedral cone, a set and a lattice map. It is hoped that they may play a similar role in non-commutative algebraic geometry to that played by toric varieties in algebraic geometry. We show that there is a toric algebra B naturally associated to every dimer model, and moreover, the center of this algebra is the ring R associated to the dimer model that we described above.

Therefore a given dimer model has two non-commutative algebras A and B and there is a natural algebra map $\hbar : A \longrightarrow B$. We call a dimer model 'algebraically consistent' if this map is an isomorphism. Algebraic and geometric consistency are the two consistency conditions that we will study in the core of the thesis.

In Chapters 5 we study some properties of zig-zag flows in a geometrically consistent dimer model. The homology class of a zig-zag flow encodes information about the 'direction' of that flow. We show that at each quiver face f, there is a 'local zig-zag fan' in the homology lattice of the torus generated by the homology classes of zig-

zag flows which intersect the boundary of f. Furthermore, the cyclic order of the intersections around the face, is the same as the order of the rays in the local zig-zag fan. There is also a 'global zig-zag fan' generated by the homology classes of all zig-zag flows. Using these fans we construct, in a very explicit way, a collection of perfect matchings indexed by the 2-dimensional cones in the global zig-zag fan. We prove that these perfect matchings are extremal perfect matchings and they are all the extremal perfect matchings. We also see that each perfect matching of this form corresponds to a different vertex of the polygon described above, so these vertices are of multiplicity one.

In Chapter 6 we prove the following main theorem

Theorem 1.2.1. *A geometrically consistent dimer model is algebraically consistent.*

The proof relies on the explicit description of extremal perfect matchings from Chapter 5. We actually prove the following proposition, which provides the surjectivity of the map $\hbar : A \longrightarrow B$, while the injectivity is provided by a result of Hanany, Herzog and Vegh (see Theorem 3.5.2 and Remark 4.4.3).

Proposition 1.2.2. *Given a geometrically consistent dimer model, for all vertices i, j in the universal cover of Q, there exists a path from i to j which avoids some extremal perfect matching.*

Thus we see that the extremal perfect matchings play a key role in the theory.

In Chapter 7 we discuss Ginzburg's definition of a Calabi-Yau algebra and prove the following main theorem

Theorem 1.2.3. *If a dimer model on a torus is algebraically consistent then the algebra A obtained from it is a Calabi-Yau algebra of global dimension 3.*

Therefore we have shown that for dimer models on the torus, algebraic consistency and consequently geometric consistency, is a sufficient condition to obtain a Calabi-Yau algebra. Thus we have produced a class of superpotential algebras which are Calabi-Yau. Finally we note that both Stienstra in [29], and Gulotta in [14] prove that for any lattice polygon V, there exists a geometrically consistent dimer model which has V as its perfect matching polygon. Therefore to every Gorenstein affine toric threefold, there is an associated geometrically consistent model. Hence, by using dimer models we can construct a Calabi-Yau algebra of global dimension 3, whose center is the coordinate ring of any given Gorenstein affine toric threefold and which is conjecturally an NCCR.

Remark 1.2.4. Recently there have been several papers proving results that are related to parts of this thesis. In [26] Mozgovoy and Reineke prove that if an algebra

obtained from a dimer model satisfies two conditions then it is a 3 dimensional Calabi-Yau algebra. Davison [9] goes on to show that the second of these conditions is actually a consequence of the first. The first condition states that the algebra should satisfy a cancellation property. This holds in algebraically consistent cases as cancellation is a property of toric algebras. Therefore the condition also holds in the geometrically consistent case. Geometric consistency, as we shall see in Section 3.3, can be checked readily and thus gives examples where the cancellation property can be easily verified.

Chapter 2

Introduction to the Dimer Model

The aim of this chapter is to provide a mathematical introduction to the theory of dimer models as introduced by Hanany *et al* (see [22, 16, 11] for example).

2.1 Quivers and Algebras from Dimer models

The theory begins with a finite bipartite tiling of a compact (oriented) Riemann surface Y. By 'bipartite tiling' we mean a polygonal cell decomposition of the surface, whose vertices and edges form a bipartite graph i.e. the vertices may be coloured black and white in such a way that all edges join a black vertex to a white vertex. In particular we note that each face must have an even number of vertices (and edges) and each vertex has valence at least 2. We call a tiling of this type, a dimer model. This definition is quite general and as we progress we will describe additional non-degeneracy conditions, the strongest of which is 'consistency'. We note here that in principle faces in a dimer model which have two edges (di-gons) and bivalent vertices are allowed. However we will see that models with these features fail to satisfy certain of the non-degeneracy conditions. Furthermore we shall observe that the 'consistency' condition forces the Riemann surface Y to be a 2-torus T. Therefore in the majority of this thesis, we shall focus on bipartite tilings of T. In this case, we may (and shall) consider the dimer model instead as a doubly periodic tiling of the plane.

Remark 2.1.1. In some of the literature it is included as part of the definition of a bipartite graph, that there are the same number of black and white vertices. We do not impose this as a condition here, however if it does hold we call the dimer model 'balanced'.

2.1.1 Examples

The two simplest bipartite tilings of the 2-torus T, are the regular ones by squares and by hexagons. In each case, a fundamental domain is indicated by the dotted line.

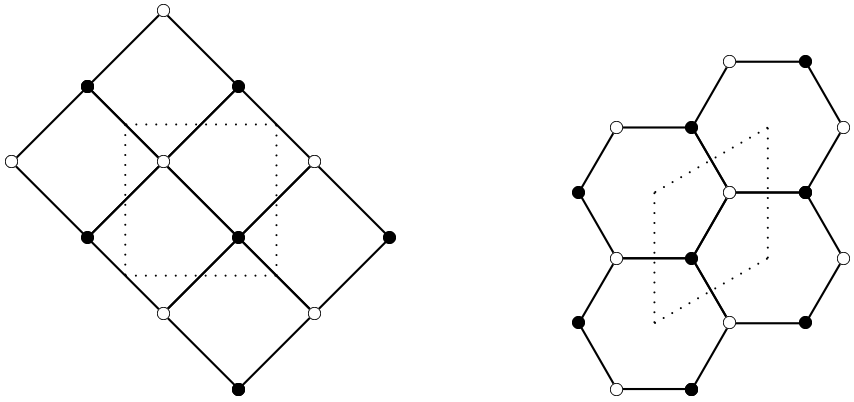

For a tiling of T which is not balanced, consider the following tiling by three rhombi:

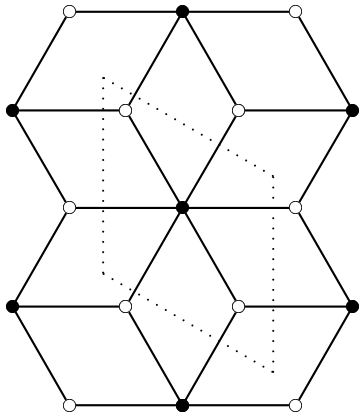

On the 2-sphere, the only regular (Platonic) bipartite tiling is the cube (shown here in stereographic projection):

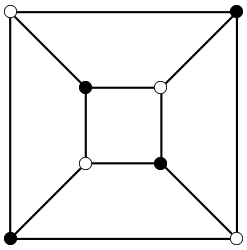

2.1.2 The quiver

Given a dimer model one can consider the dual tiling (or dual cell decomposition) with a vertex dual to every face, an edge dual to every edge and a face dual to every vertex. Crucially, since the dimer model is bipartite, the edges of the dual tiling inherit a consistent choice of orientation. In particular, it is the convention that faces dual to white vertices are oriented clockwise and faces dual to black vertices are oriented anti-clockwise. This is equivalent to requiring that black vertices are on the left and white vertices on the right of every arrow dual to a dimer edge. Thus the dual graph is a quiver Q (i.e. a directed graph), with the additional structure that it provides a tiling of the Riemann surface Y with oriented faces. We will refer to the faces of the quiver dual to black/white vertices of the dimer model, as black/white faces.

In the usual way, we denote by Q_0 and Q_1 the sets of vertices and arrows (directed edges) of the quiver and by $h, t\colon Q_1 \to Q_0$ the maps which take an arrow to its head and tail. To this information we add the set Q_2 of oriented faces. We may write down a homological chain complex for the Riemann surface Y, using the fact that this 'quiver with faces' forms a cell decomposition,

$$\mathbb{Z}_{Q_2} \xrightarrow{\partial} \mathbb{Z}_{Q_1} \xrightarrow{\partial} \mathbb{Z}_{Q_0} \tag{2.1.1}$$

where $\mathbb{Z}_{Q_i}$ denotes the free abelian group generated by the elements in Q_i. We also have the dual cochain complex

$$\mathbb{Z}^{Q_0} \xrightarrow{d} \mathbb{Z}^{Q_1} \xrightarrow{d} \mathbb{Z}^{Q_2} \tag{2.1.2}$$

where $\mathbb{Z}^{Q_i}$ denotes the $\mathbb{Z}$-linear functions on $\mathbb{Z}_{Q_i}$. Note that, because of the way the faces are oriented, the coboundary map $d\colon \mathbb{Z}^{Q_1} \to \mathbb{Z}^{Q_2}$ simply sums any function of the edges around each face (without any signs). Let $f \mapsto (-1)^f$ be the map which takes

the value +1 on black faces of Q, and -1 on white faces. Then the cycle

$$\sum_{f \in Q_2} (-1)^f f \in \mathbb{Z}_{Q_2}$$

is a generator for the kernel of the boundary map ∂. Thus it defines a fundamental class, i.e. a choice of generator of $H_2(Y) \cong \mathbb{Z}$. We note that the function $\underline{1} \in \mathbb{Z}^{Q_2}$, which takes the constant value 1 on every face, evaluates to $|B| - |W|$ on this fundamental cycle (where $|B|$ and $|W|$ denote the number of black and white faces respectively). If we have a balanced dimer model, i.e. $|B| = |W|$, then this implies that the function $\underline{1} \in \mathbb{Z}^{Q_2}$ is exact.

2.1.3 The quiver algebra

We construct the path algebra $\mathbb{C}Q$ of the quiver; this is a complex algebra with generators $\{e_i \mid i \in Q_0\}$ and $\{x_a \mid a \in Q_1\}$ subject to the relations $e_i^2 = e_i$, $e_i e_j = 0$ for $i \neq j$ and $e_{ta} x_a e_{ha} = x_a$. The e_i are idempotents of the algebra which, we observe, has a monomial basis of paths in Q. Following Ginzburg [13], let $[\mathbb{C}Q, \mathbb{C}Q]$ be the complex vector space in $\mathbb{C}Q$ spanned by commutators and denote by $\mathbb{C}Q_{\text{cyc}} := \mathbb{C}Q/[\mathbb{C}Q, \mathbb{C}Q]$ the quotient space. This space has a basis of elements corresponding to cyclic paths in the quiver. The consistent orientation of any face f of the quiver means that we may interpret ∂f as a cyclic path in the quiver. Therefore the set of faces determines an element of $\mathbb{C}Q_{\text{cyc}}$ which, following the physics literature [11], we refer to as the 'superpotential'

$$W = \sum_{f \in Q_2} (-1)^f \partial f. \tag{2.1.3}$$

Remark 2.1.2. In this thesis we will use the notation ∂f for several distinct objects, namely the boundary of f considered as an element of $\mathbb{Z}_{Q_1}$, the boundary of f considered as an element of $\mathbb{C}Q_{\text{cyc}}$, and the set of arrows which are contained in the boundary of f. It should be clear from context which of these we mean in any given instance.

For each arrow $a \in Q_1$ there is a linear map $\frac{\partial}{\partial x_a} : \mathbb{C}Q_{\text{cyc}} \to \mathbb{C}Q$ which is a (formal) cyclic derivative. The image of a cyclic path is obtained by taking all the representatives in $\mathbb{C}Q$ which start with x_a, removing this and then summing them. We note that because of the cyclicity, this is equivalent to taking all the representatives in $\mathbb{C}Q$ which end with x_a, removing this and then summing. The image of a cycle is in fact an element in $e_{ha}\mathbb{C}Qe_{ta}$, and if the cycle contains no repeated arrows then this is just the path which begins at ha and follows the cycle around to ta.

This superpotential W determines an ideal of relations in the path algebra $\mathbb{C}Q$

$$I_W = \left(\frac{\partial}{\partial x_a} W : a \in Q_1 \right). \tag{2.1.4}$$

The quotient of the path algebra $\mathbb{C}Q$ by this ideal is the superpotential (or 'Jacobian', or quiver) algebra

$$A = \mathbb{C}Q/I_W$$

From an algebraic point of view, the output of a dimer model is this algebra, and we are interested in understanding the special properties that such algebras exhibit.

Remark 2.1.3. Each arrow $a \in Q_1$ occurs in precisely two oppositely oriented faces $f^+, f^- \in Q_2$ (this also implies that no arrow is repeated in the boundary of any one face). Therefore each relation $\frac{\partial}{\partial x_a} W$ can be written explicitly as a difference of two paths,

$$\frac{\partial}{\partial x_a} W = p_a^+ - p_a^-$$

where $p_a^\pm$ is the path from ha around the boundary of $f^\pm$ to ta. The relations $p_a^+ = p_a^-$ for $a \in Q_1$ are called 'F-term' relations. They generate an equivalence relation on paths in the quiver such that the equivalence classes form a natural basis for the algebra A.

2.1.4 Examples

Example 2.1.4. We return to the tilings of the torus by regular hexagons and by squares that we saw in Section 2.1.1. We start by considering the hexagonal tiling of the torus. The figures below both show the bipartite tiling and the dual quiver, drawn together so it is clear how they are related. The left hand figure highlights the bipartite tiling, and the right hand figure highlights the quiver.

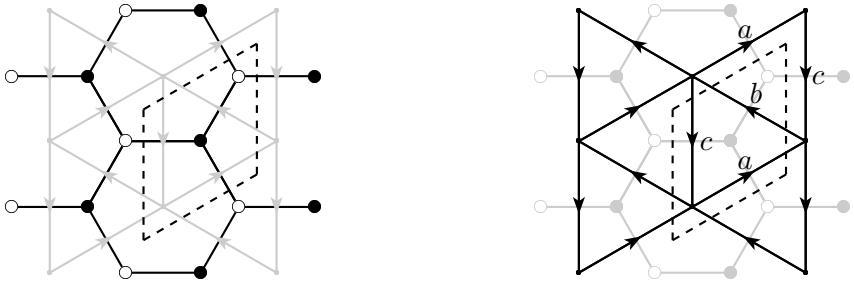

Observe that the bipartite tiling has one face, three edges and two vertices, and dually, the quiver has one vertex, three arrows and two faces. Since the quiver has one vertex,

this is the head and tail of each of the arrows. Therefore the path algebra $\mathbb{C}Q$ is actually the free algebra $\mathbb{C}\langle a, b, c\rangle$ with three generators corresponding to the three arrows. We see that the cyclic elements corresponding to the boundaries of the black and white faces, are (abc) and (acb) respectively. Thus the superpotential is:

$$W = (abc) - (acb)$$

and differentiating this with respect to each arrow, we obtain the three relations:

$$\begin{aligned} \frac{\partial W}{\partial c} &= ab - ba &= 0 \\ \frac{\partial W}{\partial b} &= ca - ac &= 0 \\ \frac{\partial W}{\partial a} &= bc - cb &= 0 \end{aligned}$$

Therefore, the ideal I_W is generated by the commutation relations between all the generators of $\mathbb{C}Q$, and the algebra

$$A = \mathbb{C}\langle a, b, c\rangle / I_W = \mathbb{C}[a, b, c]$$

is the polynomial ring in three variables.

Example 2.1.5. The tiling of the torus by squares has two faces and is therefore slightly more complicated. We show the bipartite tiling and the quiver below.

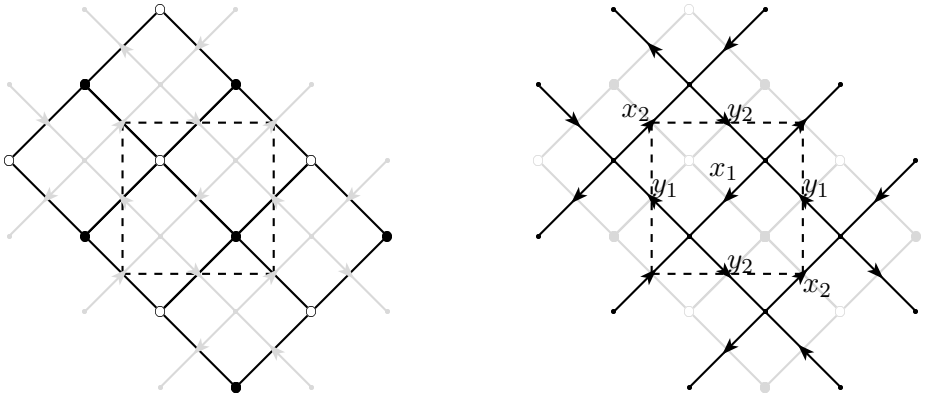

Observe that the quiver has two vertices, with two arrows in each direction between them:

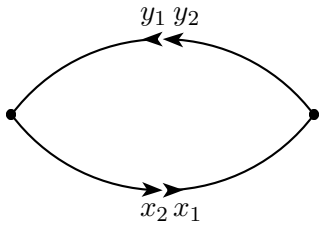

Thus, the path algebra $\mathbb{C}Q$ is generated by two idempotents and elements corresponding to the four arrows. As in the previous example, the quiver has two faces so the superpotential has two terms. The cyclic elements corresponding to the boundaries of the black and white faces, are $(x_1y_2x_2y_1)$ and $(x_1y_1x_2y_2)$ respectively, and so the superpotential is:

$$W = (x_1y_2x_2y_1) - (x_1y_1x_2y_2)$$

Applying the cyclic derivative with respect to each arrow, we obtain four relations:

$$\begin{array}{rrl} \frac{\partial W}{\partial x_1} = & y_2x_2y_1 - y_1x_2y_2 & = 0 \\ \frac{\partial W}{\partial x_2} = & y_1x_1y_2 - y_2x_1y_1 & = 0 \\ \frac{\partial W}{\partial y_1} = & x_1y_2x_2 - x_2y_2x_1 & = 0 \\ \frac{\partial W}{\partial y_2} = & x_2y_1x_1 - x_1x_1x_2 & = 0 \end{array}$$

We note that unlike in the hexagonal tiling example above, the algebra $A = \mathbb{C}Q/I_W$ is a non-commutative algebra. We will see later that its centre is isomorphic to the coordinate ring of the threefold ordinary double point, or conifold singularity. It is known that A is a non-commutative crepant resolution of this singularity (see Proposition 7.3 of [31], [30]), and for this reason the example is usually referred to as the 'non-commutative conifold' in the physics literature [22, 16, 17].

Example 2.1.6. We now give an example which has the same algebra A, as the conifold example above.

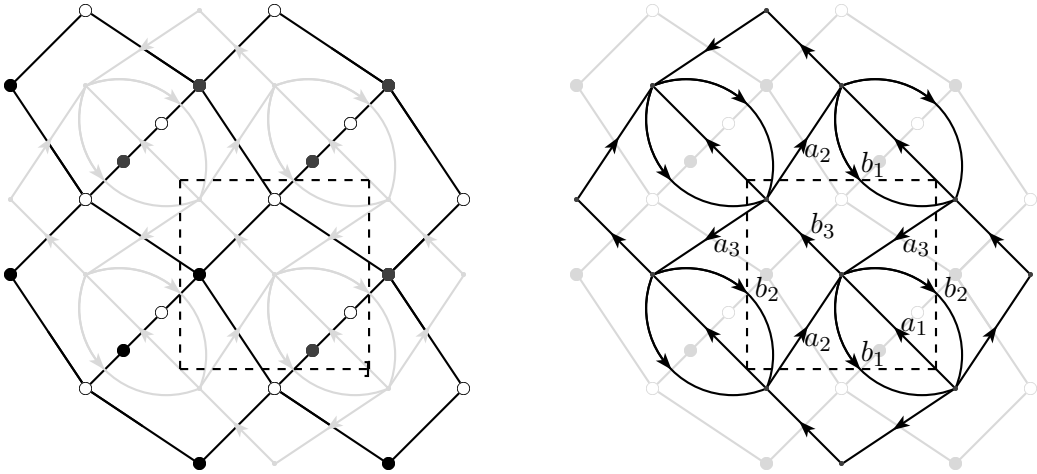

This quiver also has two vertices, there are three arrows in each direction between them. Thus, the path algebra $\mathbb{C}Q$ is generated by two idempotents and elements corresponding to the six arrows. The quiver has four faces so the superpotential has four terms:

$$W = (a_3 b_1) - (a_3 b_3) + (b_3 a_2 b_2 a_1) - (b_1 a_1 b_2 a_2)$$

Applying the cyclic derivative with respect to each arrow, we now obtain six relations:

$$\begin{array}{rcl} \frac{\partial W}{\partial a_1} = & b_3 a_2 b_2 - b_2 a_2 b_1 & = 0 \\ \frac{\partial W}{\partial a_2} = & b_2 a_1 b_3 - b_1 a_1 b_2 & = 0 \\ \frac{\partial W}{\partial a_3} = & b_1 - b_3 & = 0 \\ \frac{\partial W}{\partial b_1} = & a_3 - a_1 b_2 a_2 & = 0 \\ \frac{\partial W}{\partial b_2} = & a_1 b_3 a_2 - a_2 b_1 a_1 & = 0 \\ \frac{\partial W}{\partial b_3} = & a_2 b_2 a_1 - a_3 & = 0 \end{array}$$

We can use the relations $\frac{\partial W}{\partial a_3}$ and $\frac{\partial W}{\partial b_3}$ respectively, to write b_3 and a_3 in terms of the other generators, namely, $b_3 = b_1$ and $a_3 = a_2 b_2 a_1$. The path algebra subject to these two relations, is patently isomorphic to the path algebra of the quiver from the conifold example. Furthermore, substituting b_3 and a_3 into the relations, we obtain four relations:

$$\begin{array}{rcl} \frac{\partial W}{\partial a_1} = & b_1 a_2 b_2 - b_2 a_2 b_1 & = 0 \\ \frac{\partial W}{\partial a_2} = & b_2 a_1 b_1 - b_1 a_1 b_2 & = 0 \\ \frac{\partial W}{\partial b_1} = & a_2 b_2 a_1 - a_1 b_2 a_2 & = 0 \\ \frac{\partial W}{\partial b_2} = & a_1 b_1 a_2 - a_2 b_1 a_1 & = 0 \end{array}$$

which are the relations in the conifold example. Therefore we have demonstrated a

dimer model which outputs the same algebra A.

2.1.5 Minimality

As we have just seen, it is possible for two distinct dimer models to have the same quiver algebra A. In fact, if we choose any vertex of dimer model, we can 'split' this into two vertices of the same colour, connected together via a bivalent vertex of the other colour:

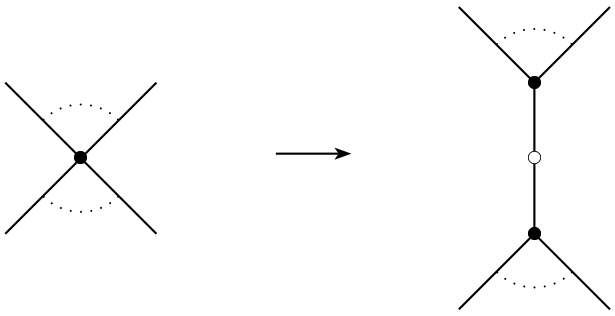

The resulting dimer model has two additional edges and so the quiver has two additional arrows. However the relations dual to these arrows equate the new arrows to paths which previously existed, and the resulting quiver algebras for the two dimer models are in fact the same. We call a dimer model 'non-minimal' if it can be obtained from a dimer model with fewer edges in this way. Note that Example 2.1.6 is non-minimal as it can be obtained from Example 2.1.5.

If a dimer model has a bivalent vertex which is connected to two distinct vertices, then is possible to do the converse of the above process, i.e. remove the bivalent vertex and contract its two neighbours to a single vertex. For an example where it is not possible to remove the bivalent vertices, see (2.3.1).

2.2 Symmetries

A *global* symmetry is a one-parameter subgroup $\rho\colon \mathbb{C}^* \to \mathrm{Aut}(A)$ that arises from an action on the arrow fields

$$\rho(t)\colon x_a \mapsto t^{v_a} x_a,$$

for some $v \in \mathbb{Z}^{Q_1}$, which we may think of as a 1-cochain in the complex (2.1.2). Then its coboundary $dv \in \mathbb{Z}^{Q_2}$ gives precisely the weights of the ρ-action on the terms in the

superpotential W.

Thus, ρ is a well-defined map to $\mathrm{Aut}(A)$ when it acts homogeneously on all terms in the superpotential W, in other words, when

$$dv = \lambda \underline{1} \tag{2.2.1}$$

for some constant $\lambda \in \mathbb{Z}$, which we will also call the *degree* of ρ.

Using intentionally toric notation, we shall write

$$N = d^{-1}(\mathbb{Z}\underline{1}) \subset \mathbb{Z}^{Q_1} \quad \text{and} \quad N^+ = N \cap \mathbb{N}^{Q_1} \tag{2.2.2}$$

Then N is the one-parameter subgroup lattice of a complex torus $\mathbb{T} \leq \mathrm{Aut}(A)$ containing all global symmetries.

The other differential in the cochain complex (2.1.2) also has a natural interpretation in this context. The lattice $N_{in} = \mathbb{Z}^{Q_0}$ is the one-parameter subgroup lattice of a complex torus $\mathbb{T}_{in}$ of invertible elements of A, namely

$$\mathbb{T}_{in} = \{ \sum_{i \in Q_0} t_i e_i : t_i \in \mathbb{C}^* \},$$

where $e_i \in A$ are the idempotents corresponding to the vertices of Q. Then the lattice map $d\colon \mathbb{Z}^{Q_0} \to N$ corresponds to the map $\mathbb{T}_{in} \to \mathbb{T} \leq \mathrm{Aut}(A)$ giving the action on A by inner automorphisms, i.e. by conjugation. Then the cokernel of $d\colon \mathbb{Z}^{Q_0} \to N$ is the lattice of one-parameter subgroups of outer automorphisms arising from global symmetries. In other words, we have an exact sequence of complex tori

$$1 \to \mathbb{C}^* \to \mathbb{T}_{in} \to \mathbb{T} \to \mathbb{T}_o \to 1,$$

with corresponding exact sequence of one parameter subgroup lattices

$$0 \to \mathbb{Z} \to N_{in} \to N \to N_o \to 0 \tag{2.2.3}$$

In the physics literature (e.g. [22]), elements of N_{in} are usually referred to as *baryonic* symmetries, and elements of N_o as *mesonic* symmetries.

Finally in this section we define the notion of an *R-symmetry*, whose name comes from physics, but which is important mathematically as it makes A into a graded algebra with finite dimensional graded pieces.

Definition 2.2.1. An R-symmetry is a global symmetry that acts with strictly positive weights (or 'charges') on all the arrows.

The R-symmetries are the 'interior lattice points' of the cone N^+. In the physics literature (e.g. [22]) it is traditional to normalise the R-symmetries so they are of degree 2, (i.e. they act homogeneously with weight 2 on the superpotential) but also to extend the definition to allow the weights to be real, i.e. in $\mathbb{R}^{Q_1}$. By this definition, R-symmetries are real one-parameter subgroups whose weights lie in the interior of the degree 2 slice of the real cone corresponding to N^+. Since this is a rational polyhedral cone, the interior is non-empty if and only if it contains rational points and hence if and only if N^+ itself contains integral points with all weights strictly positive. Therefore for the purposes of this thesis we consider R-symmetries to be integral, as we defined above, and we do not impose the degree 2 normalisation.

Note finally that the existence of an R-symmetry is equivalent to the fact that N^+ is a 'full' cone, i.e. it spans N.

2.3 Perfect matchings

A *perfect matching* on a bipartite graph is a collection of edges such that each vertex is the end point of precisely one edge. The edges in a perfect matching are sometimes also referred to as dimers and the perfect matching as a dimer configuration.

Using the notation from (2.1.2), we take the essentially equivalent dual point of view; we consider a perfect matching to be a 1-cochain $\pi \in \mathbb{Z}^{Q_1}$, with all values in $\{0, 1\}$, such that $d\pi = \underline{1}$. This is equivalent to requiring that $\pi \in \mathbb{N}^{Q_1}$ and $d\pi = \underline{1}$, and so perfect matchings are the degree 1 elements of N^+.

Not every dimer model has a perfect matching. This is obvious for dimer models which are not balanced, but even those with equal numbers of black and white vertices need not have a perfect matching. For example, the following case drawn on the torus:

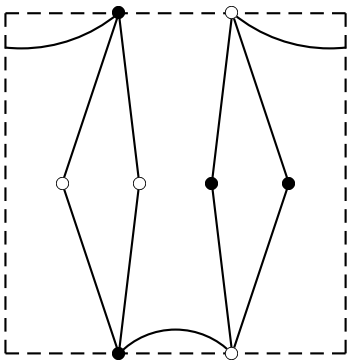

(2.3.1)

The condition that a perfect matching does exist is provided by Hall's (Marriage) Theorem:

Lemma 2.3.1. *A bipartite graph admits a perfect matching if and only if it has the same number of black and white vertices and every subset of black vertices is connected to at least as many white vertices.*

In the example in figure 2.3.1 above, it can be see that the two black vertices in the interior of the fundamental domain are connected to just one vertex and so there are no perfect matchings.

Remark 2.3.2. The above example contains bivalent vertices which can not be removed in the way explained in Section 2.1.5. However these are not the source of the 'problem', in fact by doubling one of the edges ending at each bivalent vertex:

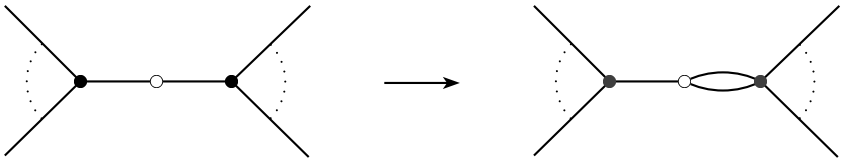

we obtain a new dimer model which, by Lemma 2.3.1, admits a perfect matching if and only if the original dimer model did. The resulting dimer model doesn't have bivalent vertices, but it does have di-gons. We can in turn replace each di-gon as follows:

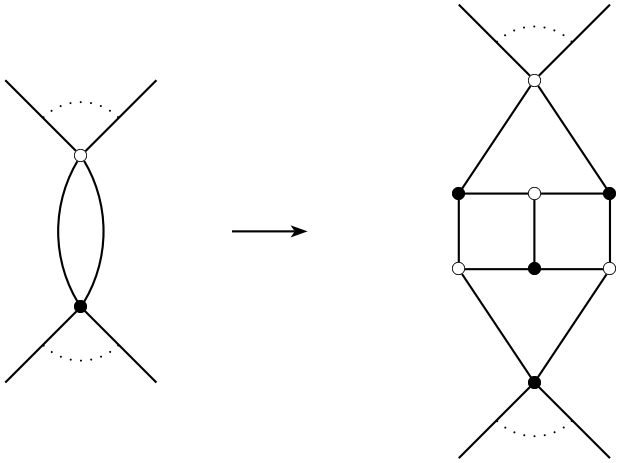

It is simple to check (again using Lemma 2.3.1) that the altered dimer model has a perfect matching if and only if the original did. Therefore, in the example, if we replaced each bivalent vertex and then each di-gon as above, we would obtain a dimer model without bivalent vertices or di-gons but which still has no perfect matchings. The moral of this is that for simplicity we can leave the bivalent vertices alone (and let di-gons be di-gons)!

We will be particularly interested in dimer models which satisfy a slightly stronger condition.

Definition 2.3.3. We call a dimer model *non-degenerate* when every edge in the bipartite graph is contained in some perfect matching.

Given a non-degenerate dimer model, the sum all perfect matchings (as an element of N^+) is strictly positive on every arrow. Therefore it defines an R-symmetry.

In fact, the existence of an R-symmetry and the non-degeneracy condition are equivalent. This is a straightforward consequence of the following integral version of the famous Birkhoff-von Neumann Theorem for doubly stochastic matrices [3].

Lemma 2.3.4. *The cone N^+ is integrally generated by the perfect matchings, all of which are extremal elements.*

Proof. We adapt the standard argument [2] to the integral case. Every perfect matching is an element of N^+ and therefore the cone generated by the perfect matchings is contained in N^+. Conversely, choose any element $v \in N^+$, and suppose $\deg v > 0$. We construct a graph G_v whose vertex set is the same as the dimer model (bipartite graph) and whose edges are the subset of edges e of the dimer model, such that v evaluated on the dual arrow a_e is non-zero.

We claim that G_v satisfies the conditions of Lemma 2.3.1. To see this, let A be any subset of vertices of one colour (black or white) and denote by $N(A)$ the set of neighbours of A, i.e. the vertices (of the other colour) which have an edge connecting them to some element of A. In an abuse of notation we shall also consider $A, N(A) \subseteq Q_2$ as sets of faces of the dual quiver Q. We note that

$$\deg v.|A| = \sum_{f\in A}\langle d(v), f\rangle = \sum_{\substack{f\in A\\ g\in N(A)}} \langle v, \partial f \cap \partial g\rangle$$

where $\partial f \cap \partial g$ denotes the class in $\mathbb{Z}_{Q_1}$ corresponding to the sum of the arrows which are in the boundary of faces f and g. If $B = N(A)$, then since $A \subseteq N(B)$,

$$|B| = \frac{1}{\deg v} \sum_{\substack{f\in B\\ g\in N(B)}} \langle v, \partial f \cap \partial g\rangle \geq \frac{1}{\deg v} \sum_{\substack{f\in B\\ g\in A}} \langle v, \partial f \cap \partial g\rangle = |A|$$

Thus $|N(A)| \geq |A|$ as required.

Applying Lemma 2.3.1, we see that G_v has a perfect matching which extends by zero to a perfect matching $\pi \in \mathbb{Z}^{Q_1}$ of the dimer model. Since by construction, v takes strictly positive integral values on all the arrows on which π is non-zero, we see that $v - \pi \in N^+$, and has degree $\deg v - 1$. We proceed inductively and, using the fact that 0 is the only degree zero element in N^+, we see that v is equal to a sum of $\deg v$ perfect matchings.

To show that all perfect matchings are extremal elements it is sufficient to prove that no perfect matching is a non-trivial convex sum of distinct perfect matchings. However if $\sum_{s=1}^{n} \kappa_s \pi_s$ is a non-trivial convex sum, i.e. $\kappa_s > 0$ for all $s = 1, \ldots, n$ and $\sum_{s=1}^{n} \kappa_s = 1$, then this sum evaluates to a number in the closed interval $[0, 1]$ on every arrow in Q. Furthermore we see that the values $\{0, 1\}$ are attained if and only if all of the perfect matchings evaluate to the same number on that arrow. Therefore if this convex sum is a perfect matching, i.e. a $\{0, 1\}$-valued function, then π_s evaluate to the same number on every arrow for all $s = 1, \ldots, n$, so the perfect matchings are not distinct. □

Remark 2.3.5. Another straightforward corollary of Hall's theorem states that a dimer model is non-degenerate if and only if the bipartite graph has an equal numbers of black and white vertices and every proper subset of the black vertices of size n is connected to at least $n+1$ white vertices. We shall refer to this condition as the 'strong marriage' condition. Using this, it is easy to construct examples of dimer models which have a perfect matching but do not satisfy the non-degeneracy condition. In the following example the two white vertices in the interior of the fundamental domain are connected to two black vertices, so it is degenerate. It can also be checked directly that the edge marked in grey must be contained in every perfect matching. Therefore the other edges which share an end vertex with this edge are not contained in any perfect matching.

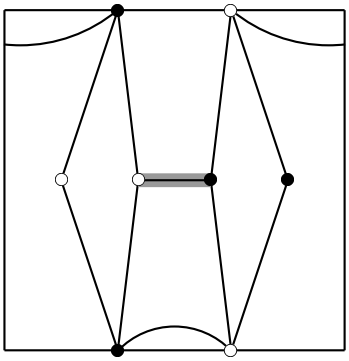

Let N_o^+ be the saturation of the projection of the cone $N^+ \subset N$ into the rank $2g+1$ lattice N_o, where g is the genus of Y. In other words N_o^+ is the intersection of N_o with the real cone generated by the image of N^+ in $N_o \otimes_{\mathbb{Z}} \mathbb{R}$. Because of Theorem 2.3.4, it is natural to use the perfect matchings to describe N_o^+. From its construction there is a short exact sequence

$$0 \to H^1(Y;\mathbb{Z}) \longrightarrow N_o \xrightarrow{deg} \mathbb{Z} \to 0 \tag{2.3.2}$$

and, since every perfect matching has degree 1, their images in N_o span a lattice polytope in a rank $2g$ affine sublattice such that N_o^+ is the cone on this polytope. By choosing some fixed reference matching π_0, this polytope may be translated into $H^1(Y;\mathbb{Z})$ and described more directly as follows: for any perfect matching π, the difference $\pi - \pi_0$ is a cocycle and hence has a well-defined cohomology class. We call this the relative cohomology class of π. The lattice polytope described above, is the convex hull of all relative cohomology classes of perfect matchings. We note that there is usually not a 1-1 correspondence between perfect matchings and lattice points in the polytope.

Definition 2.3.6. The *multiplicity* of a lattice point in the polytope is defined to be the number of perfect matchings whose relative cohomology class is that point.

In the cases which will be of most interest, when the Riemann surface is a torus, then N_o is a rank 3 lattice, and the images of the perfect matchings span a polygon in a rank 2 affine sublattice.

Definition 2.3.7. A lattice point is called *external* if it lies on a facet of the polygon, and *extremal* if it lies at a vertex of the polygon. A perfect matching is external (extremal) if it corresponds to an external (extremal) lattice point.

The translated polygon in $H^1(T;\mathbb{Z}) \cong \mathbb{Z}^2$ may be computed by various explicit methods, e.g using the Kastelyn determinant as in [16].

From the point of view of toric geometry, it is natural to think of N^+ and N_o^+ as describing two (normal) affine toric varieties X and X_o, such that $X_o = X//\mathbb{T}_{in}$ where the $\mathbb{T}_{in}$ action is determined by the map $N_{in} \to N$. Furthermore, X and X_o both have Gorenstein singularities, since the corresponding cones are generated by hyperplane sections.

Chapter 3

Consistency

In Chapter 2 we saw some non-degeneracy conditions which we can impose on dimer models. For example we saw what it means for a dimer model to be balanced (2.1.1) and non-degenerate (2.3.3). We now come to the most important and strongest of these conditions which are called *consistency* conditions. We describe the types of consistency which appear in the physics literature and state how they relate to each other. We will see in later chapters that some kind of consistency condition is needed in order to prove properties we are interested in, such as the Calabi-Yau property.

3.1 A Further Condition on the R-symmetry

We defined, in Section 2.2, an *R-symmetry* to be a global symmetry that acts with strictly positive weights on all the arrows. We recall that the existence of an R-symmetry is equivalent to non-degeneracy of a dimer model. The first definition of consistency is a strengthening of this, and states that a dimer model is consistent if there exists an 'anomaly-free' R-symmetry.

We recall that in the physics literature (e.g. in [22]) it is traditional to allow real R-symmetries, but to normalise so they are of degree 2, i.e. a real R-symmetry $R \in \mathbb{R}^{Q_1}$ which acts on each arrow $a \in Q_1$ with weight R_a, satisfies

$$\sum_{a \in \partial f} R_a = 2 \qquad \forall f \in Q_2 \tag{3.1.1}$$

Of these real R-symmetries, physicists are particularly interested in ones which have no 'anomalies'. Formulated mathematically, these are R-symmetries which satisfy the

following 'anomaly-vanishing' condition at each vertex of the quiver

$$\sum_{a \in H_v \cup T_v} (1 - R_a) = 2 \qquad \forall v \in Q_0 \tag{3.1.2}$$

where $H_v := \{b \in Q_1 \mid hb = v\}$ and $T_v := \{b \in Q_1 \mid tb = v\}$.

As stated before, we usually work with integral R-symmetries, without any normalisation, and let $\deg(R)$ be the degree of an R-symmetry $R \in \mathbb{Z}^{Q_1}$. Therefore, if R acts on each arrow $a \in Q_1$ with weight $R_a \in \mathbb{Z}$, it satisfies

$$\sum_{a \in \partial f} R_a = \deg(R) \qquad \forall f \in Q_2 \tag{3.1.3}$$

The corresponding un-normalised 'anomaly-vanishing' condition at each vertex of the quiver is given by

$$\sum_{a \in H_v \cup T_v} R_a = \deg(R)(|H_v| - 1) \qquad \forall v \in Q_0 \tag{3.1.4}$$

We note that since Q is dual to a bipartite tiling, the arrows around any given vertex v alternate between outgoing and incoming arrows, so $|H_v| = |T_v|$.

Remark 3.1.1. Since the conditions (3.1.4) are rational linear equations, the intersection of their zero locus and the cone N^+ is a rational cone. Thus, using a similar argument to that in Section 2.2, we see that there exists an 'anomaly-free' real R-symmetry if and only if there exists an 'anomaly free' integral R-symmetry.

Definition 3.1.2. A dimer model is called *consistent* if there exists an R-symmetry satisfying the condition (3.1.4).

We note that in particular a consistent dimer model has an R-symmetry and so it is non-degenerate (Definition 2.3.3). Up to this point we have considered dimer models on an arbitrary Riemann surface Y. However the following argument, given by Kennaway in Section 3.1 of [22], shows that consistency forces this surface to be a torus.

Consider an R-symmetry which satisfies conditions (3.1.3) and (3.1.4). Summing these equations over all the quiver faces Q_2 and the quiver vertices Q_0 respectively and using the fact that each arrow is in exactly two faces and has two ends we observe that:

$$\deg(R)|Q_2| = 2 \sum_{a \in Q_1} R_a = \deg(R)(|Q_1| - |Q_0|) \tag{3.1.5}$$

Hence $|Q_0| - |Q_1| + |Q_2| = 0$. Since the quiver gives a cell decomposition of the surface Y, this implies that Y has Euler characteristic zero and must be a 2-torus.

3.2 Rhombus Tilings

We now define another consistency condition which we call 'geometric consistency'. This will imply the consistency condition (Definition 3.1.2) and when it holds, it gives a geometric interpretation of the conditions (3.1.1) and (3.1.2). This was first understood by Hanany and Vegh in [17]. In practice it is not easy to see directly if a dimer model is geometrically consistent, however we will explain an equivalent characterisation in terms of 'train tracks' on the 'quad graph' due to Kenyon and Schlenker which will be easier to check.

Given a dimer model on a torus, we construct the 'quad graph' associated to it. This is a tiling of the torus whose set of vertices is the union of the vertices of the bipartite tiling and its dual quiver Q. The edges of the quad graph connect a dimer vertex f to a quiver vertex v if and only if the face dual to f has vertex v in its boundary. The faces of this new tiling, which we call 'quads' to avoid confusion, are by construction quadrilaterals and are in 1-1 correspondence with the arrows in the quiver Q; given any arrow a in the quiver we have remarked previously (Remark 2.1.3) that it lies in the boundary of exactly two quiver faces f_+ and f_- of different colours. Therefore, there are edges in the quad graph between each of $f_\pm$ and both ha and ta. These four edges form the boundary of a quad, and every quad is of this form. In particular, the corresponding arrow and dual edge in the dimer are the two diagonals of the quad.

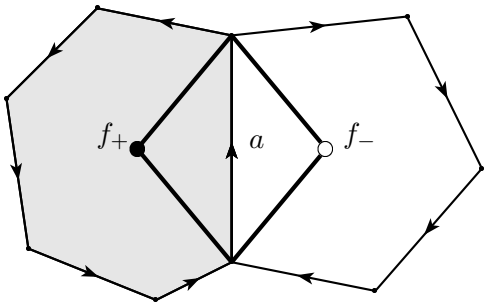

We draw the bipartite graph, the quiver and the quad graph of the hexagonal tiling below as an example.

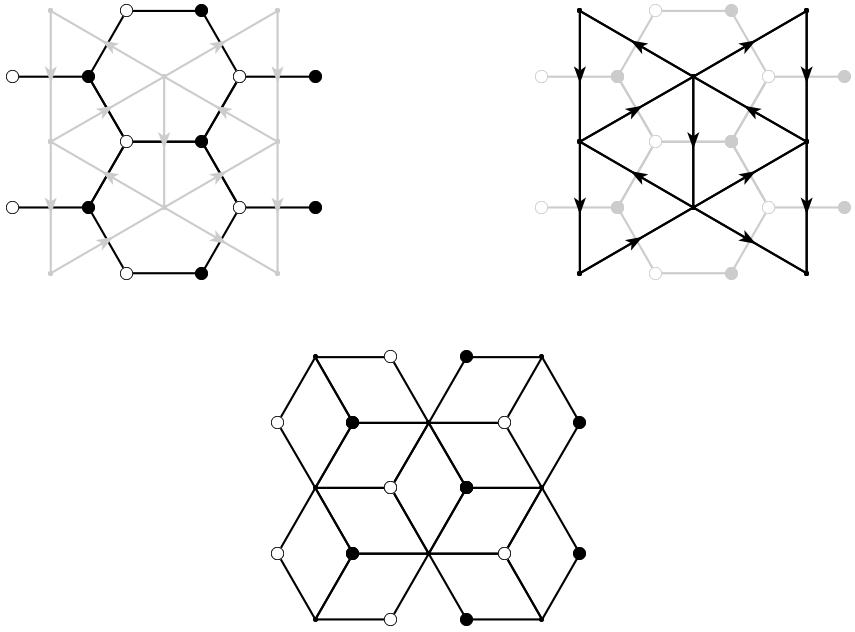

Definition 3.2.1. A dimer model on a torus is called *geometrically consistent* if there exists a rhombic embedding of the quad graph associated to it, i.e. an embedding in the torus such that all edges are line segments with the same length.

There exists a flat metric on the torus, so line segments are well defined, and each quad in a rhombic embedding is a rhombus. We note that the hexagonal tiling example above, is a geometrically consistent dimer model and the quad graph drawn is a rhombic embedding.

Suppose we have a geometrically consistent dimer model and consider a single rhombus in the rhombus embedding. The interior angles at opposite corners are the same, and the total of the internal angles is 2π, so its shape is determined by one angle. To each rhombus, and so to each arrow a of the quiver, we associate R_a, the interior angle of the rhombus at the dimer vertices divided by π.

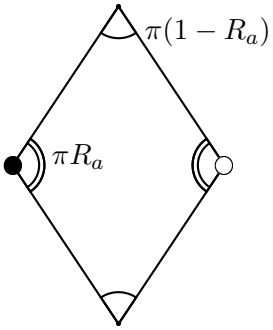

The conditions that the rhombi fit together around each dimer vertex and each quiver vertex, are exactly the conditions (3.1.1) and (3.1.2) for an 'anomaly free' real R-charge, normalised with $\deg(R) = 2$. Thus, recalling Remark 3.1.1, every geometrically consistent dimer model is consistent.

The converse however is not true. Given a normalised anomaly-free R-symmetry, we certainly require the additional condition that $R_a < 1$ for all $a \in Q_1$ in order to be able to produce a genuine rhombus embedding with angles in $(0, \pi)$. This does not hold in all cases; for example, the following dimer model is consistent but not geometrically consistent, as we shall see shortly.

Example 3.2.2.

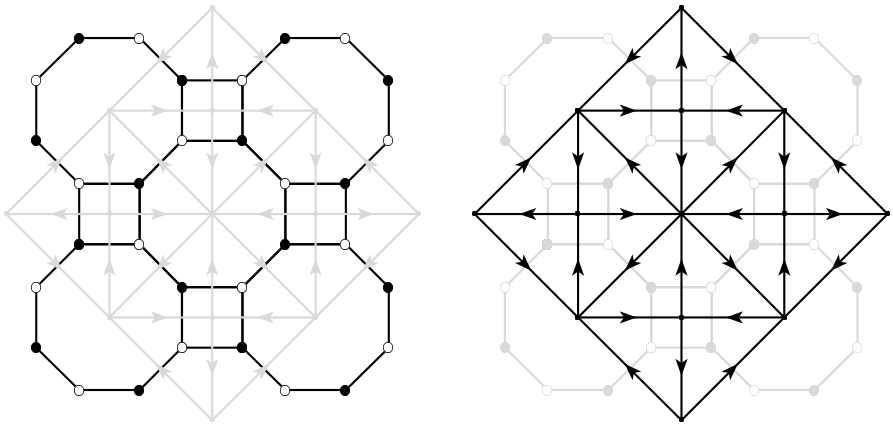

In [24], Kenyon and Schlenker prove a necessary and sufficient condition for the existence of a rhombus embedding, and thus in the dimer model case, for geometric consistency. They define a 'train track' to be a path of quads (each quad being adjacent along an edge to the previous quad) which does not turn, i.e. for each quad in the train

track, its shared edges with the previous and subsequent quads are opposite each other. Train tracks are assumed to extend in both directions as far as possible. The shaded quads in the example below, form part of a train track.

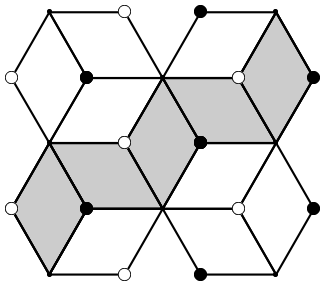

Theorem 3.2.3. (Theorem 5.1, [24]) *Suppose G is a quad graph on a torus. Then G has a rhombic embedding on a torus if and only if the following two conditions are satisfied:*

1. *Each train track is a simple closed curve.*
2. *The lift of two train tracks to the universal cover intersect at most once.*

The knowledge of a quad, and a pair of opposite edges is enough to completely determine a train track. Thus there are at most two train tracks containing any given quad, and since there are a finite number of quads on the torus, there are a finite number of train tracks. Therefore Theorem 3.2.3 gives a practical way of checking if a dimer model is geometrically consistent.

It will sometimes be more convenient to consider (and draw) paths, rather than paths of quads. For this reason we define the *spine* of a train track t to be the path which, on each quad of t, connects the mid-points of the opposite edges which are in adjacent quads in t. The diagram below shows part of a train track, with its spine dawn in grey:

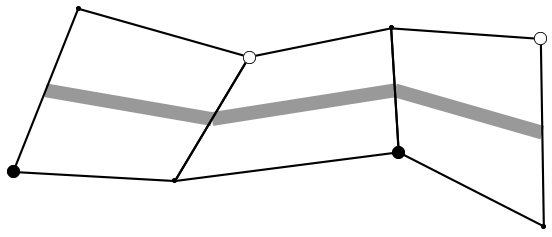

The spine of a train track is a closed curve on the torus. We note that two train tracks intersect in a quad if and only if their spines intersect, and the intersection of two spines may be assumed to be transversal.

Returning to Example 3.2.2 above, we draw part of the universal cover of the quad graph. The grey paths are lifts of the spines of two train tracks which can be seen to intersect more than once. Using Theorem 3.2.3, this shows that the example is not geometrically consistent.

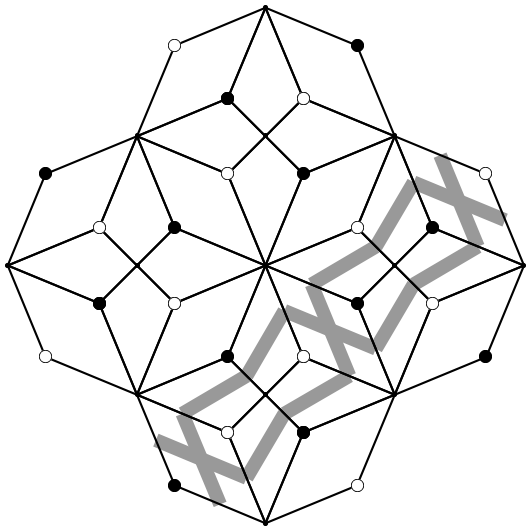

3.3 Zig-Zag Flows

Although we now have a way of checking if a given dimer model is geometrically consistent, this is done on the quad graph and we would prefer to return to the language of quivers which we used in previous chapters. We consider how the properties of train tracks transfer to the quiver.

We saw in the previous section that there is a 1-1 correspondence between quads and arrows, for example the arrow corresponding to a quad is the one in the boundary of the quiver faces dual to the dimer vertices of the quad. Therefore, if two quads are adjacent along an edge $\{v, f\}$, the corresponding arrows a, b have $ha = v = tb$, and are both in the boundary of f. Furthermore, since the dimer vertices on opposite edges of a quad, are different colours, the pairs of arrows corresponding to adjacent quads in a train track alternate between being in the boundary of black and white faces.

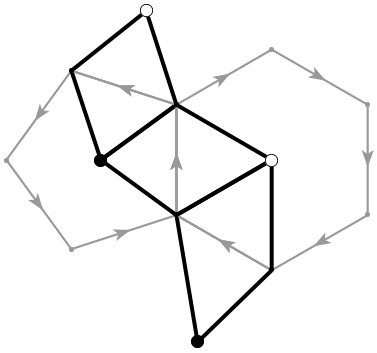

Definition 3.3.1. A *zig-zag path* η is a map $\eta : \mathbb{Z} \longrightarrow Q_1$ such that,

i) $h\eta_n = t\eta_{n+1}$ for each $n \in \mathbb{Z}$.

ii) η_{2n} and η_{2n+1} are both in the boundary of the same black face and, η_{2n-1} and η_{2n} are both in the boundary of the same white face.

We observe that shifting the indexing by an even integer, generates a different zig-zag path with the same image. We call this a reparametrisation of the path, and we will always consider paths up to reparametrisation.

Definition 3.3.2. An arrow a in a zig-zag path η is called a zig (respectively a zag) of η if it is the image of an even (respectively odd) integer.

This is independent of the choice of parametrisation.

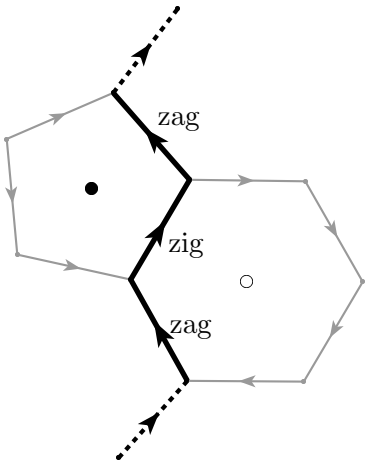

We saw in the previous section that the knowledge of a quad, and a pair of opposite edges is enough information to completely determine a train track. Let a be any arrow

in Q and suppose we decide that it is a zig (respectively zag). Then similarly,we see that this is enough to uniquely determine a zig-zag path (up to reparametrisation). Thus every arrow is in at most two zig-zag paths. Furthermore since there are a finite number of arrows in Q, we see that all zig-zag paths are periodic.

We now turn our attention to the universal cover $\widetilde{Q}$ of Q, and maps $\widetilde{\eta} : \mathbb{Z} \longrightarrow \widetilde{Q}_1$ into this, which satisfy the same 'zig-zag' property.

Definition 3.3.3. A *zig-zag flow* $\widetilde{\eta}$ is a map $\widetilde{\eta} : \mathbb{Z} \longrightarrow \widetilde{Q}_1$ such that,

i) $h\widetilde{\eta}_n = t\widetilde{\eta}_{n+1}$ for each $n \in \mathbb{Z}$.

ii) $\widetilde{\eta}_{2n}$ and $\widetilde{\eta}_{2n+1}$ are both in the boundary of the same black face and, $\widetilde{\eta}_{2n-1}$ and $\widetilde{\eta}_{2n}$ are both in the boundary of the same white face.

We define reparametrisation, zigs and zags in the same way as above, and observe that if we decide that an arrow $a \in \widetilde{Q}_1$ is a zig (respectively zag), then this is enough to uniquely determine a zig-zag flow (up to reparametrisation).

Remark 3.3.4. We use the terms zig-zag path and zig-zag flow in order to distinguish between objects on the quiver Q, and on its universal cover $\widetilde{Q}$. We note that composing a zig-zag flow with the projection from the universal cover $\widetilde{Q}$ to the quiver Q produces a zig-zag path. The 'zig-zag' property may also be characterised by saying that the path turns 'maximally left' at a vertex, then 'maximally right' at the following vertex, and then left again and so on. This is how it is defined in the physics literature, for example in [23]. In this language, knowing that a is a zig or a zag of a zig-zag path or flow, is equivalent to knowing whether the zig-zag path or flow turns left or right at the head of a.

Since there exists a unique zig-zag path or flow containing any given arrow a as a zig (respectively zag), we will refer to this as the zig-zag path or flow generated by the zig (respectively zag) a. In particular, the lift of a single zig or zag of a zig-zag path η to $\widetilde{Q}$, (remembering that it is a zig or zag), generates a zig-zag flow $\widetilde{\eta}$ which projects down to η.

Let $\widetilde{\eta}$ be a zig-zag flow and denote by η, the zig-zag path obtained by projecting this down to Q. Since η is periodic, there is a well defined element $(\eta) \in \mathbb{Z}_{Q_1}$ which is the sum of the arrows in a single period. This is obviously closed and has a homology class $[\eta] \in H_1(Q)$ i.e. in the homology of the torus. Thus each zig-zag flow $\widetilde{\eta}$ (and zig-zag path η), has a corresponding homology class.

Remark 3.3.5. The 2-torus is the quotient of the plane by the fundamental group $\pi_1(T)$ which is isomorphic to $H_1(T)$ as it is abelian. The action is by deck transformations. Given a point x on the plane and a homology class λ we find a curve on the

torus with this homology class which passes through the projection of x. We lift this curve to a path in the plane starting at x and define $\lambda.x$ to be the end point. This depends only on the homology class, and not on the choice of curve. We note that in particular, the action of $[\eta] \in H_1(Q)$ on an arrow $\widetilde{\eta}_n$ in a representative zig-zag flow $\widetilde{\eta}$, is the arrow $\widetilde{\eta}_{n+\varpi}$, where ϖ is the length of one period of $\widetilde{\eta}$.

We note that there is an obvious homotopy between the spine of a train track and the zig-zag path corresponding to that train track.

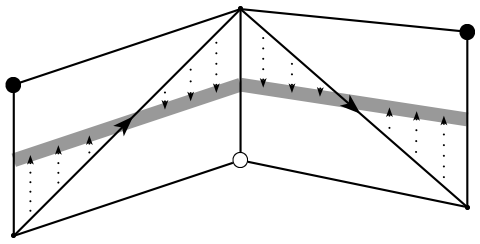

Therefore the spine of a train track and the corresponding zig-zag path have the same class in the homology of the torus.

Remark 3.3.6. We will often talk about the intersection between two zig-zag paths or flows. We have defined a zig-zag path or flow as a doubly infinite sequence of arrows, and as such, we will consider them to intersect if and only if they have an arrow in common. Thus there may exist zig-zag paths which share a vertex but not intersect. This is consistent with the train tracks definitions where two paths of quads intersect if and only if they have a quad in common which happens if and only if the spines of the train tracks intersect. Furthermore since the spines of zig-zag paths intersect each other transversally, each intersection of spines counts as ± 1 in the intersection product of the corresponding homology classes. Thus each arrow in the intersection between two zig-zag paths contributes ± 1 to the intersection number, and the intersection number is the sum of these contributions. In particular if a is a zag of $[\eta]$ and a zig of $[\eta']$, then it contributes $+1$ to $[\eta] \wedge [\eta']$.

We now give a proposition that describes necessary and sufficient conditions for a dimer model to be geometrically consistent in terms of zig-zag flows. We note that unlike Theorem 3.2.3, all conditions are formulated on the universal cover.

Proposition 3.3.7. *A dimer model is geometrically consistent if and only if the following conditions hold.*

(a) No zig-zag flow $\widetilde{\eta}$ in $\widetilde{Q}$ intersects itself, i.e. $\widetilde{\eta}$ is an injective map.

(b) If $\widetilde{\eta}$ and $\widetilde{\eta}'$ are zig-zag flows and $[\eta], [\eta'] \in H_1 Q$ are linearly independent, then they intersect in precisely one arrow.

(c) If $\widetilde{\eta}$ and $\widetilde{\eta}'$ are zig-zag flows and $[\eta], [\eta'] \in H_1 Q$ are linearly dependent, then they do not intersect.

Proof. First we suppose conditions (a)-(c) hold, and prove that these imply conditions (1) and (2) of Theorem 3.2.3. As there are a finite number of quads on the torus, all train tracks are closed. Therefore to prove condition (1), we need to show that they are simple. Suppose there is a train track which is not, and so intersects itself in a quad. This quad corresponds to an arrow in the quiver Q, which is contained in the corresponding zig-zag path as both a zig and a zag. Lifting this arrow to an arrow a in the universal cover, we consider the flows generated by a considered as a zig and as a zag. We either obtain one zig-zag flow which intersects itself, contradicting condition (a), or we obtain two zig-zag flows which intersect in the arrow a. By construction these project down to the same zig-zag path η, and therefore have the same corresponding homology class, but this contradicts condition (c). Therefore we have shown that condition (1) of Theorem 3.2.3 holds. Since the lift of a train track corresponds to a zig-zag flow, we observe that condition (2) of Theorem 3.2.3 follows directly from (b) and (c).

Now conversely, assuming that we have a geometrically consistent dimer model, so conditions (1) and (2) of Theorem 3.2.3 hold, we show that (a)-(c) hold. First we consider the case where $\widetilde{\eta}$ and $\widetilde{\eta}'$ are distinct zig-zag flows which project down to the same zig-zag path η, and show that they don't intersect. If they did, then there is an arrow $a \in \widetilde{Q}$ which is (without loss of generality) a zig of $\widetilde{\eta}$ and a zag of $\widetilde{\eta}'$. This projects down to an arrow which is both a zig and a zag of η. Thus η intersects itself and the corresponding train track is not a simple closed curve. This contradicts (1), and so $\widetilde{\eta}$ and $\widetilde{\eta}'$ do not intersect. This proves part of condition (c).

Now we prove that (a) holds. A zig-zag flow can intersect itself in two ways. If an arrow a occurs as a zig and a zag in $\widetilde{\eta}$, then $\widetilde{\eta}$ projects down to a zig-zag path η which contains the image of a as a zig and a zag. Thus η intersects itself and the corresponding train track is not a simple closed curve. This contradicts (1).

On the other hand, suppose an arrow a occurs more than once as a zig (or zag) in $\widetilde{\eta}$. Then $\widetilde{\eta}$ is a periodic sequence of arrows, whose support is a finite closed path in $\widetilde{Q}$. In particular, the corresponding homology class $[\eta] = 0$. Let $\widetilde{\eta}'$ be the zig-zag flow generated by a considered as a zag (or zig). We note that if $\widetilde{\eta}$ and $\widetilde{\eta}'$ are the same then they contain a as a zig and a zag which we showed could not happen in the case above. Therefore they must be distinct. Since $[\eta] = 0$, we see that $[\eta]$ and $[\eta']$ have zero

intersection number. We know from Remark 3.3.6 that each arrow in the intersection of η and η' contributes either ± 1 to the intersection number, so they must intersect in an even number of arrows. They intersect in at least one, namely the image of a, and so they must intersect at least twice which contradicts (2).

Finally we complete the proof of (b) and (c). We may suppose $\widetilde{\eta}$ and $\widetilde{\eta}'$ are zig-zag flows which project down to distinct zig-zag paths η and η' in Q, as the other case of (c) was already done above. Then $\widetilde{\eta}$ and $\widetilde{\eta}'$ correspond to the lifts of two distinct train tracks, and so by condition (2) they intersect at most once.

To prove (b) we suppose $\widetilde{\eta}$ and $\widetilde{\eta}'$ are zig-zag flows with the property that $[\eta]$ and $[\eta']$ are linearly independent. If v is any vertex of $\widetilde{\eta}$, then repeatedly applying the deck transformations corresponding to the homology classes $\pm[\eta]$ we obtain a sequence of vertices of $\widetilde{\eta}$ which lie on a line ℓ in the plane which has gradient given by $[\eta]$. In particular $\widetilde{\eta}$, and therefore the spine of the corresponding train track, lie within a bounded region of ℓ. Similarly, the spine of the train track corresponding to $\widetilde{\eta}'$ lies within a bounded region of a line ℓ' which has gradient given by $[\eta']$. Since $[\eta]$ and $[\eta']$ are linearly independent, the lines ℓ and ℓ' are not parallel and so intersect. Using the boundedness we see that the two spines must also intersect at least once. Thus $\widetilde{\eta}$ and $\widetilde{\eta}'$ intersect at least once and therefore exactly once. This proves (b).

Finally suppose $[\eta]$ and $[\eta']$ are linearly dependent, so there exists a non-zero homology class $c = k[\eta] = k'[\eta']$ which is a common multiple of $[\eta]$ and $[\eta']$. If $\widetilde{\eta}$ and $\widetilde{\eta}'$ intersect in an arrow a, we consider applying the deck transformation corresponding to c to this arrow. The image is an arrow which is both k periods along $\widetilde{\eta}$ from a, and k' periods along $\widetilde{\eta}'$ from a. Thus the image of a is a second arrow which is contained in both $\widetilde{\eta}$ and $\widetilde{\eta}'$. This is a contradiction, so $\widetilde{\eta}$ and $\widetilde{\eta}'$ do not intersect. This completes the proof of condition (c).

□

Remark 3.3.8. We note here that the property that a zig-zag flow $\widetilde{\eta}$ doesn't intersect itself (condition (a) of Proposition 3.3.7) implies that the homology class $[\eta]$ is non-zero. Also, condition (1) of Theorem 3.2.3 implies that the homology class corresponding to any zig-zag flow is primitive (or zero). Thus the homology class corresponding to any zig-zag flow in a geometrically consistent dimer model is non-zero and primitive. This observation will be useful in the next chapter.

Remark 3.3.9. Suppose we have a geometrically consistent dimer model and $\widetilde{\eta}$ and $\widetilde{\eta}'$ are such that $[\eta] \wedge [\eta'] > 0$. Considering the lines ℓ and ℓ' as in the proof of part (b) in the proposition above, we note that ℓ crosses ℓ' from left to right. Since $\widetilde{\eta}$ and $\widetilde{\eta}'$ lie within a bounded region of ℓ and ℓ' respectively and $\widetilde{\eta}$ and $\widetilde{\eta}'$ intersect exactly once,

we see that $\widetilde{\eta}$ crosses $\widetilde{\eta}'$ from left to right. Therefore this intersection is a zag of $\widetilde{\eta}$ and a zig of $\widetilde{\eta}'$.

3.4 Marginal Geometric Consistency

We saw in Section 3.2 that geometric consistency is a stronger condition than consistency. We discuss in this section two ways of weakening the geometric consistency condition, which we obtain by weakening the original definition, and the conditions of Proposition 3.3.7 respectively. We conjecture that these weakened conditions are equivalent.

Remark 3.4.1. We note here that Stienstra in [29], and Gulotta in [14] both prove that for any lattice polygon V, there exists a geometrically consistent dimer model which has V as its perfect matching polygon (as defined in Section 2.3). Thus to every lattice polygon, and so to every Gorenstein affine toric threefold, we can associate a geometrically consistent model. Therefore, in order to construct a CY3 algebra associated to every Gorenstein affine toric threefold it is sufficient to prove the CY3 condition in the geometrically consistent case and considering marginally geometrically consistent dimer models is not required.

3.4.1 Rhombus Tilings

We recall that in the quad graph associated to a dimer model, each quad has opposite vertices which are either both dimer vertices or both quiver vertices. Given a rhombus with this property, then it can be 'flattened', so it has no area, in two distinct ways. Namely, we can consider the limits as the two dimer vertices, or the two quiver vertices come together. These are equivalent to letting the interior angle of the rhombus at the dimer vertices, tend to π or zero respectively, i.e. using the notation of Section 3.2 letting $R_a \to 1$ or $R_a \to 0$ respectively. We call a dimer model on a torus *marginally geometrically consistent* if there exists a rhombus embedding of the quad graph, where we allow 'flat' rhombi whose dimer vertices coincide but not those whose quiver vertices coincide.

Using the same argument as in Section 3.2, we see that we can construct an anomaly free R-symmetry given such an embedding. Therefore marginal geometric consistency implies consistency. The weakened condition allows examples where the normalised R-symmetry has $R_a = 1$ for some $a \in Q_1$. Returning again to Example 3.2.2, we see that this has a rhombus embedding with flat rhombi of the correct sort, obtained by flattening the shaded quads in the diagram below:

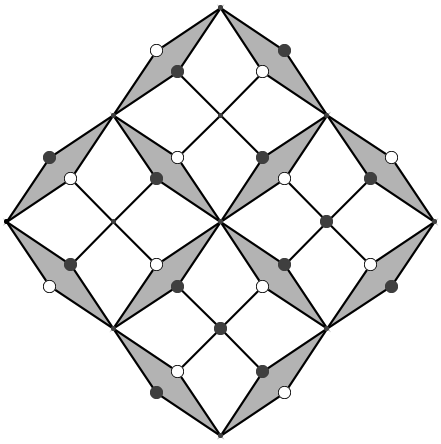

We saw at the end of Section 3.2 that it is not geometrically consistent. Therefore, this is an example of a marginally geometrically consistent dimer model which is not geometrically consistent. In the physics literature, it is described as a 'non-mimimal toric phase' of F_0, on the other hand, the 'mimimal toric phase' is geometrically consistent [17].

3.4.2 Zig-Zag Flows

We now consider how one might weaken the conditions of Proposition 3.3.7 and still obtain a sensible and hopefully equivalent definition of marginal consistency. One might consider weakening condition (c) of Proposition 3.3.7 to allow certain zig-zag flows with dependent homology classes to intersect. Looking at the marginally geometrically consistent Example 3.4.1, we see that the two zig-zag flows which do intersect more than once, have dependent homology classes which are negative rational multiples of each other. However, the two zig-zag flows which intersect more than once in the following example, satisfy these same properties, but the way they intersect forces any rhombus tiling to have rhombi which are flattened in the 'wrong' way.

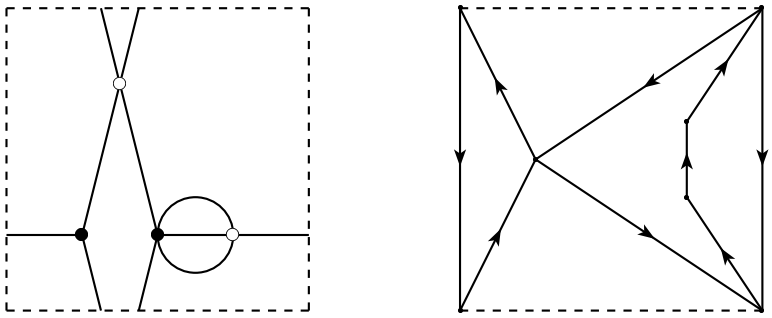

Remark 3.4.2. We note here that di-gons are 'bad'. If a dimer model has a di-gon, then looking at the two quads corresponding to the two edges of the face, we see that they can not both be rhombi, even allowing flat rhombi where the dimer vertices come together (see the diagram below). Therefore any dimer model with di-gons is not marginally geometrically consistent.

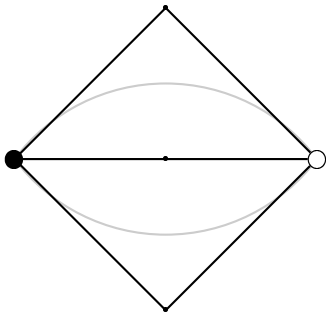

There are also examples of dimer models which are marginally geometrically consistent, which have zig-zag flows whose corresponding homology classes are linearly independent, and which intersect more than once. In the example below, we can obtain a rhombic embedding by flattening the light grey quads. The dark grey lines are the lifts of the spines of two train tracks which can be seen to intersect, but have linearly dependent homology classes. Two periods of each are shown.

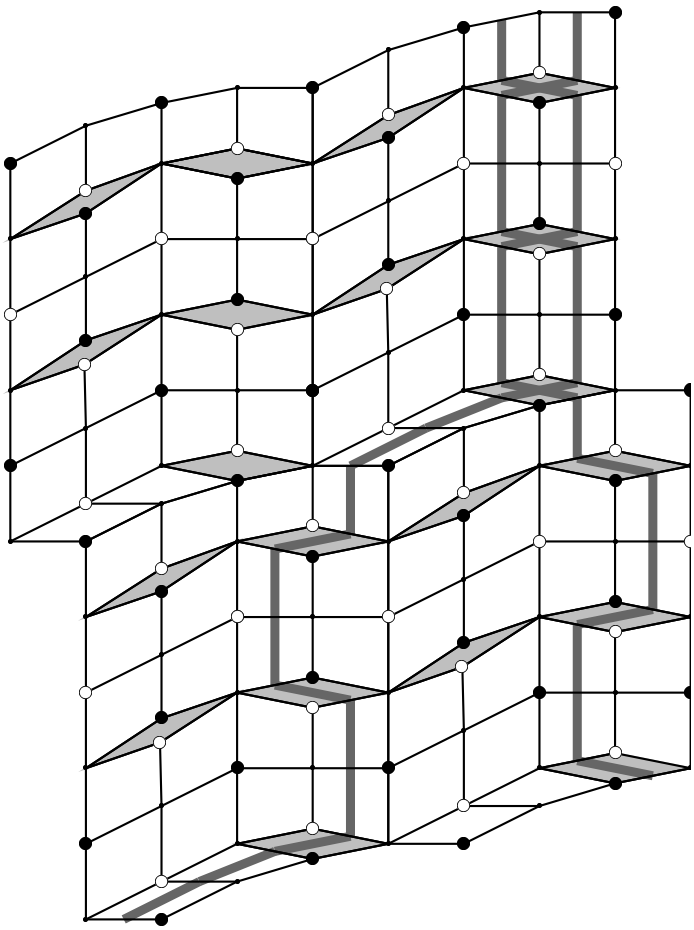

Therefore we need to consider more carefully how zig-zag flows intersect. We suggest the following conditions:

(a) No zig-zag flow $\widetilde{\eta}$ in $\widetilde{Q}$ intersects itself in an arrow.

(b) Suppose $\widetilde{\eta}$ and $\widetilde{\eta}'$ are zig-zag flows which intersect more than once, and let $\widetilde{\eta}_{k_1} = \widetilde{\eta}'_{n_1}$ and $\widetilde{\eta}_{k_2} = \widetilde{\eta}'_{n_2}$ be any two arrows in their intersection. If $k_1 < k_2$, then $n_1 > n_2$.

We conjecture that these conditions are equivalent to marginal geometric consistency.

3.5 Some Consequences of Geometric Consistency

We now return to dimer models that are geometrically consistent. In Section 2.1 we explained the construction of the algebra A which from an algebraic point of view is the output of a dimer model. This is quotient of the path algebra $\mathbb{C}Q$ by the ideal generated by 'F-term relations'. If a dimer model is geometrically consistent, a theorem of Hanany, Herzog and Vegh gives a concrete criterion for two paths to be F-term equivalent. In

this section we set up the notation required and then state this result. This will also act as motivation for the definition of 'non-commutative toric algebras' which we shall introduce in Chapter 4.

Recall that every arrow $a \in Q_1$ occurs in precisely two oppositely oriented faces $f^+, f^- \in Q_2$. Then each F-term relation can be written explicitly as an equality of two paths $p_a^+ = p_a^-$ for some $a \in Q_1$, where $p_a^\pm$ is the path from ha around the boundary of $f^\pm$ to ta. We say that two paths differ by a single F-term relation if they are of the form $q_1 p_a^+ q_2$ and $q_1 p_a^- q_2$ for some paths q_1, q_2 and some $a \in Q_1$. The F-term relations generate an equivalence relation on paths in the quiver.

Definition 3.5.1. Two paths p_1 and p_2 in Q are F-term equivalent denoted $p_1 \sim_F p_2$ if there is a finite sequence of paths $p_1 = \sigma_0, \sigma_1, \ldots, \sigma_k = p_2$ such that σ_i and σ_{i+1} differ by a single F-term relation for $i = 0, \ldots, k-1$.

The F-term equivalence classes of paths form a natural basis for A.

We recall that the quiver Q gives a cellular decomposition of the Riemann surface Y of a dimer model which, in consistent examples, is a 2-torus. Therefore there exist corresponding chain and cochain complexes

$$\mathbb{Z}_{Q_2} \xrightarrow{\partial} \mathbb{Z}_{Q_1} \xrightarrow{\partial} \mathbb{Z}_{Q_0} \tag{3.5.1}$$

$$\mathbb{Z}^{Q_0} \xrightarrow{d} \mathbb{Z}^{Q_1} \xrightarrow{d} \mathbb{Z}^{Q_2} \tag{3.5.2}$$

In Section 2.2 we defined a sublattice $N := d^{-1}(\mathbb{Z}\underline{1}) \subset \mathbb{Z}^{Q_1}$. We now wish to consider the dual lattice to N which we denote by M. This is the quotient of $\mathbb{Z}_{Q_1}$ by the sub-lattice $\partial(\underline{1}^\perp)$, where $\underline{1}^\perp := \{u \in \mathbb{Z}_{Q_2} \mid \langle u, \underline{1} \rangle = 0\}$. Since $\partial(\underline{1}^\perp)$ is contained in the kernel of the boundary map, this boundary map descends to a well defined map $\partial : M \to \mathbb{Z}_{Q_0}$ on the quotient.

Every path p in Q defines an element of $(p) \in \mathbb{Z}_{Q_1}$, obtained by simply summing up the arrows in the path. This in turn defines a class $[p]_M \in M$, for which $\partial[p]_M = hp - tp$. Now consider any F-term relation $p_a^+ = p_a^-$ for some $a \in Q_1$. Since $p_a^\pm$ is the path from ha around the boundary of $f^\pm$ to ta, we note that $(p_a^\pm) + (a) = \partial f^\pm$. In particular $(p_a^+) - (p_a^-) = \partial(f^+ - f^-)$ in $\mathbb{Z}_{Q_1}$, so $[p_a^+]_M = [p_a^-]_M$. Thus we see that it is necessary for F-term equivalent paths to have the same class in M. The result due to Hanany, Herzog and Vegh says that for geometrically consistent dimer models, this condition is also sufficient i.e. if two paths have the same class in M then they are F-term equivalent.

Let $M_o := \partial^{-1}(0)$ and note that this is a rank 3 lattice which is dual to N_o.

Therefore it sits in the short exact sequence dual to (2.3.2)

$$0 \longrightarrow \mathbb{Z} \longrightarrow M_o \xrightarrow{H} H_1(T;\mathbb{Z}) \longrightarrow 0 \tag{3.5.3}$$

The kernel of H is spanned by the class $\Box = \partial[f]_M$ for any face $f \in Q_2$. If R is any R-symmetry then by definition $\langle R, \Box \rangle = \deg R \neq 0$. Therefore, from (3.5.3), we observe that p and q have the same class in M, i.e. $[p]_M - [q]_M = 0$, precisely when they are *homologous*, i.e. $H([p]_M - [q]_M) = 0$, and they have the same weight under R, i.e. $\langle R, [p]_M \rangle = \langle R, [q]_M \rangle$.

Theorem 3.5.2. *(Hanany, Herzog, Vegh, Lemma 5.3.1 in [15]) For a geometrically consistent dimer model, two paths in Q are F-term equivalent (i.e. represent the same element of A) if and only if they are homologous and have the same weight under a fixed R-symmetry.*

Remark 3.5.3. In the terminology of [15] homologous paths are called 'homotopic' and paths which evaluate to the same integer on a fixed R-symmetry are said to be of the same 'length'.

Chapter 4

Toric Algebras and Algebraic Consistency

In this chapter we introduce the concept of (non-commutative, affine, normal) toric algebras. We prove some general properties, and relate the definition back to dimer models by showing that there is a toric algebra naturally associated to every dimer model. This leads to the definition of another consistency condition which we call 'algebraic consistency'. This will play a key role in the rest of this thesis. Finally we give some examples of algebraically consistent, and non algebraically consistent dimer models.

4.1 Toric Algebras

We start the story with two objects, a finite set Q_0, and a lattice N. Suppose this pair is equipped with two further pieces of information: Firstly a map of lattices

$$\mathbb{Z}^{Q_0} \xrightarrow{d} N$$

with the property that its kernel is $\mathbb{Z}\underline{1}$, and secondly a subset $N^+ \subset N$ which is the intersection of a strongly convex rational polyhedral cone in $N \otimes_{\mathbb{Z}} \mathbb{R}$ with the lattice N. Following the standard abuse of notation from toric geometry, we will simply refer to N^+ as a cone.

We consider the corresponding dual map of dual lattices

$$\mathbb{Z}_{Q_0} \xleftarrow{\partial} M$$

where $M = N^\vee := \mathrm{Hom}(N, \mathbb{Z})$ contains the dual cone of N^+,

$$M^+ = (N^+)^\vee := \{u \in M \mid \langle u, v\rangle \geq 0 \quad \forall v \in N^+\}$$

Let $M_{ij} := \partial^{-1}(j-i)$ for $i, j \in Q_0$, and denote the intersection with cone M^+ by $M_{ij}^+ := M_{ij} \cap M^+$. We define M^{gen} to be the submonoid of M^+ generated by the elements of M_{ij}^+ for all $i, j \in Q_0$.

Definition 4.1.1. We call (N, Q_0, d, N^+) *non-commutative toric data* if it satisfies the following two conditions:

1. M_{ij}^+ is non-empty for all $i, j \in Q_0$
2. $N^+ = (M^{gen})^\vee := \{v \in N \mid \langle u, v\rangle \geq 0 \quad \forall u \in M^{gen}\}$

Given some non-commutative toric data, we can associate a *non-commutative toric algebra*

$$B = \mathbb{C}[\underline{M}^+] = \bigoplus_{i,j \in Q_0} \mathbb{C}[M_{ij}^+]$$

where $\mathbb{C}[M_{ij}^+]$ is the vector space with a basis of monomials of the form x^m for $m \in M_{ij}^+$. The algebra may be considered as a formal matrix algebra

$$B = \begin{pmatrix} \mathbb{C}[M_{11}^+] & \dots & \mathbb{C}[M_{1n}^+] \\ \vdots & & \vdots \\ \mathbb{C}[M_{n1}^+] & \dots & \mathbb{C}[M_{nn}^+] \end{pmatrix}$$

with product

$$\mathbb{C}[M_{ij}^+] \otimes \mathbb{C}[M_{jk}^+] \to \mathbb{C}[M_{ik}^+] \colon x^{m_1} \otimes x^{m_2} \mapsto x^{m_1+m_2}$$

Remark 4.1.2. We note that $M_{ii} = \partial^{-1}(0)$ is obviously independent of the vertex $i \in Q_0$. We denote it by $M_o := \partial^{-1}(0)$, and let $M_o^+ := M_o \cap M^+$. Then $\mathbb{C}[M_o^+]$ is the coordinate ring of a commutative (affine normal) toric variety where $\mathbb{C}[M_o]$ is the coordinate ring of its torus.

4.2 Some Examples

Example 4.2.1. If $Q_0 = \{\bullet\}$ is the set with one element and N is any lattice, then the zero map

$$\mathbb{Z}^{Q_0} \xrightarrow{0} N$$

has kernel $\mathbb{Z}\underline{1}$. If N^+ is a cone in N then (N, Q_0, d, N^+) satisfies all the conditions for non-commutative toric data. In particular $M_{\bullet\bullet} = M$ so $M^+_{\bullet\bullet} = M^+ = (N^+)^\vee$, and

$$B = \mathbb{C}[M^+]$$

is a commutative ring. Thus we get the usual toric construction of the coordinate ring of the (normal) affine toric variety, defined by the cone N^+ in N.

Example 4.2.2. Let $Q_0 = \{i, j\}$ and let $N \cong \mathbb{Z}^2$ be a rank 2 lattice with some chosen basis. The map

$$\mathbb{Z}^{Q_0} \xrightarrow{\left(\begin{smallmatrix} 1 & -1 \\ -1 & 1 \end{smallmatrix}\right)} N$$

has kernel $\mathbb{Z}\underline{1}$. We consider the family of cones N^+_k for $k \in \mathbb{N}$ with rays which have primitive generators $(1, 0)$ and $(-k, k+1)$.

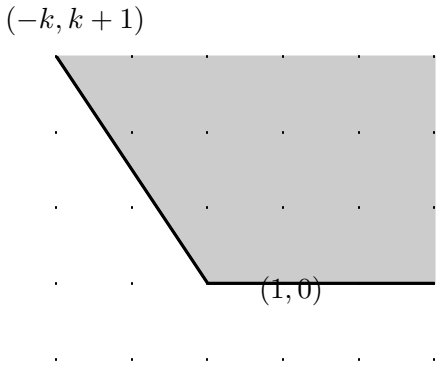

Then the dual cone $(M_k)^+$ in the dual lattice M_k is shown below. We can see that the slices $(M_k)^+_o$, $(M_k)^+_{ij}$ and $(M_k)^+_{ji}$ are all non-empty, and also that $(M^{gen})^\vee = N^+$.

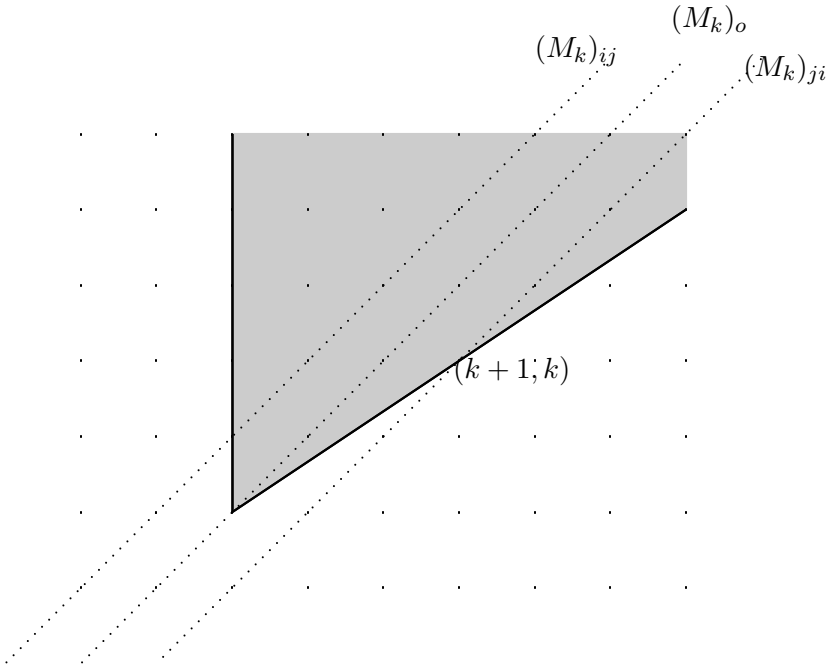

Therefore we have well defined non-commutative data, and the corresponding non-commutative toric algebra is

$$B = \mathbb{C}[\underline{M}_k^+] = \begin{pmatrix} \mathbb{C}[XY] & Y\mathbb{C}[XY] \\ X^{k+1}Y^k\mathbb{C}[XY] & \mathbb{C}[XY] \end{pmatrix}$$

Example 4.2.3. Let $Q = (Q_0, Q_1)$ be a strongly connected quiver and consider any sublattice $L \subset \mathbb{Z}_{Q_1}$ with a torsion free quotient, which is contained in the kernel of the boundary map $\partial : \mathbb{Z}_{Q_1} \to \mathbb{Z}_{Q_0}$. Using this we can construct some non-commutative toric data and the corresponding algebra. We define $M := \mathbb{Z}_{Q_1}/L$ to be the quotient lattice and let $N := M^\vee$. Since L is in the kernel, the boundary map descends to a map $\partial : M \to \mathbb{Z}_{Q_0}$ which has a dual map $d : \mathbb{Z}^{Q_0} \to N$. Furthermore, as the quiver is connected, we see that the kernel of d is $\mathbb{Z}\underline{1}$ as we required.

Let M^{ef} be the image of $\mathbb{N}_{Q_1}$ in M under the quotient map, and define $N^+ := (M^{ef})^\vee$. This is a strongly convex rational polyhedral cone in N.

We now see that (N, Q_0, d, N^+) is non-commutative toric data. First note that M^{ef} is generated by the images of the arrows in M^+. The image of an arrow is in $M^+_{ta,ha}$, so $M^{ef} \subseteq M^{gen} \subseteq M^+$. Dualising this we see that

$$N^+ = (M^+)^\vee \subseteq (M^{gen})^\vee \subseteq (M^{ef})^\vee = N^+$$

so condition (2) of Definition 4.1.1 is satisfied. Condition (1) is a consequence of the fact that Q is strongly connected. Given any two vertices $i, j \in Q_0$, there exists an (oriented) path from i to j. This defines an element of $\mathbb{N}_{Q_1}$ and therefore a class in $M^{ef} \subset M^+$. Furthermore since the path is from i to j, applying the boundary map to the class we get the element $(j - i) \in \mathbb{Z}_{Q_0}$, and we have therefore constructed an element in M^+_{ij}.

4.3 The Centre

Lemma 4.3.1. The centre $Z(B)$ of a non-commutative toric algebra $B = \mathbb{C}[\underline{M}^+]$ is isomorphic to $R := \mathbb{C}[M^+_o]$.

Proof. First we note that we can consider B as an R-algebra, using the map $R \to R\,\mathrm{Id} \subset B$, where Id is the identity element of B (which exists because M^+_o is a cone). This is true because $x^m x^{m_{kl}} = x^{m+m_{kl}} = x^{m_{kl}} x^m$ for any $m \in M^+_o$ and $m_{kl} \in M^+_{kl}$. In particular $R\,\mathrm{Id} \subset Z(B)$.

Now suppose $\underline{z} = (z_{ij}) \in Z(B)$. For every $k, l \in Q_0$, by definition M^+_{kl} is non-empty, so we may fix some $m_{kl} \in M^+_{kl}$. Let $x^{m_{kl}} \in B$ be the corresponding element in B. Then

$$(\underline{z} x^{m_{kk}})_{ij} = \begin{cases} z_{ik} x^{m_{kk}} & j = k \\ 0 & \text{otherwise} \end{cases}$$

and

$$(x^{m_{kk}} \underline{z})_{ij} = \begin{cases} x^{m_{kk}} z_{kj} & i = k \\ 0 & \text{otherwise} \end{cases}$$

Since $\underline{z}$ is central these must be equal and thus for all $i \neq k$ we have $z_{ik} x^{m_{kk}} = 0$. We note that $\mathbb{C}[M^+_{ik}]$ is a torsion free right $\mathbb{C}[M^+_{kk}]$- module and therefore $z_{ik} = 0$ for all $i \neq k$. Thus every off-diagonal entry in $\underline{z}$ is zero.

Similarly considering $(\underline{z} x^{m_{kl}})_{kl}$ and $(x^{m_{kl}} \underline{z})_{kl}$ we observe that $z_{kk} x^{m_{kl}} = x^{m_{kl}} z_{ll}$. Therefore $z_{kk} x^{m_{kl}} = z_{ll} x^{m_{kl}}$ and so $z_{kk} = z_{ll}$ in R. Thus $Z(B) \subseteq R\,\mathrm{Id}$ and we are done. □

4.4 Relationship with dimer models and Algebraic Consistency

We observe that there is a non-commutative toric algebra naturally associated to every non-degenerate dimer model. Given any dimer model, we saw in Section 2.1.3 that

there is a corresponding quiver. This quiver is strongly connected. This follows from the fact that the quiver is a tiling and given any unoriented path we can construct an oriented one by replacing any arrow a which occurs with the wrong orientation by the path from ha to ta around the boundary of one of the faces containing a. Let $L := \partial(\underline{1}^{\perp})$ be the sublattice of $\mathbb{Z}_{Q_1}$ where $\underline{1}^{\perp} := \{u \in \mathbb{Z}_{Q_2} \mid \langle u, \underline{1}\rangle = 0\}$, as defined in Section 3.5. We recall that this is contained in the kernel of the boundary map, and that the quotient $M = \mathbb{Z}_{Q_1}/L$ is torsion free. Then using Section 4.2.3 we can associate to this a non-commutative toric algebra $B := \mathbb{C}[\underline{M}^{+}]$.

Remark 4.4.1. We observe that the notation has been set up in a consistent way, i.e. the objects N, Q_0, d, N^{+} and also M, M^{+}, M_o corresponding to this toric algebra are the objects of the same name, seen in Sections 2.2 and 3.5 respectively.

We are now in a position to introduce a final consistency condition which we shall call 'algebraic consistency'. We saw in Section 3.5 that every path p from i to j in Q defines a class $[p]_M \in M$ which has boundary $j - i$. Since this was obtained by summing the arrows in the path it is clear that this class actually lies in $M_{ij}^{ef} \subset M_{ij}^{+}$. Furthermore we saw that if two paths are F-term equivalent, then they define the same class.

The F-term equivalence classes of paths in the quiver form a natural basis for the quiver algebra A. By definition the classes in M_{ij}^{+} for all $i, j \in Q_0$ form a basis for the algebra $B = \mathbb{C}[\underline{M}^{+}]$. Therefore, since it is defined on a basis, there is a well defined $\mathbb{C}$-linear map from A to B. It follows from the definition that if paths p and q are composable then $[pq]_M = [p]_M + [q]_M$ and thus the map respects the multiplication, i.e. we have defined an algebra morphism:

$$\hbar : A \longrightarrow \mathbb{C}[\underline{M}^{+}]; \qquad p \mapsto x^{[p]_M} \tag{4.4.1}$$

Definition 4.4.2. A dimer model is called algebraically consistent if the morphism (4.4.1) is an isomorphism.

We note that the map is an isomorphism if and only if restricts to an isomorphism on each i, jth piece, i.e. $e_i A e_j \xrightarrow{\cong} \mathbb{C}[M_{ij}^{+}]$ for each $i, j \in Q_0$.

Remark 4.4.3. Theorem 3.5.2 says that for a geometrically consistent dimer model two paths are F-term equivalent if and only if they have the same class in M. This is equivalent to saying that for geometrically consistent dimer models the map $\hbar$ is injective.

4.5 Example

We will construct a large class of examples of dimer models which are algebraically consistent in Chapter 6. For now we look at an example which is not algebraically consistent to see how things can go wrong.

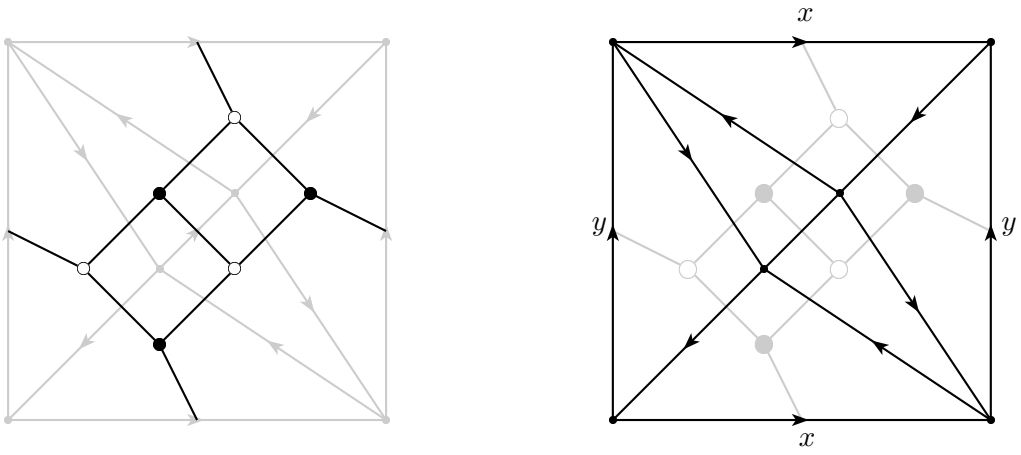

In this example the map $\hbar$ is neither injective nor surjective. To see the lack of injectivity we consider the two paths xy and yx around the boundary of the fundamental domain in the diagram above. Neither path can be altered using F-term relations and so they are distinct elements in A. However, considered as sum of arrows in $\mathbb{Z}_{Q_1}$, they are the same element, so they have the same class in M.

To see the lack of surjectivity we consider the path x which is a loop at a vertex. Therefore this path maps to an element $m \in M_o^+$. If the map $\hbar$ is surjective, then there must also be a path in e_1Ae_1 and e_2Ae_2 which maps to m, where e_1, e_2 are the idempotents corresponding to the other two vertices. However, no such paths exist.

Chapter 5

Zig-zag flows and perfect matchings

In Chapter 3 we saw how properties of the intersections of zig-zag flows could be used to characterise geometric consistency. In this chapter we assume geometric consistency, and use this to prove some properties about the intersections between zig-zag flows and paths. We will be particularly interested in zig-zag flows which intersect the boundary of a given face. We define 'zig-zag fans' which encode information about intersections of these flows, and use some of their properties to explicitly write down all the external and extremal perfect matchings (as defined in Section 2.3) of a geometrically consistent dimer model. We prove that the extremal perfect matchings have multiplicity one and that the multiplicities of the external perfect matchings are binomial coefficients. Several of the ideas and results introduced in this chapter will be important throughout the remainder of this thesis.

We start by recalling (Definition 3.3.3) that a zig-zag flow $\widetilde{\eta}$ is a doubly infinite path $\widetilde{\eta} : \mathbb{Z} \longrightarrow \widetilde{Q}_1$ such that, $\widetilde{\eta}_{2n}$ and $\widetilde{\eta}_{2n+1}$ are both in the boundary of the same black face and, $\widetilde{\eta}_{2n-1}$ and $\widetilde{\eta}_{2n}$ are both in the boundary of the same white face. We called an arrow a in a zig-zag flow $\widetilde{\eta}$, a zig (respectively a zag) of $\widetilde{\eta}$ if it is the image of an even (respectively odd) integer.

Remark 5.0.1. For a geometrically consistent dimer model, a zig-zag flow does not intersect itself in an arrow. Therefore each arrow in a zig-zag flow $\widetilde{\eta}$ is either a zig or a zag of $\widetilde{\eta}$ but can not be both. Furthermore we recall that knowledge that an arrow is a zig (or a zag) in a zig-zag flow, is enough to uniquely determine that zig-zag flow. Thus every arrow is in precisely two zig-zag flows, and is a zig in one and a zag in the other.

5.1 Boundary Flows

We start by defining the 'boundary flows' of a zig-zag flow $\widetilde{\eta}$. By definition, for each $n \in \mathbb{Z}$ we see that the 'zig-zag pair' $\widetilde{\eta}_{2n}$ and $\widetilde{\eta}_{2n+1}$ both lie in the boundary of a black face f_n. The other arrows in the boundary of this face form an oriented path $p^{(n)}$ from $h\widetilde{\eta}_{2n+1} = t\widetilde{\eta}_{2(n+1)}$ to $t\widetilde{\eta}_{2n} = h\widetilde{\eta}_{2n-1}$, i.e. a finite sequence of consecutive arrows.

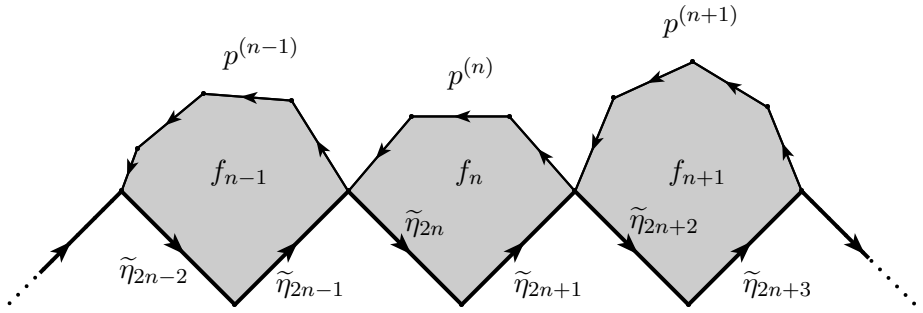

We piece these $p^{(n)}$ together in the obvious way, to construct a doubly infinite sequence of arrows which we call the black boundary flow of $\widetilde{\eta}$. By considering pairs of arrows $\widetilde{\eta}_{2n-1}$ and $\widetilde{\eta}_{2n}$ which lie in the boundary of a white face for each $n \in \mathbb{Z}$, (i.e. the 'zag-zig pairs') we can similarly construct the white boundary flow of $\widetilde{\eta}$. The two boundary flows of a zig-zag flow $\widetilde{\eta}$, project down to 'boundary paths' of the zig-zag path η. The construction we have just described, is well defined on the quiver Q and so the boundary paths can be constructed directly in Q. Since η is periodic, it follows that each boundary path is also periodic.

We recall from Section 3.3 that the image of a single period of η is a closed cycle $(\eta) \in \mathbb{Z}_{Q_1}$ which defines a homology class $[\eta] \in H_1(Q)$. Similarly the image of a single period of a boundary path is a closed cycle in $\mathbb{Z}_{Q_1}$ and also defines a homology class. Each 'zig-zag pair' of η is in the boundary of a unique black face. Summing these faces over a single period of η, defines an element in $\mathbb{Z}_{Q_0}$ whose boundary, by construction contains all the arrows in a period of η. If we subtract the cycle $(\eta) \in \mathbb{Z}_{Q_1}$ from this boundary, we obtain a cycle which is the sum of all arrows in the boundary of each of the faces except the zig-zag pair of η. Thus we see that by construction this cycle is the one corresponding to the black boundary flow of $\widetilde{\eta}$. The same argument follows through with white faces and zag-zig pairs. Thus we have shown:

Lemma 5.1.1. *For each zig-zag flow $\widetilde{\eta}$, the black and white boundary flows on $\widetilde{Q}$ project to boundary paths on Q whose corresponding homology classes are both $-[\eta] \in H_1(Q)$.*

5.2 Some Properties of zig-zag flows

It will now be useful to consider the intersections of zig-zag flows and more general paths. We consider a path in $\widetilde{Q}$ to be a (finite or infinite) sequence of arrows (a_n) such that $ha_n = ta_{n+1}$. We will call a path *simple* if it contains no repeated arrows. We will also consider 'unoriented' paths, where we do not have to respect the orientation of the arrows. These can be considered as paths in the doubled quiver and where we denote the opposite arrow to a by a^{-1}. We call an unoriented path *simple* if it contains no arrow which is repeated with either orientation.

Remark 5.2.1. We note that the support of a simple path does not have to be a simple curve in the usual sense, and may intersect itself as long as the intersections occur at vertices.

Lemma 5.2.2. *Let p be a (possibly unoriented) finite simple closed path in $\widetilde{Q}$ and $\widetilde{\eta}$ be any zig-zag flow. If p and $\widetilde{\eta}$ intersect in an arrow a, then they must intersect in at least two arrows.*

Proof. Without loss of generality we can consider the case when the support of p is a Jordan curve. Indeed, if the support of p is not simple, there is a path p' containing a whose support is a simple closed curve which is contained in the support of p. This is true because the curve only intersects itself at vertices of the quiver. The path p' can be constructed by considering the path starting at a, and each time a vertex is repeated, removing all the arrows between the repeated vertices. If $\widetilde{\eta}$ intersects p' in at least two arrows, it must intersect p in at least these arrows.

Since the universal cover $\widetilde{Q}$ is planar we may apply the Jordan curve theorem which implies that p is the boundary of the union of a finite number of faces. Let F denote the set consisting of these faces. We observe that the arrows in the path p are those which are contained in the boundary of precisely one face in F. We say that an arrow is 'interior' if it is contained in the boundary of two distinct faces in F. In particular since F contains a finite number of faces, there are a finite number of arrows in the interior.

Since $a = \widetilde{\eta}_k$ is an arrow in p, it is in the boundary of one face $f \in F$. Using the zig-zag property, one of the arrows $\widetilde{\eta}_{k-1}$ or $\widetilde{\eta}_{k+1}$ in $\widetilde{\eta}$ must also be in the boundary of f. Either this arrow in the path p, and we are done, or it lies in the interior. Without loss of generality, assume that $\widetilde{\eta}_{k+1}$ lies in the interior. There are a finite number of arrows in the interior, and $\widetilde{\eta}$ is an infinite sequence of arrows which, by geometric consistency, never intersects itself. Therefore, there exists a first arrow $\widetilde{\eta}_{k'}$ with $k' > k+1$, which is not in the interior.

In particular the arrow $\widetilde{\eta}_{k'-1}$ is in the interior, and therefore is in the boundary of two faces in F. Using the zig-zag property, we see that $\widetilde{\eta}_{k'}$ is in the boundary of one of these faces and, because it is not in the interior, it must be an arrow in p. Finally, since $a = \widetilde{\eta}_k$ and $\widetilde{\eta}_{k'}$ are both in $\widetilde{\eta}$, which does not intersect itself, they must be distinct. □

Now let f be a face in the universal cover $\widetilde{Q}$, and consider the the intersections between zig-zag flows and the boundary of f.

Lemma 5.2.3. *If $\widetilde{\eta}$ is a zig-zag flow which intersects the boundary of f, then it intersects in exactly two arrows which form a zig-zag pair of $\widetilde{\eta}$ if f is black and a zag-zig pair if f is white.*

Proof. Let $\widetilde{\eta}$ be a zig-zag flow that intersects the boundary of f. We assume that f is black, the result for white faces follows by a symmetric argument. Using the zig-zag property we see that each intersection between $\widetilde{\eta}$ and the boundary of f must occur as a pair of arrows and by definition, this is a zig-zag pair of $\widetilde{\eta}$.

Suppose for a contradiction that some zig-zag flow intersects the boundary of face f in more than one pair. We choose such a flow $\widetilde{\eta}$ so that the number of arrows around the boundary of f, from one zig-zag pair $(\widetilde{\eta}_0, \widetilde{\eta}_1)$ to another pair $(\widetilde{\eta}_k, \widetilde{\eta}_{k+1})$, where $k \geq 2$, is minimal (it could be zero). We note that minimality ensures that $\widetilde{\eta}$ does not intersect the part of the boundary of f between $\widetilde{\eta}_1$ and $\widetilde{\eta}_k$. The arrow $\widetilde{\eta}_1$ is a zig of a different zig-zag flow which we call $\widetilde{\eta}'$, and without loss of generality $\widetilde{\eta}_1 = \widetilde{\eta}'_0$. By the zig-zag property, $\widetilde{\eta}'_1$ is also in the boundary of f.

If the number of arrows around the boundary of f, between $h\widetilde{\eta}_1 = h\widetilde{\eta}'_0$ and $t\widetilde{\eta}_k$ is zero then $\widetilde{\eta}'_1 = \widetilde{\eta}_k$ and $\widetilde{\eta}$ and $\widetilde{\eta}'$ intersect in at least two arrows, which contradicts geometric consistency. Otherwise there are two finite oriented simple paths from $h\widetilde{\eta}_1 = h\widetilde{\eta}'_0$ to $t\widetilde{\eta}_k$; the path p along the boundary of f and the path q which is part of $\widetilde{\eta}$. Then pq^{-1} is a (finite) simple closed path which intersects $\widetilde{\eta}'$ in the arrow $\widetilde{\eta}'_0$. Simplicity follows since p and q are both simple and $\widetilde{\eta}$ does not intersect p. Applying Lemma 5.2.2 we see that $\widetilde{\eta}'$ must intersect pq^{-1} in another arrow. It can not intersect q otherwise $\widetilde{\eta}$ and $\widetilde{\eta}'$ intersect in at least two arrows, so it must intersect p in a second arrow. We show that this leads to a contradiction.

First note that it can not intersect p in an arrow $\widetilde{\eta}'_l$ for $l \geq 2$, as this would contradict the minimality condition above. Suppose it intersects in an arrow $\widetilde{\eta}'_l$ for $l < 1$. Without loss of generality assume there are no other intersections of $\widetilde{\eta}'$ with the boundary between $\widetilde{\eta}'_1$ and $\widetilde{\eta}'_l$. Then since $\widetilde{\eta}'$ doesn't intersect itself, the path along the boundary from $h\widetilde{\eta}'_1$ to $t\widetilde{\eta}'_l$ followed by the path along $\widetilde{\eta}'$ from $t\widetilde{\eta}'_l$ to $h\widetilde{\eta}'_1$ is a simple closed path. However this intersects $\widetilde{\eta}$ in the single arrow $\widetilde{\eta}_1 = \widetilde{\eta}'_0$, which contradicts Lemma 5.2.2.

□

Corollary 5.2.4. *A zig-zag flow does not intersect its black (or white) boundary flow.*

5.3 Right and left hand sides

Intuitively, one can see that since zig-zag flows do not intersect themselves in a geometrically consistent dimer model, any given zig-zag flow $\widetilde{\eta}$ splits the universal cover of the quiver into two pieces. We formalise this idea by defining an equivalence relation on the vertices as follows.

Lemma 5.3.1. *There is an equivalence relation on $\widetilde{Q}_0$, where $i, j \in \widetilde{Q}_0$ are equivalent if and only if there exists a (possibly unoriented) finite path from i to j in $\widetilde{Q}$ which doesn't intersect $\widetilde{\eta}$ in any arrows. There are exactly two equivalence classes.*

Proof. It is trivial to check that the equivalence relation is well defined. To prove that there are two equivalence classes we consider the following sets of vertices

$$R(\widetilde{\eta}) := \{v \in \widetilde{Q}_0 \mid v = ha \text{ where } a \text{ is a zig of } \widetilde{\eta}\}$$
$$L(\widetilde{\eta}) := \{v \in \widetilde{Q}_0 \mid v = ta \text{ where } a \text{ is a zig of } \widetilde{\eta}\}$$

The black and white boundary flows of $\widetilde{\eta}$ don't intersect $\widetilde{\eta}$ in an arrow by Corollary 5.2.4. We note that the black (white) flow is a path which passes through all the vertices of $L(\widetilde{\eta})$ (respectively $R(\widetilde{\eta})$). Thus all the vertices in $L(\widetilde{\eta})$ (respectively $R(\widetilde{\eta})$) lie in a single equivalence class. We show that these two classes are distinct.
If they were not, then for any zig a of $\widetilde{\eta}$, there would exist a (possibly unoriented) finite path in $\widetilde{Q}$ from $ha \in R(\widetilde{\eta})$ to $ta \in L(\widetilde{\eta})$ which doesn't intersect $\widetilde{\eta}$ in an arrow. By removing the part of the path between any repeated arrows (including the arrows themselves if they occur with opposite orientations), we may assume the path is simple. We prove that such a path does not exist. If p is any finite simple path from ha to ta which doesn't intersect $\widetilde{\eta}$, then in particular it doesn't contain a, so ap is a finite simple closed path. Then as $\widetilde{\eta}$ intersects this in the arrow a, by Lemma 5.2.2 it must intersect in another distinct arrow. Thus $\widetilde{\eta}$ must intersect p in an arrow which is a contradiction.
Finally we prove that the equivalence classes containing $L(\widetilde{\eta})$ and $R(\widetilde{\eta})$ are the only two equivalence classes. Let $v \in \widetilde{Q}_0$ be any vertex. The quiver $\widetilde{Q}$ is strongly connected so, if a is some zig in $\widetilde{\eta}$, there exists a finite path from v to ha. Either the path doesn't intersect $\widetilde{\eta}$ in an arrow, and we are done, or it does. Let b be the first arrow in the

intersection. Then by construction the path from v to tb doesn't intersect $\widetilde{\eta}$ and tb is obviously in $L(\widetilde{\eta})$ or $R(\widetilde{\eta})$. □

Definition 5.3.2. We say a vertex $v \in \widetilde{Q}_0$ is on the left (right) of a zig-zag flow $\widetilde{\eta}$ if it is in the same equivalence class as an element of $L(\widetilde{\eta})$ (respectively $R(\widetilde{\eta})$) under the equivalence relation defined above.

Corollary 5.3.3. *Any path which passes from one side of a zig-zag flow to the other side, must intersect the flow in an arrow.*

Remark 5.3.4. We note here that the above definition is consistent with the usual understanding of right and left, however it also gives a well defined notion of right or left to vertices which actually lie on the zig-zag flow itself. We recall that the lift spine of the corresponding train track (see the end of Section 3.2) to the universal cover of the quad graph is a periodic path which doesn't pass through any quiver vertices. This splits $\widetilde{Q}_0$ into the same two classes.

5.4 Zig-zag fans

We have seen that if a zig-zag flow intersects the boundary of a face, then it does so in a single zig-zag pair. We now consider the collection of zig-zag flows which intersect the boundary of a given face and construct fans in the integer homology lattice generated by the classes of these flows. We observe that these fans encode the information about the intersections of zig-zag flows which occur around the boundary of the face.

If f is some face of $\widetilde{Q}$, we define:

$$\mathcal{X}(f) = \{\widetilde{\eta} \mid \widetilde{\eta} \text{ intersects the boundary of } f\}.$$

For any zig-zag flow $\widetilde{\eta}$, recall (Remark 3.3.8) that $[\eta]$ is a non-zero primitive homology class in the integer homology lattice $H_1(Q)$. We consider the collection of rays in $H_1(Q)$ generated by the classes $[\eta]$ where $\widetilde{\eta} \in \mathcal{X}(f)$.

Lemma 5.4.1. *Given a ray γ generated by $[\eta]$ where $\widetilde{\eta} \in \mathcal{X}(f)$, there exists $\widetilde{\eta}' \in \mathcal{X}(f)$ such that the ray generated by $[\eta']$ is at an angle less than π in an anti-clockwise direction from γ.*

Proof. Since $\widetilde{\eta} \in \mathcal{X}(f)$, by Lemma 5.2.3 it intersects the boundary of f in a zig and a zag. The zag of $\widetilde{\eta}$ is a zig of a uniquely defined zig-zag flow $\widetilde{\eta}' \in \mathcal{X}(f)$ which crosses $\widetilde{\eta}$ from right to left. This intersection contributes $+1$ to the intersection number $[\eta] \wedge [\eta']$, and therefore recalling Remark 3.3.9 this implies that intersection number is strictly

positive. Therefore the ray generated by $[\eta']$ is at an angle less than π in an anti-clockwise direction from γ. □

Definition 5.4.2. The local zig-zag fan $\xi(f)$ at the face f of $\widetilde{Q}$, is the complete fan of strongly convex rational polyhedral cones in $H_1(Q)$ whose rays are generated by the homology classes corresponding to zig-zag flows in $\mathcal{X}(f)$.

Since they are primitive, we note that if the homology classes corresponding to $\widetilde{\eta}$ and $\widetilde{\eta}'$ are linearly dependent, then $[\eta] = \pm[\eta']$. We say $\widetilde{\eta}$ and $\widetilde{\eta}'$ are *parallel* if $[\eta] = [\eta']$, and *anti-parallel* if $[\eta] = -[\eta']$.

Lemma 5.4.3. *If $\widetilde{\eta}$ and $\widetilde{\eta}'$ are distinct parallel zig-zag flows, then at most one of them intersects the boundary of any given face.*

Proof. Without loss of generality let f be a black face. Suppose $\widetilde{\eta}, \widetilde{\eta}' \in \mathcal{X}(f)$ are parallel. Since they don't intersect by Proposition 3.3.7, all vertices of $\widetilde{\eta}$ lie on the same side of $\widetilde{\eta}'$ and vice-versa. Both $\widetilde{\eta}$ and $\widetilde{\eta}'$ intersect the boundary of f in a zig-zag pair, and, by geometric consistency, these pairs of arrows are distinct. By considering paths around the boundary of f we observe that all vertices of $\widetilde{\eta}$ lie on the left of $\widetilde{\eta}'$ and all vertices of $\widetilde{\eta}'$ lie on the left of $\widetilde{\eta}$.

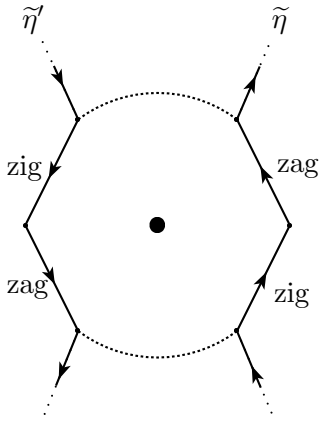

However, choosing any other zig-zag flow which is not parallel to $\widetilde{\eta}$, this intersects each of $\widetilde{\eta}$ and $\widetilde{\eta}'$ in precisely one arrow. Recalling Remark 3.3.9, we see that these arrows are either both zigs of their respective flows, or both zags. Therefore, by considering the path along the zig-zag flow between these two arrows, we see that if all vertices of $\widetilde{\eta}$ lie on the left of $\widetilde{\eta}'$ then all vertices of $\widetilde{\eta}'$ lie on the right of $\widetilde{\eta}$. This is a contradiction. □

Remark 5.4.4. We have just shown that for every ray γ of $\xi(f)$, there is a unique representative zig-zag flow which intersects the boundary of f, i.e. a unique flow which

intersects the boundary of f and whose corresponding homology class is the generator of γ. Together with Lemma 5.2.3 this also implies that if a zig-zag *path* intersects a face then it does so in a zig and a zag.

Proposition 5.4.5. *Two rays γ^+ and γ^- span a two dimensional cone in $\xi(f)$ if and only if they have representative zig-zag flows $\widetilde{\eta}^+$ and $\widetilde{\eta}^-$ which intersect each other in the boundary of f.*

Proof. Without loss of generality we assume that f is black, as the general result follows by symmetry. Suppose zig-zag flows $\widetilde{\eta}^+$ and $\widetilde{\eta}^-$ intersect in arrow a contained in the boundary of f. Without loss of generality we assume that $\widetilde{\eta}^+$ crosses $\widetilde{\eta}^-$ from right to left. As in the proof of Lemma 5.4.1 we see that corresponding ray γ^- is at an angle less than π in a clockwise direction from γ^+. We prove that γ^+ and γ^- span a two dimensional cone in $\xi(f)$. If they do not, then there is a zig-zag flow $\widetilde{\eta}$ which intersects the boundary of f in zig-zag pair $(\widetilde{\eta}_0, \widetilde{\eta}_1)$ and whose ray in the local zig-zag fan lies strictly between γ_1 and γ_2 (so $\widetilde{\eta}$ is not parallel or anti-parallel to $\widetilde{\eta}^+$ or $\widetilde{\eta}^-$.) Therefore $\widetilde{\eta}$ crosses $\widetilde{\eta}^-$ from right to left and crosses $\widetilde{\eta}^+$ from left to right. Let b be the intersection of $\widetilde{\eta}$ and $\widetilde{\eta}^-$ which we note is a zig of $\widetilde{\eta}$.

By considering paths around the boundary of f we see that vertex $v := h\widetilde{\eta}_0$ is on the left of both $\widetilde{\eta}^+$ and $\widetilde{\eta}^-$. Therefore it must occur in $\widetilde{\eta}$ before $\widetilde{\eta}$ intersects $\widetilde{\eta}_2$ but after $\widetilde{\eta}$ intersects $\widetilde{\eta}_1$.

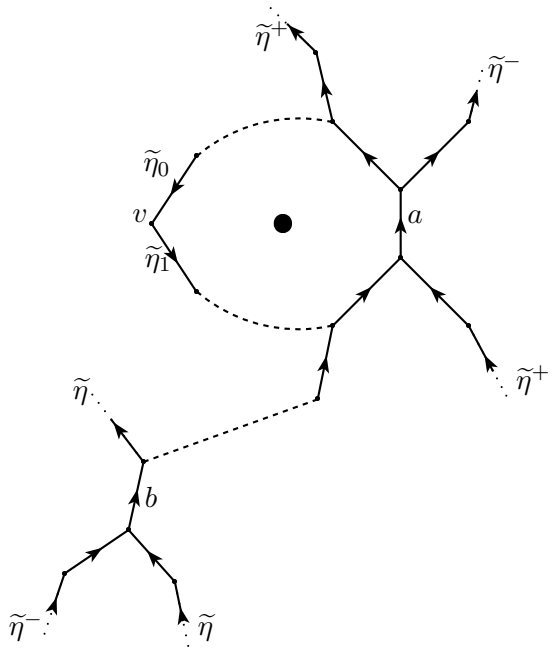

In particular $\widetilde{\eta}$ crosses $\widetilde{\eta}^-$ before it crosses $\widetilde{\eta}^+$ and the vertex hb must be on the

left of $\widetilde{\eta}^+$. Since $\widetilde{\eta}^-$ crosses $\widetilde{\eta}^+$ from left to right, we see that b occurs before a in $\widetilde{\eta}^-$. The path from hb to ta along $\widetilde{\eta}_1$ doesn't intersect $\widetilde{\eta}$ (since geometric consistency implies that b is the unique arrow where they intersect). Therefore ta is on the right of $\widetilde{\eta}$. However there is a path around the boundary of f from hb_1 to ta which doesn't intersect $\widetilde{\eta}$. This implies that ta is on the left of $\widetilde{\eta}$. Therefore we have a contradiction and so γ_1 and γ_2 generate a two-dimensional cone in $\xi(f)$, where γ_1 is the negative ray. □

Remark 5.4.6. The previous two lemmas together imply that the zig-zag flows which intersect the boundary of a face f, intersect it in pairs of arrows in such a way that the cyclic order of these pairs around the face is (up to orientation) the same as the cyclic order of the corresponding rays around the local zig-zag fan. In [14] Gulotta also observes that this is an important property. He calls a dimer model where this is satisfied at each face 'properly ordered' and proves that this happens if and only if the number of quiver vertices is equal to twice the area of the polygon whose edges are normal to the directions of the zig-zag paths. He proposes this as an alternative 'consistency condition'.

Given a two-dimensional cone σ in the local zig-zag fan of some face f, we call the unique arrow in the boundary of f, which is the intersection of representative zig-zag flows of the rays of σ, the arrow corresponding to σ.

Definition 5.4.7. The global zig-zag fan Ξ in $H_1(Q) \otimes_{\mathbb{Z}} \mathbb{R}$, is the fan whose rays are generated by the homology classes corresponding to all the zig-zag flows on $\widetilde{Q}$.

This is a refinement of each of the local zig-zag fans and is therefore a well defined fan.

5.5 Constructing Some Perfect Matchings

In this section we use the zig-zag fans we have just introduced to construct a particular collection of perfect matchings that will play a key role in the rest of this thesis. The construction is a local one in the sense that the restriction of the perfect matching to the arrows in the boundary of a quiver face is determined by the local zig-zag fan at that face.

We start by noting that the identity map on $H_1(Q)$ is a well defined map of fans $\iota_f : \Xi \to \xi(f)$ for each $f \in Q_2$. If σ is a two dimensional cone in Ξ, its image in $\xi(f)$ is contained in a unique two dimensional cone which we shall denote σ_f.

The cone σ_f corresponds to a unique arrow in the boundary of f. We define $P_f(\sigma) \in \mathbb{Z}^{Q_1}$ to be the function which evaluates to 1 on this arrow, and zero on all other arrows in Q. Finally we define the following function:

$$P(\sigma) := \frac{1}{2} \sum_{f \in Q_2} P_f(\sigma)$$

Lemma 5.5.1. *The function $P(\sigma)$ is a perfect matching.*

Proof. First we show that $P(\sigma) \in \mathbb{N}^{Q_1}$. Any arrow a is in the boundary of precisely two faces, one black and one white, which we denote f_b and f_w respectively. Since $P_f(\sigma)$ is zero on all arrows which don't lie in the boundary of f, we observe that $P(\sigma)(a) = \frac{1}{2}\left(P_{f_b}(\sigma)(a) + P_{f_w}(\sigma)(a)\right)$. If $\widetilde{\eta}^+$ and $\widetilde{\eta}^-$ are the zig-zag flows containing a then, by Lemma 5.4.5, the cones σ_b in $\xi(f_b)$ and σ_w in $\xi(f_w)$ dual to a, are both spanned by the rays generated by $[\eta^+]$ and $[\eta^-]$. Therefore the inverse image of σ_b and σ_w under the respective maps of fans is the same collection of cones in the global zig-zag fan Ξ. Thus for any cone σ in Ξ, the functions $P_{f_b}(\sigma)$ and $P_{f_w}(\sigma)$ evaluate to the same value on a. We conclude that

$$P(\sigma) = \frac{1}{2} \sum_{f \in Q_2} P_f(\sigma) = \sum_{\substack{f \in Q_2 \\ f \text{ is black}}} P_f(\sigma)$$

and evaluates to zero or one on every arrow in Q. By construction $P_f(\sigma)$ is non-zero on a single arrow in the boundary of f, and we have just seen that $P(\sigma)$ is non-zero on an arrow in the boundary of f if and only if $P_f(\sigma)$ is non-zero. Therefore $P(\sigma)$ evaluates to one on a single arrow in the boundary of each face. Recalling that the coboundary map d simply sums any function of the edges around each face we see that $d(P(\sigma)) = \underline{1}$. □

We have produced an identified perfect matching $P(\sigma) \in \mathbb{N}^{Q_1}$ for each two dimensional cone σ in the global zig-zag fan Ξ. We now consider some properties of perfect matchings of this form.

Definition 5.5.2. If η is a zig-zag path, we define $Zig(\eta) \in \mathbb{Z}^{Q_1}$ (respectively $Zag(\eta) \in \mathbb{Z}^{Q_1}$) to be the function which evaluates to one on all zigs (zags) of η and zero on all other arrows. Similarly if γ is a ray in the global zig-zag fan Ξ, then $Zig(\gamma) \in \mathbb{Z}^{Q_1}$ (respectively $Zag(\gamma) \in \mathbb{Z}^{Q_1}$) is the function which evaluates to one on all zigs (zags) of every representative zig-zag path of γ, and is zero on all other arrows.

Remark 5.5.3. We see that

$$Zig(\gamma) = \sum_{\langle [\eta] \rangle = \gamma} Zig(\eta).$$

The functions defined in Definition 5.5.2, like perfect matchings, are functions which evaluate to one on each arrow in their support. Therefore they can be thought of as sets of arrows. We now show that $P(\sigma)$ is non-zero on the zigs or zags of certain zig-zag paths, in other words that these zigs or zags are contained in the set of arrows on which $P(\sigma)$ is supported. In the language of functions, this is equivalent to the following lemma.

Lemma 5.5.4. *Suppose σ is a cone in the global zig-zag fan Ξ spanned by rays γ^+ and γ^- (see diagram below). Then the functions $P(\sigma) - Zig(\gamma^+)$ and $P(\sigma) - Zag(\gamma^-)$ are elements of $\mathbb{N}^{Q_1}$.*

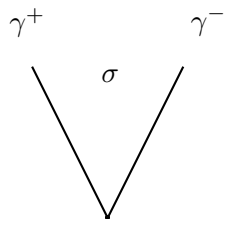

Proof. Let $f \in Q_2$ be any face. If γ^+ is not a ray in the local zig-zag fan $\xi(f)$, then by definition, no representative zig-zag flow intersects the boundary of f. Thus $Zig(\gamma^+)$ is zero on all the arrows in the boundary, and so $P(\sigma) - Zig(\gamma^+)$ is non-negative on these arrows.

If γ^+ is a ray in the local zig-zag fan $\xi(f)$, we consider the cone τ in $\xi(f)$ which is generated by γ^+ and the next ray around the fan in a clockwise direction (this is γ^- if and only if γ^- is a ray in $\xi(f)$). Since σ in the global zig-zag fan is generated by γ^+ and γ^- which is the next ray around in the clockwise direction, the image of σ under the map of fans lies in τ. Then by definition $P_f(\sigma)$, and therefore $P(\sigma)$, evaluates to 1 on the arrow in the boundary of f corresponding to the cone τ. This arrow is the intersection of the two zig-zag flows in $\mathcal{X}(f)$ corresponding the rays of τ. Since the anti-clockwise ray is γ^+, this arrow is the unique (by Lemmas 5.2.3 and 5.4.3) zig of the representative of γ^+ in the boundary of f. Therefore $P(\sigma) - Zig(\gamma^+)$ is non-negative on all the arrows in the boundary of f. The statement holds on the arrows in the boundary of all faces, and therefore in general. The result follows similarly for $P(\sigma) - Zag(\widetilde{\eta}_-)$. □

Corollary 5.5.5. *Suppose σ is a cone in Ξ spanned by rays γ^+ and γ^-. For any representative zig-zag paths η^+ of γ^+ and η^- of γ^-, the functions $P(\sigma) - Zig(\eta^+)$ and $P(\sigma) - Zag(\eta^-)$ are elements of $\mathbb{N}^{Q_1}$.*

Proof. This follows from the Lemma 5.5.4 together with Remark 5.5.3. □

5.6 The Extremal Perfect Matchings

We show that the perfect matchings we have just constructed are precisely the extremal perfect matchings of the dimer model (Definition 2.3.7).

We start by identifying an element of $M_o^{ef} \subset M_o^+$ associated to every ray γ of Ξ. We will prove that for each cone σ, the perfect matching $P(\sigma)$ evaluates to zero on two such elements which are linearly independent. Therefore the image of $P(\sigma)$ in N_o lies in a one dimensional facet of the cone N_o^+. In other words it is an extremal perfect matching.

Given a zig-zag flow, we defined its black and white boundary flows in Section 5.1. Recall that the image of a single period of a boundary path is a cycle in $\mathbb{N}_{Q_1}$.

Definition 5.6.1. The system of boundary paths $S(\gamma) \in \mathbb{N}_{Q_1}$ of a ray γ of Ξ, is the sum of all the cycles corresponding to the boundary paths (black and white) of every representative zig-zag path of γ.

Since $S(\gamma)$ is the sum of cycles it is closed and, as it is non-negative, it defines an element $[S(\gamma)]_M \in M_o^{ef} \subset M_o^+$. If σ is a two dimensional cone in Ξ spanned by rays γ^+ and γ^-, then the classes $[S(\gamma)]_M$ and $[S(\gamma)]_M$ are linearly independent: if they were not, then they would have linearly dependent homology classes (see the exact sequence (3.5.3)), however, by Lemma 5.1.1 we know that these classes are $-k^+[\eta^+]$ and $-k^-[\eta^-]$ which are linearly independent, where $k^\pm > 0$ is the number of boundary paths of $\gamma^\pm$, and $\eta^\pm$ is a representative zig-zag path of $\gamma^\pm$.

Proposition 5.6.2. *Suppose σ is a cone in Ξ spanned by rays γ^+ and γ^-. The perfect matching $P(\sigma) \in \mathbb{N}^{Q_1}$ is the unique perfect matching which evaluates to zero on the two systems of boundary paths $S(\gamma^+)$ and $S(\gamma^-)$.*

Proof. First we prove that $P(\sigma)$ evaluates to zero on the two systems of boundary paths. Let η be a representative zig-zag path of γ^+ or γ^-. Since $P(\sigma)$ is a perfect matching we know that it is non-zero on precisely one arrow in the boundary of every face. By construction, the boundary path of a zig-zag path was pieced together from paths back around faces which have a zig-zag or zag-zig pair in the boundary. By Corollary 5.5.5, $P(\sigma)$ is non-zero on either the zig or zag of η in the boundary of each

of these faces and therefore it is zero on all the arrows in the boundary path. This holds for all boundary paths of representative zig-zag paths of γ^+ or γ^-.

Now we prove that $P(\sigma)$ is the unique perfect matching which evaluates to zero on the two systems of boundary paths. Let $\widetilde{\eta}^+$ and $\widetilde{\eta}^-$ be representative zig-zag flows of γ^+ and γ^- respectively. Since they are not parallel or anti-parallel, the black boundary flows of $\widetilde{\eta}^+$ and $\widetilde{\eta}^-$ have at least one vertex in common. Let $v_{00} \in \widetilde{Q}_0$ be such a vertex and let v be its image in Q_0.

Let the finite path p_0^+ be the lift of a single period of the black boundary flow of η^+ to the universal cover, starting at v_{00} and ending at vertex v_{10}. Then let p_1^- be the lift of a single period of the black boundary flow of η^- starting at v_{10}. Similarly let p_0^- be the lift of a period of the black boundary flow of η^- starting at v_{00} and ending at v_{01}, and p_1^+ be the lift of a period of the black boundary flow of η^+ starting at v_{01}.

The paths $p_1 := p_0^+ p_1^-$ and $p_2 := p_0^- p_1^+$ have the same class $[p_1]_M = [p_2]_M$ in M. This follows trivially as $p_0^\pm$ and $p_1^\pm$ project down to the same paths in Q. This implies that both paths end at the same vertex; they have the same homology class, and start at the same vertex. Also recalling Section 3.5 we see that they are F-term equivalent.

Furthermore, since $p_0^\pm$ and $p_1^\pm$ are shifts of each other by deck transformations, i.e. by elements in the period lattice, we see that $p_1 p_2^{-1}$ forms the boundary of a region which certainly contains at least one fundamental domain of $\widetilde{Q}$. Therefore, for every face in Q, there is a lift f in $\widetilde{Q}$ such that the winding number, $\mathrm{Wind}_f(p_1 p_2^{-1}) \neq 0$.

Let $q_0 = p_1, q_1, \ldots, q_k = p_2$ be a sequence of paths such that q_i and q_{i+1} differ by a single F-term relation for $i = 0, \ldots, k-1$. Fix a face in Q, and let f be the lift to $\widetilde{Q}$ satisfying the winding number condition above. Then since

$$\mathrm{Wind}_f(p_1 p_2^{-1}) \neq 0 = \mathrm{Wind}_f(p_2 p_2^{-1})$$

there exists $i \in \{1, \ldots, k-1\}$ such that $\mathrm{Wind}_f(q_i p_2^{-1}) \neq \mathrm{Wind}_f(q_{i+1} p_2^{-1})$. As they differ by a single F-term relation we can write $q_i = \alpha_1 \epsilon_1 \alpha_2$ and $q_{i+1} = \alpha_1 \epsilon_2 \alpha_2$, where $\epsilon_1 a$ and $\epsilon_2 a$ are the boundaries of two faces $f_b, f_w \in \widetilde{Q}_2$ (one black, one white) which meet along the arrow a. Using properties of winding numbers,

$$\mathrm{Wind}_f(\epsilon_1 a) - \mathrm{Wind}_f(\epsilon_2 a) = \mathrm{Wind}_f(q_i p_2^{-1}) - \mathrm{Wind}_f(q_{i+1} p_2^{-1}) \neq 0$$

The winding number around f of the boundary of a face, is non-zero if and only if the face is f. Therefore either $f = f_b$ or $f = f_w$ so all the arrows in the boundary of f except a, lie in either q_i or q_{i+1}. Let $n \in N^+$ and suppose n evaluates to zero on the element of M^+ corresponding to the path p_1. Since they are F-term equivalent, $[p_1]_M = [q_i]_M = [q_{i+1}]_M$, so n evaluates to zero on $[q_i]_M$ and $[q_{i+1}]_M$. Using the

positivity, this implies that n evaluates to zero on every arrow in the image in Q of both q_i and q_{i+1}. In particular it evaluates to zero on all the arrows in the boundary of the image of f except a. This argument holds for any face, and thus n is non-zero on a unique arrow in the boundary of each face in Q.

Suppose there exist two perfect matchings π_1 and π_2 which evaluate to zero on the both systems of boundary flows. By construction $\pi_1 + \pi_2 \in N^+$ is zero on the path p_1 and therefore by the above argument, it is non-zero on a unique arrow in the boundary of each face. Since perfect matchings are degree 1 elements of N^+ this forces π_1 and π_2 to evaluate to the same value on all the arrows in the boundary of each face. We conclude that $\pi_1 = \pi_2$ and we have proved uniqueness. □

We have just proved that for each σ in the global zig-zag fan, the image of the perfect matching $P(\sigma)$ in N_o^+ evaluates to zero on two linearly independent classes in M_o^+. Thus the perfect matchings $P(\sigma)$, map to some set of extremal vertices of the degree 1 polygon in N_o^+. Furthermore these are the unique perfect matchings to map to any of these vertices. We now prove that every extremal vertex is the image of $P(\sigma)$ for some σ.

Recall from Section 2.3 that the cone N_o^+ is the intersection of N_o with the real cone $(N^+)_{\mathbb{R}}$ generated by the image of N^+ in $N_o \otimes_{\mathbb{Z}} \mathbb{R}$. We show that the images of $P(\sigma)$ in N_o^+, for all two dimensional cones σ of Ξ, generate $(N_o^+)_{\mathbb{R}}$. Therefore perfect matchings of the form $P(\sigma)$ map to generators of all the extremal rays of N_o^+, i.e. to all the extremal vertices of the degree 1 polygon in N_o^+. Together with the uniqueness property we saw above, this shows that the perfect matchings of the form $P(\sigma)$ are precisely the extremal perfect matchings.

Lemma 5.6.3. *The real cone $(N_o^+)_{\mathbb{R}}$ is generated over $\mathbb{R}^+$ by the images in N_o^+ of $P(\sigma)$ for all two dimensional cones σ of Ξ.*

Proof. Let $\mathcal{C}_N$ be the real cone in $N_o \otimes_{\mathbb{Z}} \mathbb{R}$ generated by the images of $P(\sigma)$ for all two dimensional cones σ of Ξ, and let $\mathcal{C}_M$ be the real cone in $M_o \otimes_{\mathbb{Z}} \mathbb{R}$ generated by $[S(\gamma)]_M$ for all rays γ of Ξ. We claim that $\mathcal{C}_M^\vee = \mathcal{C}_N$. Since $[P(\sigma)] \in N_o^+$, every element of M_o^+ evaluates to a non-negative number on this class. In particular $[P(\sigma)] \in \mathcal{C}_M^\vee$ for every two dimensional cone σ in Ξ, so $\mathcal{C}_N \subseteq \mathcal{C}_M^\vee$. For the converse, we restrict to the degree 1 plane in N_o. The functions $[S(\gamma)]_M$ restrict to affine linear functions on this plane which evaluate to zero on neighbouring points $[P(\sigma^+)]$ and $[P(\sigma^-)]$, where $\sigma^\pm$ are the two, 2-dimensional cones in Ξ containing ray γ, and are non-negative on all other points $[P(\sigma)]$. These functions define a collection of half planes whose intersection is the convex hull of the points [1]. Thus the cone over this intersection, namely $\mathcal{C}_M^\vee$ equals

[1] This 'obvious' fact is the justification for the 'gift wrapping algorithm' in two dimensions [21].

the cone over the convex hull, namely $\mathcal{C}_N$.

Finally, using the fact that $\mathcal{C}_M \subseteq (M_o^+)_{\mathbb{R}}$ where $(M_o^+)_{\mathbb{R}}$ is the real cone generated by M_o^+,

$$(N_o^+)_{\mathbb{R}} = (M_o^+)_{\mathbb{R}}^\vee \subseteq \mathcal{C}_M^\vee = \mathcal{C}_N$$

since we also know that $\mathcal{C}_N \subseteq (N_o^+)_{\mathbb{R}}$, the result follows. □

Remark 5.6.4. Thus, the real cone $(M_o^+)_{\mathbb{R}} = (N_o^+)_{\mathbb{R}}^\vee$ is dual to the real cone in $N_o \otimes_{\mathbb{Z}} \mathbb{R}$ generated by the images of perfect matchings of the form $P(\sigma)$ for σ of Ξ. We have also shown that the real cone $(N_o^+)_{\mathbb{R}}$ is dual to the real cone in $M_o \otimes_{\mathbb{Z}} \mathbb{R}$ generated by $[S(\gamma)]_M$ for all rays γ of Ξ, so $(M_o^+)_{\mathbb{R}}$ is generated by the classes $[S(\gamma)]_M$.

5.7 The External Perfect Matchings

We next see that given an extremal perfect matching constructed in the previous section, we can alter it along a zig-zag path in such a way that we still have a perfect matching. Furthermore the resulting perfect matchings still evaluate to zero on one of the two systems of boundary flows and are thus external.

Lemma 5.7.1. *If σ is a cone in the global zig-zag fan spanned by the rays γ^+ and γ^-, and η^+ and η^- are representative zig-zag paths, then $P(\sigma) - Zig(\eta^+) + Zag(\eta^+)$ and $P(\sigma) - Zag(\eta^-) + Zig(\eta^-)$ are perfect matchings.*

Proof. By Lemma 5.5.5 we know $P(\sigma) - Zig(\eta^+)$ and $P(\sigma) - Zag(\eta^-)$ are elements of $\mathbb{N}^{Q_1}$. Given any face $f \in Q_2$, its boundary either does not intersect η^+ or it intersects it in a zig and a zag (see Lemma 5.2.3 and Lemma 5.4.3). Recalling that the coboundary map adds up the function on the edges in the boundary of each face, we see that in either case $d(Zig(\eta^+) - Zag(\eta^+)) = 0$. Consequently we see that:

$$d(P(\sigma) - Zig(\eta^+) + Zag(\eta^+)) = d(P(\sigma)) = \underline{1}$$

so $P(\sigma) - Zig(\widetilde{\eta}^+) + Zag(\widetilde{\eta}^+)$ is a perfect matching. Similarly we can see that $P(\sigma) - Zag(\widetilde{\eta}^-) + Zig(\widetilde{\eta}^-)$ is a perfect matching. □

We will refer to such perfect matchings as those obtained by 'resonating' $P(\sigma)$ along η^+ and η^- respectively. By resonating along all representative zig-zag paths of a ray, we can go from one extremal perfect matching to another.

Lemma 5.7.2. *Let γ be any ray in the global zig-zag fan Ξ, and let σ^+ and σ^- be the two 2-dimensional cones containing γ (see diagram below). Then $P(\sigma^-) - Zig(\gamma) = P(\sigma^+) - Zag(\gamma)$.*

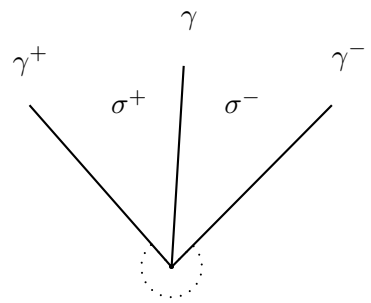

Proof. Let $f \in Q_2$ be any face. There are two cases which we consider separately. In the first case γ is a ray in the local zig-zag fan $\xi(f)$, i.e. there exists a representative zig-zag flow of γ intersecting the boundary of f. This intersection consists of a zig and a zag and therefore $d(Zig(\gamma))_f = d(Zag(\gamma))_f = 1$. Since $P(\sigma^-)$ and $P(\sigma^+)$ are perfect matchings, so are of degree 1, we note that

$$d(P(\sigma^-) - Zig(\gamma))_f = d(P(\sigma^+) - Zag(\gamma))_f = 0$$

and together with the fact that $P(\sigma^-) - Zig(\gamma), P(\sigma^+) - Zag(\gamma) \in \mathbb{N}^{Q_1}$, this implies that $P(\sigma^-) - Zig(\gamma)$ and $P(\sigma^+) - Zag(\gamma)$ are both zero on all arrows in the boundary of f.

In the second case, γ is not a ray in the local zig-zag fan $\xi(f)$. Then no representative zig-zag flow of γ intersects the boundary of f and so $Zig(\gamma)$ and $Zag(\gamma)$ both evaluate to zero on all arrows in the boundary. Furthermore, in this case we observe that the images of σ^+ and σ^- lie in the same cone in the local zig-zag fan $\xi(f)$, so $P_f(\sigma^-) = P_f(\sigma^+)$. Thus $P(\sigma^-) - Zig(\gamma)$ and $P(\sigma^+) - Zag(\gamma)$ are equal on all arrows in the boundary of f. The functions are equal on the boundary of all faces, and therefore are equal. □

Corollary 5.7.3. *The perfect matching $P(\sigma^-) = P(\sigma^+) - Zag(\gamma) + Zig(\gamma)$, i.e. $P(\sigma^-)$ can be obtained from $P(\sigma^+)$ by 'resonating' along all representative zig-zag flows of γ.*

We have seen that given an extremal perfect matching we can resonate along certain zig-zag paths. We now show that it is always possible to resonate along zig-zag paths in an external perfect matching.

Lemma 5.7.4. *Let π be any perfect matching which satisfies $\langle \pi, S(\gamma) \rangle = 0$ and let η be any representative zig-zag flow of γ. Then either $\pi - Zig(\eta) \in \mathbb{N}^{Q_1}$ or $\pi - Zag(\eta) \in \mathbb{N}^{Q_1}$.*

Proof. Using the fact that $\pi \in \mathbb{N}^{Q_1}$ and $S(\gamma) \in \mathbb{N}_{Q_1}$, we observe that $\langle \pi, S(\gamma) \rangle = 0$ if and only if $\langle \pi, a \rangle = 0$ for every arrow a in the black or white boundary path of any representative of γ. Let f_k be the black or white face with η_k and η_{k+1} in its boundary.

By construction, ever arrow in the boundary of this face except η_k and η_{k+1}, is in the boundary path of η. Therefore, the perfect matching π (which is of degree 1) must evaluate to 1 on either η_k or η_{k+1}, and to zero on all the other arrows in the boundary of f_k. Because this holds for each $k \in \mathbb{Z}$, we note that this forces π to evaluate to 1 either on all the zigs, or all the zags of $\widetilde{\eta}$. □

We now show that every external perfect matching, i.e. every perfect matching which evaluates to zero on some boundary flow can be obtained by resonating the extremal perfect matchings.

Proposition 5.7.5. *Every perfect matching π which satisfies $\langle \pi, S(\gamma) \rangle = 0$ is of the form:*

$$\pi = P(\sigma^+) - \sum_{\eta \in Z} (Zag(\eta) - Zig(\eta))$$

where Z is some set of zig-zag paths which are representatives of γ.

Proof. Let π be such a perfect matching. Let Z be the set of representative zig-zag paths η of γ for which $\pi - Zig(\eta) \in \mathbb{N}^{Q_1}$. We note that $\pi' := \pi + \sum_{\eta \in Z} (Zag(\eta) - Zig(\eta))$ is a perfect matching which satisfies $\langle \pi', S(\gamma) \rangle = 0$ and by Lemma 5.7.4 we see that $\pi' - Zag(\gamma) \in \mathbb{N}^{Q_1}$. Since

$$\pi = \pi' - \sum_{\eta \in Z} (Zag(\eta) - Zig(\eta))$$

it is sufficient to prove that any perfect matching which satisfies, $\langle \pi', S(\gamma) \rangle = 0$ and $\pi' - Zag(\gamma) \in \mathbb{N}^{Q_1}$ is equal to $P(\sigma^+)$. We will be show that if π' is such a perfect matching, then $\langle \pi', S(\gamma^+) \rangle = 0$. The result follows using the uniqueness part of Proposition 5.6.2.

Consider the elements $[\pi' - P(\sigma^+)]$ and $[P(\sigma^-) - P(\sigma^+)] \neq 0$ in $H^1(Q)$, embedded as the rank 2 sublattice of N_o consisting of degree zero elements (see equation 2.3.2). We note that the class $[S(\gamma)]_M \in M_o$ restricts to a linear map on $H^1(Q)$ which has $[\pi' - P(\sigma^+)]$ and $[P(\sigma^-) - P(\sigma^+)]$ in its kernel. The kernel is rank 1, so there exists $k \in \mathbb{Q}$ such that

$$[\pi' - P(\sigma^+)] = k[P(\sigma^-) - P(\sigma^+)]$$

We observe that $k \geq 0$ since $\langle P(\sigma^-), S(\gamma^+) \rangle > 0$ and

$$\begin{aligned} 0 \leq \langle \pi', S(\gamma^+) \rangle &= \langle [\pi' - P(\sigma^+)], [S(\gamma^+)]_M \rangle \\ &= k \langle [P(\sigma^-) - P(\sigma^+)], [S(\gamma^+)]_M \rangle \\ &= k \langle P(\sigma^-), S(\gamma^+) \rangle \end{aligned}$$

Then using Lemma 5.7.2 and the fact that $\pi' - Zag(\gamma) \in \mathbb{N}^{Q_1}$ we see that

$$\begin{aligned} 0 \geq -k\langle P(\sigma^+), S(\gamma^-)\rangle &= k\langle [P(\sigma^-) - P(\sigma^+)], [S(\gamma^-)]_M\rangle \\ &= \langle [\pi' - P(\sigma^+)], [S(\gamma^-)]_M\rangle \\ &= \langle [\pi' - P(\sigma^-) - Zag(\gamma) + Zig(\gamma)], [S(\gamma^-)]_M\rangle \\ &= \langle \pi' - Zag(\gamma) + Zig(\gamma), S(\gamma^-)\rangle \geq 0 \end{aligned}$$

so $k = 0$ and thus $\langle \pi', S(\gamma^+)\rangle = 0$.

□

Finally we see that resonating a perfect matching along different parallel zig-zag paths changes the class in N_o in the same way.

Lemma 5.7.6. *Let η, η' be representative zig-zag paths of γ. Then $Zag(\eta) - Zig(\eta) \in N$ and $Zag(\eta') - Zig(\eta') \in N$ project to the same class in N_o.*

Proof. First note that if η is any zig-zag path, then $Zag(\eta) - Zig(\eta) \in N$ and has degree zero: given any face, $\widetilde{\eta}$ either does not intersect the boundary in which case the function $Zag(\eta) - Zig(\eta)$ is non-zero on all arrows in the boundary, or it intersects in a pair of arrows one of which is a zig, and one a zag. In either case, the sum of $Zag(\eta) - Zig(\eta)$ on the arrows in the boundary is zero. Thus $Zag(\eta) - Zig(\eta)$ defines a class in $H^1(Q)$ considered as the degree zero sublattice of N_o.

Let η, η' be distinct representative zig-zag paths of γ. If η'' is any zig-zag path, then we observe that evaluating $Zag(\eta) - Zig(\eta)$ on η'' counts the number of intersections of η and η'', with signs depending on whether the intersecting arrow is a zig or zag of η''. Recalling Remark 3.3.6 we see that this is precisely the intersection number $[\eta''] \wedge [\eta]$. Therefore, since $[\eta'] = [\eta]$, the functions $Zag(\eta) - Zig(\eta)$ and $Zag(\eta') - Zig(\eta')$ evaluate to the same value on each zig-zag path. The classes of zig-zag paths span a full sublattice of $H_1(Q)$, and therefore $[Zag(\eta) - Zig(\eta)] = [Zag(\eta') - Zig(\eta')]$ in $H^1(Q)$ considered as the degree zero sublattice of N_o. □

Therefore the multiplicities of the external perfect matchings along the edge dual to $[S(\gamma)]_M$ are binomial coefficients $\binom{r}{n}$ given by choosing n zig-zag paths to resonate out of r, the total number of representative zig-zag paths of γ.

In [14] Gulotta describes the extremal and external perfect matchings for a 'properly ordered' dimer model in essentially the same way that we do. He also calculates their multiplicities. Recall from Remark 5.4.6 that a geometrically consistent dimer model is properly ordered. In [29] Stienstra also produces a correspondence between cones in

a fan and perfect matchings. At first sight this looks different to the construction in Section 5.5 but it is presumably closely related.

Remark 5.7.7. I conjecture that many of the results in this chapter can be proved in a similar way assuming only the weaker marginal geometric consistency.

Chapter 6

Geometric consistency implies algebraic consistency

In this chapter we prove the following main result.

Theorem 6.1. If a dimer model on a torus is geometrically consistent, then it is algebraically consistent.

Our proof will rely on the explicit description of extremal perfect matchings we gave in the previous chapter, together with the knowledge of their values on the boundary flows of certain zig-zag paths. We will actually prove the following proposition which we shall see in Section 6.1 implies the theorem.

Proposition 6.2. For all vertices $i, j \in \widetilde{Q}_0$ in the universal cover there exists a path from i to j on which some extremal perfect matching evaluates to zero.

Thus we see that the extremal perfect matchings play a key role in the theory.

6.1 Proving algebraic consistency

Recall that a dimer model is algebraically consistent if the algebra map $\hbar : A \longrightarrow \mathbb{C}[\underline{M}^+]$ (4.4.1) from the path algebra of the quiver modulo F-term relations to the toric algebra, is an isomorphism. We noted in Remark 4.4.3 that for a geometrically consistent dimer model injectivity is equivalent to the statement of Theorem 3.5.2. It therefore remains for us to prove that the map $\hbar$ is surjective.

Lemma 6.1.1. *If there exists a path on the universal cover $\widetilde{Q}$ from $\widetilde{i}$ to $\widetilde{j}$, which is zero on a perfect matching, for all $\widetilde{i}, \widetilde{j} \in \widetilde{Q}_0$, then the map $\hbar : A \longrightarrow \mathbb{C}[\underline{M}^+]$ is surjective.*

Proof. To prove surjectivity, we need to show that for $i, j \in Q_0$ and any element $m \in M_{ij}^+$ there exists a representative path, that is, a path p from i to j in Q such that $[p]_M = m$.

First we prove that it is sufficient to show that there exists a representative path for elements of M_{ij}^+ which lie on the boundary of the cone M^+. Recall that the cone M^+ is the dual cone of the cone N^+ which is integrally generated by the perfect matchings. Therefore the elements in the boundary of M^+, are precisely those which evaluate to zero on some perfect matching.

Suppose that there exists a representative path for all elements $m \in M_{ij}^+$ which lie on the boundary of M^+. Recall that the coboundary map $d\colon \mathbb{Z}^{Q_1} \longrightarrow \mathbb{Z}^{Q_2}$ sums the function on the edges around each face and $d(\pi) = \underline{1}$ for any perfect matching π. Thus if p is a path going once around the boundary of any quiver face $f \in Q_2$ (starting at any vertex of f) and π is a perfect matching, then $\langle \pi, p \rangle = 1$. Define $\square := [p]_M$ to be the image of p in M which we note is independent of the choice of p since the 2-torus is connected. Now let $i, j \in Q_0$ and consider any element $m \in M_{ij}^+$. If we evaluate any perfect matching π on m by definition we get an non-negative integer. Let

$$n := \min\{\langle \pi, m \rangle \mid \pi \text{ is a perfect matching } \}$$

Then for each perfect matching π, we observe that $\langle \pi, (m - n\square) \rangle = \langle \pi, m \rangle - n \geq 0$ and by construction there exists at least one perfect matching where the equality holds. In other words $(m - n\square)$ lies in the boundary of M^+. Then by assumption, there is a representative path q of $m - n\square$, from i to j in Q.

Finally we construct a representative path for m. Let f be any face which has j as a vertex, and let $p^{(n)}$ be the path which starts at j and goes n times around the boundary of f. Then the path $qp^{(n)}$ from i to j is a well defined path, and

$$[qp^{(n)}]_M = [q]_M + n[p]_M = (m - n\square) + n\square = m$$

Now we prove that if there exists a path on the universal cover $\widetilde{Q}$ from $\widetilde{i}$ to $\widetilde{j}$, which is zero on a perfect matching, for all $\widetilde{i}, \widetilde{j} \in \widetilde{Q}_0$, then there exists a representative path for all elements $m \in M_{ij}^+$ which lie on the boundary of M^+.

We start by fixing $i, j \in Q_0$, and let $m \in M_{ij}^+$ be an element in the boundary of M^+. Then some perfect matching π_m evaluates to zero on m. Recall the short exact sequence (2.3.2)

$$0 \longrightarrow \mathbb{Z} \longrightarrow M_o \xrightarrow{H} H_1(T; \mathbb{Z}) \longrightarrow 0$$

where the kernel of H is spanned by the class $\square = \partial[f]_M$ for any face $f \in Q_2$. Fix

some path p from $\widetilde{j} \in \widetilde{Q}_0$ to $\widetilde{i} \in \widetilde{Q}_0$ where $\widetilde{i}$ and $\widetilde{j}$ project down to i and j respectively. Since there is a path from $\widetilde{i}$ to every lift of j in the universal cover, there exists a path q which is zero on some perfect matching, such that pq projects down to a closed path with any given homology class. In particular, there exists a path q which is zero on some perfect matching π_p and has

$$H([p]_M + [q]_M) = H([pq]_M) = H([p]_M + m)$$

Therefore $[q]_M - m \in M_o$ is in the kernel of H, and so $[q]_M - m = k\square$ in M_o, for some $k \in \mathbb{Z}$. Since every perfect matching evaluates to 1 on $\square$, applying π_m and π_p to $[q]_M - m$, we see that

$$-\langle \pi_q, m \rangle = k = \langle \pi_m, [q]_M \rangle$$

Finally, since m and $[q]_M$ are both in M^+, we see that $k = 0$ and so $[q]_M = m$ in M_o. $\square$

Using this lemma we see that Proposition 6.2 implies Theorem 6.1. We shall prove Proposition 6.2 in Section 6.3.

6.2 Flows which pass between two vertices

We fix two vertices i, j of the universal cover of the quiver $\widetilde{Q}$. In this section we study the zig-zag flows which pass between i and j, i.e. they have i and j on opposite sides. These are important as they are the flows that intersect every path from i to j. We will see that the classes of these flows generate two convex cones in $H_1(Q) \otimes_{\mathbb{Z}} \mathbb{R}$. These will be used in proof of Proposition 6.2 in the next section.

We define the two sets of zig-zag flows which pass between i and j as follows:

$$\mathcal{X}_+ := \{\widetilde{\eta} \mid \widetilde{\eta} \text{ has } i \text{ on the left and } j \text{ on the right}\}$$

$$\mathcal{X}_- := \{\widetilde{\eta} \mid \widetilde{\eta} \text{ has } i \text{ on the right and } j \text{ on the left}\}$$

First we show that there always exist flows which pass between distinct vertices:

Lemma 6.2.1. *If $i, j \in \widetilde{Q}_0$ are distinct vertices then $\mathcal{X}_+$ and $\mathcal{X}_-$ are non-empty.*

Proof. We consider the collection of black faces which have i as a vertex. We are interested in zig-zag flows which intersect the boundary of one or more of these faces and have i on the left. Any zig-zag pair in the boundary of one of these faces defines such a flow if and only if i is not the head of the zig. Let p be any path from j to a vertex v_0 contained in one of these flows, say $\widetilde{\eta}$. We may assume that v_0 is the first

such vertex in p, so p doesn't intersect any of the flows. Since $\widetilde{\eta}$ intersects the boundary of one of the black faces, there is a path p' along $\widetilde{\eta}$ from v_0 to v_1, a vertex of one of the black faces. We may also assume that this is the first such vertex along p', so p' does not intersect the boundary of any of the black faces in an arrow; this implies that $v_1 \neq i$. We note that v_1 is the head of a zig $\widetilde{\eta}'_0$ of a zig-zag pair in the boundary of one of the black faces. Since $v_1 \neq i$ this defines a zig-zag flow $\widetilde{\eta}'$ which has i on the left.

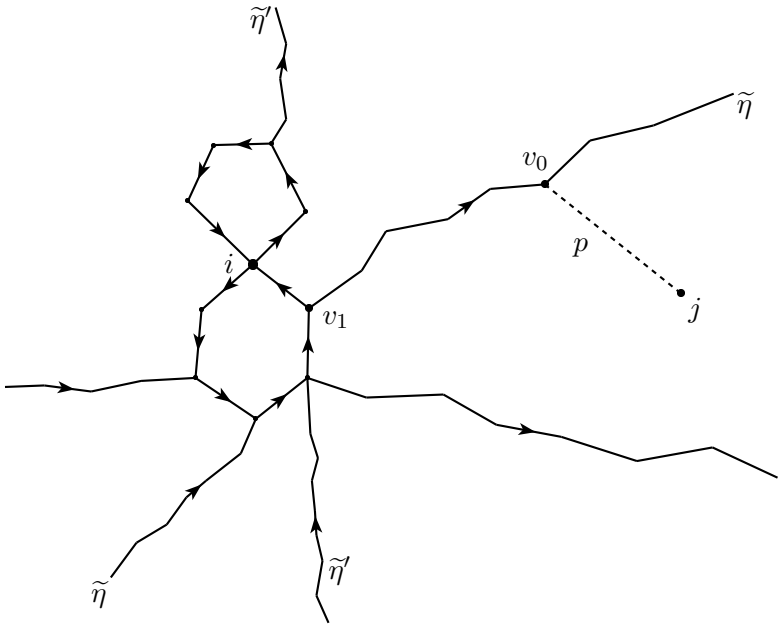

By construction, the flows $\widetilde{\eta}'$ and $\widetilde{\eta}$ intersect in either $\widetilde{\eta}'_0$ or $\widetilde{\eta}'_1$. Since this intersection is unique, $\widetilde{\eta}'$ doesn't intersect p' in an arrow. Since $\widetilde{\eta}'$ doesn't intersect p, the path pp' from j to the head of a zig of $\widetilde{\eta}'$ doesn't intersect $\widetilde{\eta}'$. Therefore j is on the right of $\widetilde{\eta}'$. □

Lemma 6.2.2. *If $\widetilde{\eta}$ and $\widetilde{\eta}'$ are parallel zig-zag flows which pass between i and j then they are both in $\mathcal{X}_+$ or both in $\mathcal{X}_-$. If $\widetilde{\eta}$ and $\widetilde{\eta}'$ are anti-parallel zig-zag flows which pass between i and j then one is in $\mathcal{X}_+$ and the other is in $\mathcal{X}_-$.*

Proof. We prove the parallel case, the anti-parallel case follows using a similar argument. Without loss of generality, suppose that $\widetilde{\eta} \in \mathcal{X}_+$. Then there is a path from i to a vertex v of $\widetilde{\eta}$ which does not intersect $\widetilde{\eta}$. In particular all vertices of this path are also on the left of $\widetilde{\eta}$. If $\widetilde{\eta}'$ is on the right of $\widetilde{\eta}$ then this path does not intersect $\widetilde{\eta}'$, and so i is on the left of $\widetilde{\eta}'$.

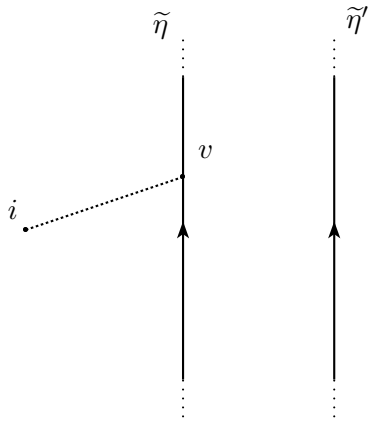

Since we assume that $\widetilde{\eta}'$ passes between i and j, we conclude that $\widetilde{\eta}' \in \mathcal{X}_+$. If $\widetilde{\eta}'$ is on the left of $\widetilde{\eta}$ then a symmetric argument works considering j instead of i. □

Consider two zig-zag flows $\widetilde{\eta}, \widetilde{\eta}'$ which are in $\mathcal{X}_+$. We see by Lemma 6.2.2 that they are not anti-parallel, and therefore their homology classes $[\widetilde{\eta}], [\widetilde{\eta}']$ generate a strongly convex cone in $H_1(Q) \otimes_{\mathbb{Z}} \mathbb{R}$. We now prove that no zig-zag flow in $\mathcal{X}_-$ has a homology class which lies in this cone.

Lemma 6.2.3. *Let $\widetilde{\eta}, \widetilde{\eta}' \in \mathcal{X}_+$ and denote the rays in $H_1(Q) \otimes_{\mathbb{Z}} \mathbb{R}$ generated by their respective homology classes by γ and γ'. Suppose that $\widetilde{\eta}''$ is a zig-zag path which passes between i and j. If $[\widetilde{\eta}''] \in H_1(Q)$ is in the cone spanned by γ and γ', then $\widetilde{\eta}'' \in \mathcal{X}_+$.*

Proof. We first note that if $[\widetilde{\eta}'']$ equals $[\widetilde{\eta}]$ or $[\widetilde{\eta}']$ then the result follows from Lemma 6.2.2.

Otherwise suppose that γ, γ' and γ'' are all distinct. Without loss of generality we assume that $\widetilde{\eta}'$ crosses $\widetilde{\eta}$ from right to left. Then since $[\widetilde{\eta}'']$ is in the cone spanned by γ and γ', we note that $\widetilde{\eta}''$ crosses $\widetilde{\eta}$ from right to left, and $\widetilde{\eta}'$ from left to right. Therefore $\widetilde{\eta}''$ intersects $\widetilde{\eta}$ in a zig $\widetilde{\eta}''_k$ and intersects $\widetilde{\eta}'$ in a zag $\widetilde{\eta}''_n$. Suppose $k < n$; the result for $k > n$ follows by a symmetric argument.

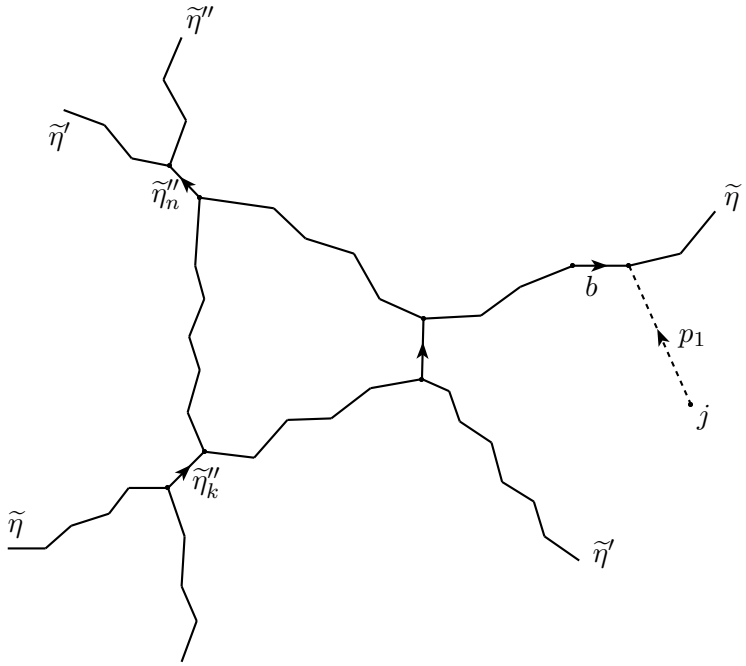

Take any (possibly unoriented) path p_1 from j to the head of some zig b of $\widetilde{\eta}$ which intersects neither $\widetilde{\eta}$ nor $\widetilde{\eta}'$. Such a path exists: since j is on the right of $\widetilde{\eta}$ there is a path from j to the head of a zig which does not intersect $\widetilde{\eta}$. If this path intersects $\widetilde{\eta}'$ we consider instead the path up to but not including the first arrow in the intersection, followed by part of the boundary flow of $\widetilde{\eta}'$.

We observe that p_1 does not intersect $\widetilde{\eta}''$ since all the vertices along it are on the right of both $\widetilde{\eta}$ and $\widetilde{\eta}'$, while all the vertices of $\widetilde{\eta}''$ are on the left of either $\widetilde{\eta}_1$ or $\widetilde{\eta}_2$ (using the fact that $k < n$, so $\widetilde{\eta}$ crosses $\widetilde{\eta}_1$ from right to left before it crosses $\widetilde{\eta}_2$ from left to right). The arrow $\widetilde{\eta}''_k$ occurs before b in $\widetilde{\eta}$, since $h\widetilde{\eta}''_k$ is on the left and hb is on the right of $\widetilde{\eta}'$.

Therefore the path p_2 along $\widetilde{\eta}$ from $h\widetilde{\eta}''_k$ to hb does not contain $\widetilde{\eta}''_k$ and so does not intersect $\widetilde{\eta}''$. Finally we see that the path $p_2 p_1^{-1}$ is a path from the head of a zig of $\widetilde{\eta}''$ to j which doesn't intersect $\widetilde{\eta}''$, so j is on the right of $\widetilde{\eta}$. If $\widetilde{\eta}''$ passes between i and j then it also has i on the left, and we are done. □

We now consider the cones generated by homology classes of flows in $\mathcal{X}_+$ and $\mathcal{X}_-$.

Definition 6.2.4. Let C_+ (resp. C_-) be the cone in $H_1(Q) \otimes_{\mathbb{Z}} \mathbb{R}$ generated by the homology classes $[\widetilde{\eta}]$ of zig-zag flows $\widetilde{\eta} \in \mathcal{X}_+$ (respectively $\widetilde{\eta} \in \mathcal{X}_-$).

We note that C_+ and C_- are non-empty by Lemma 6.2.1. If any set of rays corresponding to zig-zag flows $\widetilde{\eta} \in \mathcal{X}_+$ is not contained in some half-plane, then every

point in $H_1(Q) \otimes_{\mathbb{Z}} \mathbb{R}$ is in the cone generated by a pair of these rays. However using Lemma 6.2.3, this would then imply that C_- is empty. Therefore C_+ is contained in a some half-plane. Furthermore, by Lemma 6.2.2 we see that C_+ can not contain both rays in the boundary of this half-plane, as they are anti-parallel. Therefore C_+ is a strongly convex cone. Similarly we see that C_- is a strongly convex cone. Furthermore we note that the intersection $C_+ \cap C_- = \{0\}$. There exists a line ℓ separating C_+ and C_- which must pass through the origin. It can be chosen such that the origin is its only point of intersection with C_+ or C_-, or in fact with any ray in the global zig-zag fan. We choose such an ℓ, and let $\mathcal{H}_+$ and $\mathcal{H}_-$ be the corresponding closed half spaces containing C_+ and C_- respectively.

We consider the 2-dimensional cone σ in the global zig-zag fan which intersects the line ℓ, and lies between the clockwise boundary ray of C_+ and the anti-clockwise boundary ray of C_-. This cone σ may intersect C_+ or C_- in a ray, but is not contained in either. The diagram below shows the cones C_+ and C_-, and a possible choice of ℓ and σ.

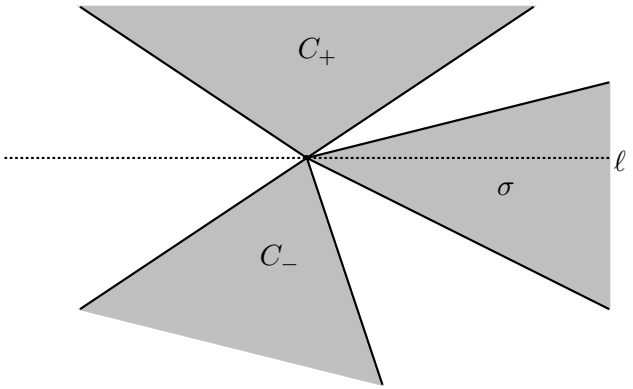

We denote the anti-clockwise and clockwise rays of σ by σ^+ and σ^- respectively. Using polar coordinates, any ray may be described by an angle in the range $(-\pi, \pi]$, where $\ell \cap \sigma$ has angle zero. Let $\alpha^+ \in (0, \pi)$ and $\alpha^- \in (-\pi, 0)$ be the angles of σ^+ and σ^- respectively.

6.3 Proof of Proposition 6.2

Finally we come to the proof of Proposition 6.2 which we showed was sufficient in order to prove Theorem 6.1.

6.3.1 Overview of proof

Fix two vertices i, j of the universal cover of the quiver $\widetilde{Q}$. We will construct a path from j to i which is zero on the extremal perfect matching $P(\sigma)$ where σ is the choice of cone in the global zig-zag fan made at the end of the previous section. First we use an iterative procedure to construct a different path p, ending at i, from pieces of the boundary flows of a sequence zig-zag flows. These zig-zag flows all have vertices i and j on the left, and satisfy a minimality condition which will allow us to prove, using results from Chapter 5, that $P(\sigma)$ evaluates to zero on p.

Similarly we construct a path q ending at i, from boundary flows of zig-zag flows which have i and j on the right. We will see that $P(\sigma)$ also evaluates to zero on q. The paths p and q intersect at some vertex $v \neq i$, and we are interested in the parts $p^{(\leq n)}$ and $q^{(\leq k)}$ of p and q respectively which go from v to i. We prove that they are F-term equivalent and observe that either $p^{(\leq n)}$ or $q^{(\leq k)}$ pass through j, or the closed path $p^{(\leq n)}(q^{(\leq k)})^{-1}$ has a non-zero winding number around j. In this case, we show that there exists an F-term equivalent path which passes through j. Since it is F-term equivalent, $P(\sigma)$ also evaluates to zero on this path. By taking the piece of this path from j to i we have the required path.

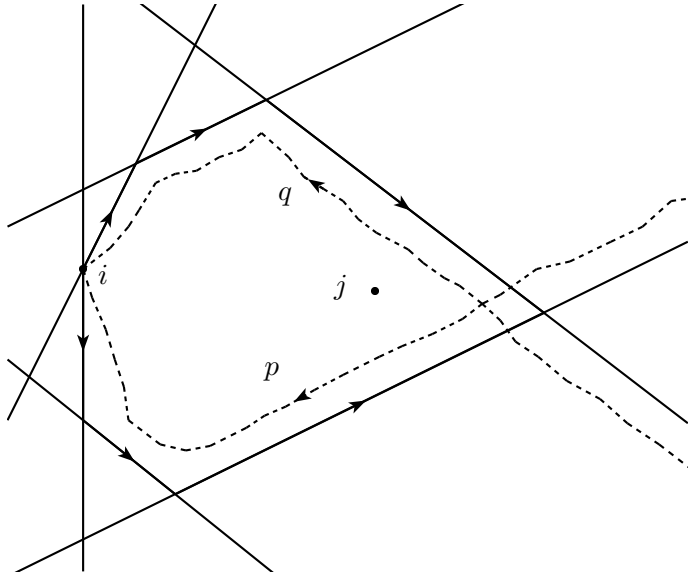

6.3.2 The starting point

In this section we find the first zig-zag flow in our sequence. This must have the property that its black boundary flow passes through i. Therefore we start by considering the black faces which have i as a vertex, and look at all the zig-zag flows which intersect the boundary of these faces.

Lemma 6.3.1. *There exists a zig-zag flow which has the following properties:*

1. *It has vertices i and j on the left,*
2. *It intersects the boundary of a black face which has i as a vertex,*
3. *The corresponding ray in Ξ has angle, measured with respect to ℓ, in the interval $(-\pi, 0]$.*

Proof. Consider the set of black faces which have i as a vertex, and let $\mathcal{Y}(i)$ be the set of zig-zag flows which intersect the boundary of one or more of these faces and have i on the left. If $\widetilde{\eta} \in \mathcal{Y}(i)$ then it intersects the boundary of the black face f in a zig-zag pair $(\widetilde{\eta}_0, \widetilde{\eta}_1)$. Without loss of generality we may assume that $t\widetilde{\eta}_0 \neq i$; otherwise we can consider instead the zig-zag pair $(\widetilde{\eta}_{-2}, \widetilde{\eta}_{-1})$ which is in the boundary of a black face which patently has i as a vertex, and $t\widetilde{\eta}_{-2} \neq i$ since in a geometrically consistent dimer model there are no quiver faces with just two arrows.

Arrow $\widetilde{\eta}_0 = \widetilde{\eta}'_1$ is the zag of another zig-zag flow $\widetilde{\eta}'$ which has i on its left. By Lemma 5.4.5 we see that the rays γ and γ' corresponding to $\widetilde{\eta}$ and $\widetilde{\eta}'$ respectively, span a convex cone in the local zig-zag fan $\xi(f)$ with γ' the clockwise ray. Thus for any ray in Ξ corresponding to a flow in $\mathcal{Y}(i)$, there is a ray of such a flow at an angle less than π in a clockwise direction. In particular, there is a ray γ corresponding to some zig-zag flow $\widetilde{\eta} \in \mathcal{Y}(i)$, whose angle is in the interval $(-\pi, 0)$, so γ lies in $\mathcal{H}_-$. We note that $\widetilde{\eta}$ satisfies properties 2 and 3, and claim that it satisfies 1 as well. If $\widetilde{\eta}$ had j on the right then by definition, γ would be in C_+, however the intersection of C_+ with $\mathcal{H}_-$ is just the origin, which gives a contradiction. □

Finally in this section we define for any face $f \in Q_2$

$$\mathcal{Z}(f) := \{\widetilde{\eta} \mid \widetilde{\eta} \text{ intersects the boundary of } f \text{ and has } i, j \text{ on left}\}$$

By Lemma 6.3.1 there exists a face f, which has i as a vertex, and where $\mathcal{Z}(f)$ is non-empty. We fix such a face, which we label $f^{(1)}$ and let $v^{(0)} := i$.

6.3.3 A sequence of faces

We construct a sequence of black faces $\{f^{(n)}\}_{n=1}^{\infty}$ and vertices $\{v^{(n)}\}_{n=0}^{\infty}$ with the property that for each $n \in \mathbb{N}^+$, the vertex $v^{(n)}$ is contained in the boundary of $f^{(n)}$ and $f^{(n+1)}$. We do this inductively as follows:
Suppose we have a black face $f^{(n)}$ with a known vertex $v^{(n-1)}$, for which $\mathcal{Z}(f^{(n)})$ is non-empty. Looking at the zig-zag flows in $\mathcal{Z}(f^{(n)})$, let $\widetilde{\eta}^{(n)}$ be the one with the maximum angle $\theta^{(n)}$ in the interval $(-\pi, \alpha^+]$. This zig-zag flow intersects the boundary of $f^{(n)}$ in a zig-zag pair $(\widetilde{\eta}^{(n)}_{2n}, \widetilde{\eta}^{(n)}_{2n+1})$. We look at the next zig-zag pair $(\widetilde{\eta}^{(n)}_{2n+2}, \widetilde{\eta}^{(n)}_{2n+3})$

which lies in the boundary of a black face which we denote by $f^{(n+1)}$. Note that the vertex $v^{(n)} := h\widetilde{\eta}^{(n)}_{2n+1}$ is contained in the boundaries of both $f^{(n)}$ and $f^{(n+1)}$. Furthermore, $\widetilde{\eta}^{(n)}$ has i and j on the left and intersects the boundary of $f^{(n+1)}$, so $\mathcal{Z}(f^{(n+1)})$ is non-empty.

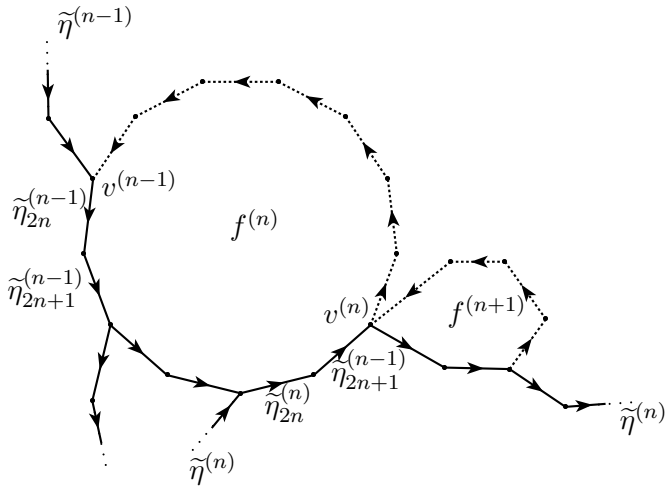

The maximality condition and Lemma 6.3.1 imply that

$$-\pi < \theta^{(n)} \leq \theta^{(n+1)} \leq \alpha^{+} \tag{6.3.1}$$

for all $n \in \mathbb{N}^{+}$. Since by Lemma 5.4.3 there is at most a unique representative zig-zag flow of any ray which intersects the boundary of a face, we note that zig-zag flows $\widetilde{\eta}^{(n)} = \widetilde{\eta}^{(n+1)}$ if and only if $\theta^{(n)} = \theta^{(n+1)}$. In particular if $\theta^{(n_0)} = \alpha^{+}$ then $\widetilde{\eta}^{(n)} = \widetilde{\eta}^{(n_0)}$ for all $n \geq n_0$.

Remark 6.3.2. We observe that if $n \neq k$ then $f^{(n)} \neq f^{(k)}$, otherwise the local zig-zag fans at $f^{(n)}$ and $f^{(k)}$ are the same so $\theta^{(n)} = \theta^{(k)}$. This implies that $\widetilde{\eta}^{(n)} = \widetilde{\eta}^{(k)}$, and so $\widetilde{\eta}^{(n)}_{2n}$ and $\widetilde{\eta}^{(n)}_{2k}$ are both arrows in the boundary of $f^{(n)}$. However this would contradict geometric consistency (in particular either Proposition 3.3.7 or Lemma 5.2.3).

6.3.4 The paths p and $\widehat{p}$

We now construct two paths by piecing together paths around the boundaries of these black faces. For each $n \in \mathbb{N}^{+}$ define $p^{(n)}$ to be the shortest oriented path around the boundary of $f^{(n)}$ from $v^{(n)}$ to $v^{(n-1)}$ and let $\widehat{p}^{(n)}$ to be the shortest oriented path around the boundary of $f^{(n)}$ from $v^{(n-1)}$ to $v^{(n)}$.

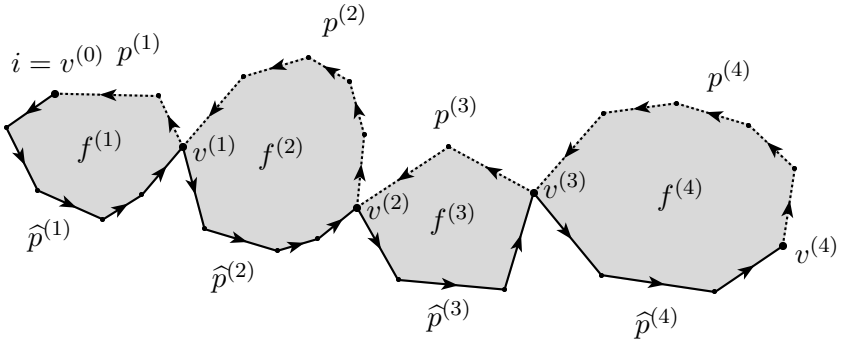

Since $hp^{(n)} = v^{(n-1)} = tp^{(n-1)}$ we can piece the paths $p^{(n)}$ together to form an infinite oriented path p which ends at $v_0 = i$. Similarly we can piece the paths $\widehat{p}^{(n)}$ together to form an infinite oriented path $\widehat{p}$ which starts at $v_0 = i$.

Remark 6.3.3. Using the property (see Remark 5.4.6) that the intersections of zig-zag flows with the boundary of face f occur in the same cyclic order as the rays of the local zig-zag fan $\xi(f)$, we note that the arrows in $\widehat{p}^{(n)}$ are the arrows in the boundary of $f^{(n)}$ which are contained in zig-zag flows with angle in the closed interval $[\theta^{(n-1)}, \theta^{(n)}]$. If $\theta^{(n-1)} = \theta^{(n)}$, then $\widehat{p}^{(n)}$ just contains the zig-zag pair $\widetilde{\eta}^{(n)}_{2n}, \widetilde{\eta}^{(n)}_{2n+1}$ and $p^{(n)}$ is the intersection of the black boundary flow of $\widetilde{\eta}^{(n)}$ with the boundary of $f^{(n)}$.

Now that we have constructed the paths p and $\widehat{p}$ we check that they satisfy some properties. Most importantly we need to show that the perfect matching $P(\sigma)$ evaluates to zero on p. Recalling the definition of $P(\sigma)$, we are interested in the image of the cone σ in the local zig-zag fan at each face. We prove the following lemma:

Lemma 6.3.4. *There are no rays in the local zig-zag fan $\xi(f^{(n)})$ with angle in the interval $(\theta^{(n)}, 0]$ for any $n \in \mathbb{N}^+$.*

Proof. Suppose to the contrary that this doesn't hold and let n' be the least value where such a ray exists. We label this ray by γ and suppose the intersection of its representative zig-zag flow with the boundary of $f^{(n')}$ is the zig-zag pair $(\widetilde{\eta}_0, \widetilde{\eta}_1)$. Denote the angle of ray γ by $\theta \in (\theta^{(n')}, 0]$. We observe that:

- The maximality condition in the construction ensures that $\widetilde{\eta}$ can not have both i and j on its left.
- If $\widetilde{\eta}$ had i on its left and j on its right then γ would be in C_+. However since $\theta \in (\theta^{(n')}, 0]$ we see that γ lies in $\mathcal{H}_-$ which would be a contradiction.

Therefore $\widetilde{\eta}$ must have i on its right. Consider the path $p^{(n'-1)}p^{(n'-2)}\dots p^{(1)}$ from $v^{(n'-1)}$ to i. Since n' is minimal, $\widetilde{\eta}$ does not intersect the boundary of any of the faces $f^{(1)},\dots,f^{(n'-1)}$. In particular it does not intersect this path. Therefore $v_{n'-1}$ is also on the right of $\widetilde{\eta}$. Since $f^{(n')}$ is a black face, all its vertices are on the left of $\widetilde{\eta}$ except for $h\widetilde{\eta}_0 = t\widetilde{\eta}_1$, so $v_{n'-1} = t\widetilde{\eta}_1$.

Recalling the construction of the sequence of faces $f^{(n)}$, we see that arrow $\widetilde{\eta}_1$ is a zig of $\widetilde{\eta}^{(n'-1)}$. Therefore $\widetilde{\eta}$ crosses $\widetilde{\eta}_{n'-1}$ from left to right and, by Lemma 5.4.5, the corresponding rays in the local zig-zag fan span a cone where γ is the clockwise ray. Then

$$-2\pi < \theta^{(n'-1)} - \pi < \theta < \theta^{(n'-1)} \leq \theta^{(n')}$$

However, this contradicts the assumption that $\theta \in (\theta^{(n')}, 0]$. □

We now use this lemma to prove the first property we required of the path p.

Lemma 6.3.5. *The perfect matching $P(\sigma)$ evaluates to zero on the path p.*

Proof. The path p was constructed locally of paths $p^{(n)}$ in the boundary of the faces $f^{(n)}$. The perfect matching $P(\sigma)$ was also defined locally at each face. Therefore it is sufficient to prove the statement locally; we must show that $P_{f^{(n)}}(\sigma)$ evaluates to zero on $p^{(n)}$ for each $n \geq 1$.

We recall that $P_{f^{(n)}}(\sigma)$ is non-zero on a single arrow, corresponding to the cone in $\xi(f^{(n)})$ which contains the image of σ. We split the proof into two cases:

If $\theta^{(n)} \neq \alpha^+$, it follows from Lemma 6.3.4 that $\gamma^{(n)}$ is the clockwise ray of the cone containing the image of σ. Then using Lemma 5.4.5, the unique arrow on which $P_{f^{(n)}}(\sigma)$ is non-zero is the zag $\widetilde{\eta}^{(n)}_{2n+1}$ in the boundary of $f^{(n)}$. By construction $h\widetilde{\eta}^{(n)}_{2n+1} = v^{(n)}$ and thus any oriented path around the boundary of $f^{(n)}$ from $v^{(n)}$, which contains this arrow, must contain a complete cycle. Each $p^{(n)}$ was defined so that this is not the case, so $P_{f_n}(\sigma)$ evaluates to zero on p_n.

If $\theta^{(n)} = \alpha^+$ then $\gamma^{(n)}$ is the image of σ^+ and $p^{(n)}$ is part of the boundary flow of $\widetilde{\eta}^{(n)}$, a representative of σ^+. By Proposition 5.6.2 we see that $P(\sigma)$ evaluates to zero on this.

□

We now show that $\widehat{p}$ is made up of sections of zig-zag flows that have the vertices i and j on their left.

Lemma 6.3.6. *Each arrow in $\widehat{p}^{(n)}$ is contained in some zig-zag flow which has i and j on the left.*

Proof. If an arrow of $\widehat{p}^{(n)}$ is in $\widetilde{\eta}^{(n-1)}$ or $\widetilde{\eta}^{(n)}$, then we are done. Otherwise the arrow is contained in a zig-zag flow $\widetilde{\eta}$ with angle in the open interval $(\theta^{(n-1)}, \theta^{(n)})$. We note that $\widetilde{\eta}$ has $v^{(n-1)}$ on its left, otherwise one obtains a contradiction in the same way as the end of the proof of Lemma 6.3.4. Using Lemma 6.3.4 directly, we see that $\widetilde{\eta}$ does not intersect the boundary of $f^{(r)}$ for any $r \leq n-1$. Therefore considering a path along the boundary of these faces, we see that $\widetilde{\eta}$ has i on its left. Because of its angle, $\widetilde{\eta}$ can not be in $\mathcal{X}_+$, and therefore it must have both i and j on the left. □

Finally in this section we see that sufficiently far away from its starting point, the path $\widehat{p}$ looks like a representative zig-zag flow of σ^+.

Lemma 6.3.7. *There exists $n' \in \mathbb{N}^+$ such that for all $n \geq n'$ we have $\widetilde{\eta}^{(n)} = \widetilde{\eta}^{+}$ which is a representative zig-zag flow of σ^+.*

Proof. Since the increasing sequence $\{\theta^{(n)}\}$ is bounded above, and there are a finite number of rays in Ξ, there exists some $n' \in \mathbb{N}^+$ such that $\theta^{(n)} = \theta^{(n')}$, and therefore $\widetilde{\eta}^{(n)} = \widetilde{\eta}^{(n')}$, for all $n \geq n'$. Thus it is sufficient to prove that $\widetilde{\eta}^{(n')}$ is a representative zig-zag flow of σ^+.

Suppose it is not. Then $\widetilde{\eta}^{(n')}$ intersects every representative zig-zag flows of σ^+ from left to right, and an infinite number of these intersections must occur after $v^{(n')}$ in $\widetilde{\eta}^{(n')}$ (so $v^{(n')}$ is on their left). The path $p^{(n')}p^{(n'-1)}\dots p^{(1)}$ from $v^{(n')}$ to i has a finite number of arrows and therefore intersects at most a finite number of these. Therefore there are an infinite number of representative zig-zag flows of σ^+ which intersect $\widetilde{\eta}^{(n')}$ after $v^{(n')}$, so intersect the boundary of $f^{(n)}$ for some $n \geq n'$, and have i on their left. Only a finite number of zig-zag flows have i on their left and j on their right; such a flow must intersect every path from i to j. Thus there exists a representative zig-zag flows of σ^+ which intersects the boundary of $f^{(n)}$ for some $n \geq n'$, and has i and j on its left. This contradicts the maximality assumption. □

In an analogous way to the construction of p and $\widehat{p}$, we construct a paths q and $\widehat{q}$ by piecing together sequences of paths $q^{(k)}$ and $\widehat{q}^{(k)}$ respectively, around the boundaries of a sequence of white faces $\{g^{(k)}\}$ with a distinguished set of vertices $\{w^{(k)}\}$. This is constructed by considering zig-zag flows $\widetilde{\beta}^{(k)}$ which have both i and j on the right and whose ray in the global zig-zag fan has minimal angle $\varpi^{(k)}$ which lies in the interval $[-\alpha^-, \pi)$. Certain corresponding properties hold, which can be proved by symmetric arguments:

1. The path q ends at the vertex i.
2. The perfect matching $P(\sigma)$ evaluates to zero on q.
3. Each arrow in $\widehat{q}^{(n)}$ is contained in some zig-zag flow which has i and j on the right.

4. There exists $k' \in \mathbb{N}^+$ such that for all $k \geq k'$ we have $\widetilde{\beta}^{(k)} = \widetilde{\beta}^-$ which is a representative zig-zag flow of σ^-.

6.3.5 p and q intersect

We now find a vertex (other than i) which is in both p and q. This will be a vertex of the zig-zag paths $\widetilde{\eta}^+$ and $\widetilde{\beta}^-$.

Lemma 6.3.8. *Let n' and k' be be the least integers such that $\widetilde{\eta}^{(n')} = \widetilde{\eta}^+$ and $\widetilde{\beta}^{(k')} = \widetilde{\beta}^-$. Then $\widetilde{\beta}^-$ does not intersect the boundary of $f^{(n)}$ for any $n \leq n'$ and $\widetilde{\eta}^+$ does not intersect the boundary of $g^{(k)}$ for any $k \leq k'$.*

Proof. First consider the case when $n < n'$ so $\theta^{(n)} \leq \alpha^-$. If $\theta_n = \alpha^-$ then $\widetilde{\eta}^{(n)}$ and $\widetilde{\beta}^-$ are parallel zig-zag flows which are distinct; i is on the left of $\widetilde{\eta}^{(n)}$ but on the right of $\widetilde{\beta}^-$. By definition $\widetilde{\eta}^{(n)}$ intersects the boundary of $f^{(n)}$, so by Lemma 5.4.3, $\widetilde{\beta}^-$ does not. If $\theta_n < \alpha^-$ then by Lemma 6.3.4 there are no rays of $\xi(f^{(n)})$ with angle in the interval $(\theta_n, 0)$ and therefore $\widetilde{\beta}^-$ does not intersect the boundary of $f^{(n)}$.

Now consider the case when $n = n'$. We have just shown that $\widetilde{\beta}_-$ does not intersect the path $p^{(n'-1)}p^{(n'-2)}\dots p^{(1)}$ from $v_{n'-1}$ to i. Therefore $v_{n'-1}$ is on the right of $\widetilde{\beta}_-$. As we have noted before, since it is a black face, there is only one zig-zag flow which intersects the boundary of $f^{(n')}$ and has $v^{(n'-1)}$ on the right. However, this crosses $\widetilde{\eta}^{(n'-1)}$ from left to right and so can not be $\widetilde{\beta}_-$ since $-\pi < \theta_{n'-1} \leq \alpha^- < 0$. Therefore $\widetilde{\beta}_-$ does not intersect the boundary of $f_{n'}$.

The proof of the other statement follows similarly. □

Corollary 6.3.9. *Let $a = \widetilde{\eta}^+_{2n} = \widetilde{\beta}^-_{2k+1}$ be the unique arrow where $\widetilde{\beta}^-$ and $\widetilde{\eta}^+$ intersect. Then ta occurs after $v^{(n')}$ in $\widetilde{\eta}^+$ and after $w^{(k')}$ in $\widetilde{\beta}^-$.*

Proof. Using the lemma we see that $\widetilde{\beta}^-$ does not intersect the path $p^{(n')}p^{(n'-1)}\dots p^{(1)}$ from $v^{(n'-1)}$ to i. Therefore $v^{(n')}$ is on the right of $\widetilde{\beta}_-$. We know that $\widetilde{\beta}_-$ crosses $\widetilde{\eta}_+$ from right to left, so $v_{n'}$ occurs in $\widetilde{\eta}_+$ before the intersection. □

Using this result we see that the paths p and q both contain the vertex ta: the arrow $a = \widetilde{\eta}^+_{2n}$ is a zig of $\widetilde{\eta}_+$ and by Corollary 6.3.9 we know that ta occurs after $v_{n'}$ in $\widetilde{\eta}_+$. Therefore $ta = v^{(n)}$ for some $n > n'$, and by construction $v^{(n)}$ is a vertex of p. Similarly we note that $ta = w^{(k)}$ for some $k > k'$ and so ta is a vertex of q.

We define paths $p^{(\leq n)} := p^{(n)}p^{(n-1)}\dots p^{(1)}$ and $q^{(\leq k)} := q^{(k)}q^{(k-1)}\dots q^{(1)}$ from ta to i. These are finite pieces of the paths p and q respectively. We note that since $P(\sigma)$ evaluates to zero on p and q, it must also evaluate to zero on $p^{(\leq n)}$ and $q^{(\leq k)}$.

Similarly we may define paths $\widehat{p}^{(\leq n)} := \widehat{p}^{(n)}\widehat{p}^{(n-1)}\dots\widehat{p}^{(1)}$ and $\widehat{q}^{(\leq k)} := \widehat{q}^{(k)}\widehat{q}^{(k-1)}\dots\widehat{q}^{(1)}$ from i to ta.

6.3.6 The path from j to i

We want to be able to use F-term relations on the path $p^{(\leq n)}$ to change it into a path which passes through the vertex j. We start by showing that the paths $p^{(\leq n)}$ and $q^{(\leq k)}$ are F-term equivalent.

Lemma 6.3.10. *The elements $[p^{(\leq n)}]_M$ and $[q^{(\leq k)}]_M$ are equal, i.e. the paths $p^{(\leq n)}$ and $q^{(\leq k)}$ are homologous.*

Proof. Recall the short exact sequence (2.3.2):

$$0 \longrightarrow \mathbb{Z} \longrightarrow M_o \xrightarrow{H} H_1(T;\mathbb{Z}) \longrightarrow 0$$

where the kernel of H is spanned by the class $\square = \partial[f]_M$ for any face $f \in Q_2$. Since $p^{(\leq n)}$ and $q^{(\leq k)}$ start and finish at the same vertices in the universal cover $\widetilde{Q}$, the element $[p^{(\leq n)}]_M - [q^{(\leq k)}]_M \in M_o$ is in the kernel of H. Therefore it is some multiple of class $\square$. The perfect matching $P(\sigma)$, by definition, evaluates to 1 on the boundary of every face, and therefore it evaluates to 1 on $\square$. Since it evaluates to zero on $[p^{(\leq n)}]_M - [q^{(\leq k)}]_M$, we conclude that this multiple of $\square$ is zero, and so $[p^{(\leq n)}]_M = [q^{(\leq k)}]_M$. $\square$

Consider the paths $\widehat{p}^{(\leq n)}$ and $\widehat{q}^{(\leq k)}$. These are constructed out of sections of zig-zag flows which have the vertex j on the left and right respectively. Then the path $\widehat{p}^{(\leq n)}(\widehat{q}^{(\leq k)})^{-1}$ is constructed of sections of zig-zag flows that have j consistently on the left. Thus this path either passes through j or has a non-zero winding number around j. We note that the 'boundary path' $p^{(\leq n)}(q^{(\leq k)})^{-1}$ has the same property. If j is a vertex of $\widehat{p}^{(\leq n)}(\widehat{q}^{(\leq k)})^{-1}$ then it is a vertex of one of the faces $f^{(r)}$ or $g^{(s)}$. Neighbouring zig-zag flows in the boundary of this face which pass through j, have j on different sides. This forces j to be one of the distinguished vertices on the face, and so it is a vertex of $p^{(\leq n)}(q^{(\leq k)})^{-1}$ as well. Finally, since the boundary of a face either contains a vertex, or has zero winding number about that vertex, we note that either $p^{(\leq n)}(q^{(\leq k)})^{-1}$ passes through j or the winding number of $p^{(\leq n)}(q^{(\leq k)})^{-1}$ around j is non-zero.

To complete the proof of Proposition 6.2, it is sufficient to show that there exists a path which is F-term equivalent to $p^{(\leq n)}$ and $q^{(\leq k)}$, and which passes through vertex j. F-term equivalence implies that $P(\sigma)$ evaluates to zero on this path as well, and we obtain the required path from j to i by looking at the appropriate piece.

Lemma 6.3.11. *Suppose p, q are F-term equivalent oriented paths in $\widetilde{Q}$ from vertex v_1 to v_2, which do not pass through vertex v. If $\mathrm{Wind}_v(pq^{-1})$ is non-zero, then there exists an oriented path p' which is F-term equivalent to p and q and passes through v.*

Proof. Since p and q are F-term equivalent, there exists a sequence of paths $p_0 = p, p_1, \ldots, p_{s'} = q$ such that p_s and p_{s+1} differ by a single F-term relation for $s = 0, \ldots, s' - 1$.

Suppose that neither $p_s q^{-1}$ nor $p_{s+1} q^{-1}$ pass through v for some $s \in \{0, \ldots, s' - 1\}$, i.e. $\mathrm{Wind}_v(p_s q^{-1})$ and $\mathrm{Wind}_v(p_{s+1} q^{-1})$ are well defined. Since p_s and p_{s+1} differ by a single F-term relation we can write $p_s = \alpha_1 r_s \alpha_2$ and $p_{s+1} = \alpha_1 r_{s+1} \alpha_2$, where $r_s {r_{s+1}}^{-1}$ is the boundary of the union D of the two faces which meet along the arrow dual to the relation. Since $\mathrm{Wind}_v(p_s q^{-1})$ and $\mathrm{Wind}_v(p_{s+1} q^{-1})$ are well defined, then

$$\mathrm{Wind}_v(p_s q^{-1}) - \mathrm{Wind}_v(p_{s+1} q^{-1}) = \mathrm{Wind}_v(p_s {p_{s+1}}^{-1}) = \mathrm{Wind}_v(r_s {r_{s+1}}^{-1}) = 0$$

as there are no vertices in the interior of D. However

$$\mathrm{Wind}_v(p q^{-1}) \neq 0 = \mathrm{Wind}_v(q q^{-1})$$

and so there must exist $s \in \{0, \ldots, s' - 1\}$ such that $p_s q^{-1}$ passes through v. Then $p' := p_s$ is F-term equivalent to p and q and passes through v.

□

Chapter 7

Calabi-Yau Algebras from Algebraically Consistent dimers

In this chapter we prove one of the main theorems of this thesis:

Theorem 7.1. If a dimer model on a torus is algebraically consistent then the algebra A obtained from it is CY3.

This gives a whole class of superpotential algebras which are Calabi-Yau and which can be written down explicitly. We start by recalling Ginzburg's definition of a Calabi-Yau algebra [13]. A theorem due to Ginzburg shows that superpotential algebras are CY3 if a particular sequence of maps gives a bimodule resolution of the algebra. We formulate this for algebras coming from dimer models and show that, because they are graded, it is sufficient to prove that a one sided complex of right A modules is exact. We then prove that this is the case for algebras obtained from algebraically consistent dimer models.

7.1 Calabi-Yau Algebras

The notion of a Calabi-Yau algebra we use here was introduced by Ginzburg in [13]. Consider the contravariant functor $M \mapsto M^! := \mathrm{RHom}_{A-Bimod}(M, A \otimes A)$ on the 'perfect' derived category of bounded complexes of finitely generated projective A-bimodules. We use the outer bimodule structure on $A \otimes A$ when taking RHom and the result $M^!$ is an A-bimodule using the inner structure.

Definition 7.1.1. An algebra A is said to be a Calabi-Yau algebra of dimension $d \geq 1$ if it is homologically smooth, and there exists an A-module quasi-isomorphism

$$f : A \xrightarrow{\cong} A^![d] \quad \text{such that} \quad f = f^![d]$$

In [13] Ginzburg gives a way of proving that superpotential algebras are CY3 by checking that a particular sequence of maps is a resolution of the algebra. He gives an explicit description of this sequence of maps which we follow here.

Let Q be a finite quiver with path algebra $\mathbb{C}Q$. As in Section 2.1.3, let $[\mathbb{C}Q, \mathbb{C}Q]$ be the complex vector space in $\mathbb{C}Q$ spanned by commutators and denote by $\mathbb{C}Q_{\text{cyc}} := \mathbb{C}Q/[\mathbb{C}Q, \mathbb{C}Q]$ the quotient space. This space has a basis of elements corresponding to cyclic paths in the quiver. For each arrow $a \in Q_1$ there is a linear map

$$\frac{\partial}{\partial x_a} : \mathbb{C}Q_{\text{cyc}} \to \mathbb{C}Q$$

which is a (formal) cyclic derivative. The image of a cyclic path is obtained by taking all the representatives of the path in $\mathbb{C}Q$ which starts with x_a, removing this and then summing. We can write this map in a different way using a formal left derivative $\frac{\partial_l}{\partial_l x_a} : \mathbb{C}Q \to \mathbb{C}Q$ defined as follows:
Every monomial is of the form $x_b x$ for some $b \in Q_1$. Then we define:

$$\frac{\partial_l}{\partial_l x_a} x_b x := \begin{cases} x & \text{if } a = b, \\ 0 & \text{otherwise.} \end{cases}$$

We extend this to the whole of $\mathbb{C}Q$ by linearity. The formal right derivative $\frac{\partial_r}{\partial_r x_a}$ is defined similarly. Then we have

$$\frac{\partial}{\partial x_a}(x) = \sum_{\substack{x' \in \mathbb{C}Q \\ (x')=(x)}} \frac{\partial_l}{\partial_l x_a} x' = \sum_{\substack{x' \in \mathbb{C}Q \\ (x')=(x)}} \frac{\partial_r}{\partial_r x_a} x' \tag{7.1.1}$$

where as before (x) denotes the cyclic element in $\mathbb{C}Q_{\text{cyc}}$ corresponding to $x \in \mathbb{C}Q$.

For each arrow $a \in Q_1$ there is another linear map which we denote by:

$$\frac{\partial}{\partial x_a} : \mathbb{C}Q \to \mathbb{C}Q \otimes \mathbb{C}Q \qquad x \mapsto \left(\frac{\partial x}{\partial x_a}\right)' \otimes \left(\frac{\partial x}{\partial x_a}\right)''$$

This is defined on monomials as follows: for each occurrence of x_a in a monomial, the monomial can be written in the form $x x_a y$. This defines an element $x \otimes y \in \mathbb{C}Q \otimes \mathbb{C}Q$ and the sum of these elements over each occurrence of x_a in the monomial is the image of the monomial. We extend this linearly for general elements of $\mathbb{C}Q$. Following Ginzburg we use the same notation for both the cyclic derivative and this map.

The algebra $S := \bigoplus_{i \in Q_0} \mathbb{C}e_i$ is semi-simple and is the sub-algebra of $\mathbb{C}Q$ generated by paths of length zero. We define $T_1 := \bigoplus_{b \in Q_1} \mathbb{C}x_b$ with the natural structure of an S, S-bimodule. For each arrow $b \in Q_1$, there is a relation $R_b := \frac{\partial}{\partial x_b} W$ which is the

cyclic derivative of the superpotential W. Let $T_2 := \bigoplus_{b \in Q_1} \mathbb{C}R_b$ be the S, S-bimodule generated by these. For each vertex $v \in Q_0$, we obtain from the super-potential W a syzygy

$$W_v := \sum_{b \in T_v} x_b R_b = \sum_{b \in H_v} R_b x_b$$

Finally we define $T_3 := \bigoplus_{v \in Q_0} \mathbb{C}W_v$ which is isomorphic to S and has an S, S-bimodule structure. We consider the following maps:

$$\mu_0 : A \otimes_S A \longrightarrow A \qquad x \otimes y \mapsto xy$$

is given by the multiplication in A.

$$\begin{aligned} \mu_1 :& A \otimes_S T_1 \otimes_S A \longrightarrow A \otimes_S A \\ & x \otimes x_a \otimes y \ \mapsto x x_a \otimes y - x \otimes x_a y \end{aligned}$$

$$\begin{aligned} \mu_2 :& A \otimes_S T_2 \otimes_S A \longrightarrow A \otimes_S T_1 \otimes_S A \\ & x \otimes R_a \otimes y \ \mapsto \sum_{b \in Q_1} x \left(\frac{\partial R_a}{\partial x_b} \right)' \otimes x_b \otimes \left(\frac{\partial R_a}{\partial x_b} \right)'' y \end{aligned}$$

$$\begin{aligned} \mu_3 :& A \otimes_S T_3 \otimes_S A \longrightarrow A \otimes_S T_2 \otimes_S A \\ & x \otimes W_v \otimes y \ \mapsto \sum_{b \in T_v} x x_b \otimes R_b \otimes y - \sum_{b \in H_v} x \otimes R_b \otimes x_b y \end{aligned}$$

Piecing these maps together we can write down the following sequence of maps:

$$0 \longleftarrow A \xleftarrow{\mu_0} A \otimes_S A \xleftarrow{\mu_1} A \otimes_S T_1 \otimes_S A \xleftarrow{\mu_2} A \otimes_S T_2 \otimes_S A \xleftarrow{\mu_3} A \otimes_S T_3 \otimes_S A \longleftarrow 0 \quad (7.1.2)$$

which is the complex in Proposition 5.1.9 of [13]. Then Corollary 5.3.3 of [13] includes the following result:

Theorem 7.1.2. *A is a Calabi-Yau algebra of dimension 3 if and only if the complex (7.1.2) is a resolution of A.*

Remark 7.1.3. It is not actually necessary to check that the complex is exact everywhere as the first part of it is always exact. By Theorem 5.3.1 of [13] we see that it is sufficient to check exactness at $A \otimes_S T_2 \otimes_S A$ and $A \otimes_S T_3 \otimes_S A$.

7.2 The one sided complex

Recall from Section 2.3 that any element in the interior of the perfect matching cone N^+ defines a (positive) $\mathbb{Z}$-grading of A. We define the graded radical of A by $\operatorname{Rad} A := \bigoplus_{n\geq 1} A^{(n)}$ and note that $S = A^{(0)}$ where $A^{(n)}$ denotes the nth graded piece. Algebra S is also the quotient of A by the graded radical, and we can use the quotient map $A \to A/\operatorname{Rad} A \cong S$ to consider S as an A, A-bimodule. Using this bimodule structure we consider the functor $\mathcal{F} = S \otimes_A -$ from the category of A, A-bimodules to itself. We apply this to the complex (7.1.2) and get the following complex:

$$0 \longleftarrow S \xleftarrow{\mathcal{F}(\mu_0)} A \xleftarrow{\mathcal{F}(\mu_1)} T_1 \otimes_S A \xleftarrow{\mathcal{F}(\mu_2)} T_2 \otimes_S A \xleftarrow{\mathcal{F}(\mu_3)} T_3 \otimes_S A \longleftarrow 0 \tag{7.2.1}$$

We usually forget the left A-module structure, and treat this as a complex of right A-modules. We call this the one sided complex. The maps are:

$$\begin{aligned} \mathcal{F}(\mu_1) : & T_1 \otimes_S A \longrightarrow A \\ & x_a \otimes y \ \mapsto -x_a y \end{aligned}$$

$$\begin{aligned} \mathcal{F}(\mu_2) : & T_2 \otimes_S A \longrightarrow T_1 \otimes_S A \\ & R_a \otimes y \ \mapsto \sum_{b \in Q_1} x_b \otimes \left(\frac{\partial_l R_a}{\partial_l x_b} \right) y \end{aligned}$$

$$\begin{aligned} \mathcal{F}(\mu_3) : & T_3 \otimes_S A \longrightarrow T_2 \otimes_S A \\ & W_v \otimes y \ \mapsto - \sum_{b \in H_v} R_b \otimes x_b y \end{aligned}$$

Something stronger is actually true. There is a natural transformation of functors from the identity functor on the category of A, A-bimodules to $\mathcal{F}$. In particular we have the following commutative diagram, where $\alpha : t \mapsto 1_S \otimes_A t$.

$$\begin{array}{ccccccccc} A & \xleftarrow{\mu_0} & A \otimes_S A & \xleftarrow{\mu_1} & A \otimes_S T_1 \otimes_S A & \xleftarrow{\mu_2} & A \otimes_S T_2 \otimes_S A & \xleftarrow{\mu_3} & A \otimes_S T_3 \otimes_S A \\ \downarrow{\scriptstyle \alpha} & & \downarrow{\scriptstyle \alpha} & & \downarrow{\scriptstyle \alpha} & & \downarrow{\scriptstyle \alpha} & & \downarrow{\scriptstyle \alpha} \\ S & \xleftarrow{\mathcal{F}(\mu_0)} & A & \xleftarrow{\mathcal{F}(\mu_1)} & T_1 \otimes_S A & \xleftarrow{\mathcal{F}(\mu_2)} & T_2 \otimes_S A & \xleftarrow{\mathcal{F}(\mu_3)} & T_3 \otimes_S A \end{array}$$

We define a grading on all the objects in this diagram. Since the super-potential W is a homogeneous element of $\mathbb{C}Q$, it can be seen that the syzygies $\{W_v \mid v \in Q_0\}$

are homogeneous elements, and furthermore the relations $\{R_a \mid a \in Q_1\}$ are also homogeneous. Therefore we can extend the grading to a grading of $A \otimes_S T_\bullet \otimes_S A$ where the grade of a product of homogeneous elements is given by the sum of the grades in each of the three positions. We call this the total grading of $A \otimes_S T_\bullet \otimes_S A$. Similarly we can define a total grading of $T_\bullet \otimes_S A$. We note that the maps μ, $\mathcal{F}(\mu)$ and α in the commutative diagram above all respect the total grading.

Finally, using the diagram, we show that $\mathcal{F}(\mu)$ is the 'leading term' of μ. For any $u \in T_\bullet \otimes_S A$, we note that

$$\mu_\bullet : 1 \otimes u \mapsto 1 \otimes v + \sum x \otimes w$$

for some $v, w \in T_{\bullet-1} \otimes_S A$ and $x \in \operatorname{Rad} A$. Then

$$v = \alpha(\mu_\bullet(1 \otimes u)) = \mathcal{F}(\mu_\bullet)(\alpha(1 \otimes u)) = \mathcal{F}(\mu_\bullet)(u)$$

Using the fact that $\mu_\bullet$ is an A, A-bimodule map we see that for $y \in A$:

$$\mu_\bullet : y \otimes u \mapsto y \otimes \mathcal{F}(\mu_\bullet)(u) + \sum yx \otimes w \tag{7.2.2}$$

for some $w \in T_{\bullet-1} \otimes_S A$ and $x \in \operatorname{Rad} A$.

Proposition 7.2.1. *The full complex 7.1.2 is exact if and only if the one-sided complex 7.2.1 is exact.*

Proof. First we suppose the one-sided complex is exact and prove that the full complex is exact. Since the total grading is respected by all the maps we need only look at the dth graded pieces of each space. Let $\phi_0 \in (A \otimes_S T_n \otimes_S A)^{(d)}$ be closed with respect to μ, where $n \in \{0, 1, 2, 3\}$ and $T_0 = S$. We can write ϕ_0 in the form

$$\sum_{y \in Y} y \otimes u_y + \{\text{terms with higher grade in the first position}\}$$

where Y is a linearly independent set of monomials in the graded piece $A^{(d_0)}$ with least possible grade, and $u_y \in (T_n \otimes_S A)^{(d-d_0)}$.

Applying the differential μ and using (7.2.2), we see that closedness translates into the condition:

$$0 = \sum_y y \otimes \mathcal{F}(\mu)(u_y) + \{\text{terms with higher grade in the first position}\}$$

Since the monomials $y \in Y$ are linearly independent this implies that for all $y \in Y$

$$\mathcal{F}(\mu)(u_y) = 0$$

Using the exactness of the one-sided complex, we conclude that there exist elements $v_y \in (T_{n+1} \otimes_S A)^{(d-d_0)}$ (where $T_4 := 0$) such that $\mathcal{F}(\mu)(v_y) = u_y$ for each $y \in Y$. We construct an element:

$$\psi_1 := \sum_{y \in Y} y \otimes v_y \in (A \otimes_S T_{n+1} \otimes_S A)^{(d)}$$

and apply the differential μ to get

$$\mu\psi_1 = \sum_{y \in Y} y \otimes u_y + \{\text{terms with higher grade in the first position}\}$$

We observe that $\phi_1 := \phi_0 - \mu\psi_1$ is in the kernel of μ and has been constructed such that its terms have strictly higher grade in the first position than ϕ_0. We iterate the procedure, noting that the grade in the first position is strictly increasing but is bounded above by the total grade d. Therefore after a finite number of iterations we must get $\phi_r = \phi_0 - \sum_{i=1}^{r} \mu\psi_i = 0$. We conclude that $\phi_0 = \mu(\sum_{i=1}^{r} \psi_i)$ and the complex is exact at $A \otimes_S T_n \otimes_S A$.

Conversely, we note that full complex 7.1.2 is a projective A, A-bimodule resolution of A, and that A itself has the structure of a projective left A module. Therefore it is an exact sequence of projective left modules and so is split exact. As a consequence it remains exact when we tensor with S on the left, i.e. when we apply the functor $\mathcal{F}$.

□

7.3 Key Lemma

The following lemma is going to play an important part in the proof of the main theorem. We recall from Section 3.5 that the lattice M is a quotient of $\mathbb{Z}_{Q_1}$ and that the boundary map we get by considering the quiver as a cellular decomposition of the torus, descends to a well defined map $\partial : M \to \mathbb{Z}_{Q_0}$. Furthermore, by summing the arrows, every path p in Q determines a class $[p]_M \in M$, which lies in $M_{ij} = \partial^{-1}(j - i)$ where $tp = i$ and $hp = j$.

Lemma 7.3.1. *Let $v, j \in Q_0$ be quiver vertices, and consider an element $m \in M_{vj}$. Suppose that for all arrows $b \in Q_1$ with $hb = v$, we have $m + [b]_M \in M_{ij}^+$ where $i = tb$. Then $m \in M_{vj}^+$.*

Proof. We consider the vertex v, and label the outgoing arrows $a_1, \ldots, a_k$ and the incoming arrows $b_1, \ldots, b_k$ around v as below. We also label the paths completing the boundary of each face p_i and q_i as below.

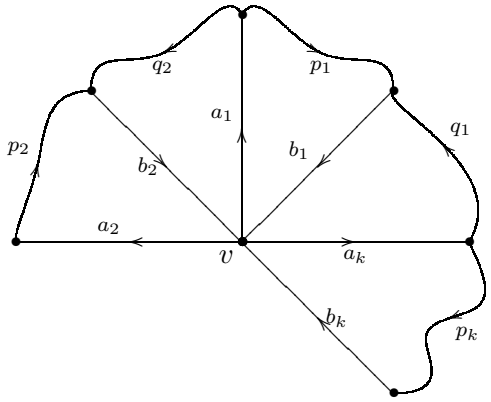

(7.3.1)

Let $m_i := m + [b_i]_M \in M^+_{tb_ij}$. We start by noting that $p_i b_i = q_{i+1} b_{i+1}$ is the F-term relation dual to a_i, so $[p_i]_M + [b_i]_M = [q_{i+1}]_M + [b_{i+1}]_M$ in M. Adding m to both sides we see that:

$$m_i + [p_i]_M = m_{i+1} + [q_{i+1}]_M \tag{7.3.2}$$

Since $m_i \in M^+_{tb_ij}$, using algebraic consistency, there exist paths y_i such that $[y_i]_M = m_i$ for all i. We lift each path y_i to a path in the universal cover $\widetilde{Q}$. From equation (7.3.2), again using algebraic consistency, we observe that the two paths $p_i y_i$ and $q_{i+1} y_{i+1}$ are F-term equivalent.

We seek a path σ which is F-term equivalent to $p_\alpha y_\alpha$ for some $\alpha \in \{1, \ldots, k\}$, and which passes through the vertex v. Either there exists some α such that y_α passes through v, in which case we define $\sigma := p_\alpha y_\alpha$, or we can consider the closed curves $\gamma_i := y_i^{-1} p_i^{-1} q_{i+1} y_{i+1}$ which have well defined winding numbers $\mathrm{Wind}_v(\gamma_i)$ around v for all i. In this case

$$\sum_{i=1}^{k} |\operatorname{Wind}_v(\gamma_i)| \geq |\operatorname{Wind}_v(\gamma_1 \ldots \gamma_k)| = |\operatorname{Wind}_v(p_1^{-1} q_2 \ldots p_k^{-1} q_1)| = 1$$

since the path $p_1^{-1} q_2 \ldots p_k^{-1} q_1$ is the boundary of the union of all faces containing v, which is homeomorphic to a disc in the plane with v an interior point. Therefore there exists $\alpha \in \{1, \ldots, k\}$ such that $\mathrm{Wind}_v(\gamma_\alpha)$ is well defined and nonzero. Thus we may apply Corollary 6.3.11 to the paths $p_\alpha y_\alpha$ and $q_{\alpha+1} y_{\alpha+1}$ and we obtain an F-term equivalent oriented path σ which passes through v.

To prove the result we need to show that $\langle \pi, m \rangle \geq 0$ for every perfect matching π.

Let π be a perfect matching and suppose that $\langle \pi, [b_i]_M \rangle = 0$ for some i. Then

$$\langle \pi, m \rangle = \langle \pi, m_i - [b_i]_M \rangle = \langle \pi, m_i \rangle \geq 0$$

since $m_i \in M^+$, and we are done. Otherwise $\langle \pi, [b_i]_M \rangle = 1$ for all $i = 1, \ldots, k$. Since the path σ passes through v then by construction it must contain an arrow b_i for some i, and

$$\langle \pi, [\sigma]_M \rangle \geq \langle \pi, [b_i]_M \rangle = 1 \tag{7.3.3}$$

Since σ and $p_\alpha y_\alpha$ are F-term equivalent,

$$[\sigma]_M = [p_\alpha y_\alpha]_M = [p_\alpha]_M + [b_\alpha]_M + m \tag{7.3.4}$$

Now $p_\alpha b_\alpha a_\alpha$ is the boundary of a face in the quiver, so perfect matching π is non-zero on a single arrow of $p_\alpha b_\alpha a_\alpha$. We know that $\langle \pi, [b_\alpha]_M \rangle = 1$, so $\langle \pi, [p_\alpha]_M \rangle = 0$. We apply our perfect matching π to (7.3.4) and use (7.3.3) to see that

$$1 \leq \langle \pi, [\sigma]_M \rangle = 1 + \langle \pi, m \rangle$$

Thus we have shown that $\langle \pi, m \rangle \geq 0$ as required. □

7.4 The main result

We are now in the position to prove the main theorem of this chapter.

Theorem 7.4.1. *If we have an algebraically consistent dimer model on a torus then the sequence of maps*

$$T_1 \otimes_S A \xleftarrow{\mathcal{F}(\mu_2)} T_2 \otimes_S A \xleftarrow{\mathcal{F}(\mu_3)} T_3 \otimes_S A \longleftarrow 0 \tag{7.4.1}$$

is exact, and hence A is a CY3 algebra.

Proof. First we prove exactness at $T_2 \otimes_S A$. Consider any element $\phi \in T_2 \otimes_S A$ which is closed. We can write ϕ in the form

$$\phi = \sum_{b \in Q_1} R_b \otimes u_b$$

We need to show that ϕ is in the image of the differential. We can write any $\psi \in T_3 \otimes_S A$

in the form $\psi := \sum_{v \in Q_0} W_v \otimes c_v \in T_3 \otimes_S A$ and we note that

$$\mu(\psi) = \sum_{v \in Q_0} \sum_{b \in H_v} R_b \otimes x_b c_v$$

Therefore ϕ is in the image of the differential if and only if the following statement holds. *For each vertex $v \in Q_0$ there is an element $c_v \in A$ such that $u_b = x_b c_v$ for all arrows $b \in H_v$.*

We now prove this statement. Applying the differential to ϕ we observe that

$$0 = \sum_{a,b \in Q_1} x_a \otimes \frac{\partial_l R_b}{\partial_l x_a} u_b = \sum_{a,b \in Q_1} x_a \otimes \frac{\partial_r R_a}{\partial_r x_b} u_b$$

By construction the set $\{x_a \mid a \in Q_1\}$ is linearly independent in T_1, so

$$\sum_{b \in Q_1} \frac{\partial_r R_a}{\partial_r x_b} u_b = 0 \qquad \forall a \in Q_1 \tag{7.4.2}$$

The algebra $A = \bigoplus_{j \in Q_0} Ae_j$ naturally splits into pieces using the idempotents. Without loss of generality we assume $u_b \in Ae_j$ for some $j \in Q_0$, so for each $b \in Q_1$ we have $u_b \in e_{tb} A e_j$.

Using algebraic consistency we work on the toric algebra side. For $b \in Q_1$, the element corresponding to u_b is of the form

$$\widetilde{u_b} = \sum_{m \in M^+_{tb,j}} \alpha_b^m z^m \in \mathbb{C}[\underline{M}^+]$$

where $\alpha_b^m \in \mathbb{C}$. Because $M^+_{tb,j} \subset M$ where subtraction is well defined, we can write each element in the form $m = (m - [b]_M) + [b]_M$. Therefore we can re-write $\widetilde{u_b}$ as

$$\widetilde{u_b} = z^{[b]_M} \sum_{m \in M_{vj}} \alpha_b^{m+[b]_M} z^m$$

where $\alpha_b^{m+[b]_M}$ is take to be zero where it was not previously defined, i.e. when $m + [b]_M \notin M^+_{tb,j}$. We need to show that $\sum_{m \in M_{vj}} \alpha_b^{m+[b]_M} z^m$ is the same for all $b \in Q_1$ which have the same head, and that it is a well defined element of $\mathbb{C}[\underline{M}^+]$.

Let $v \in Q_0$ be any vertex and consider the following diagram, for any arrow a with

$ta = v$.

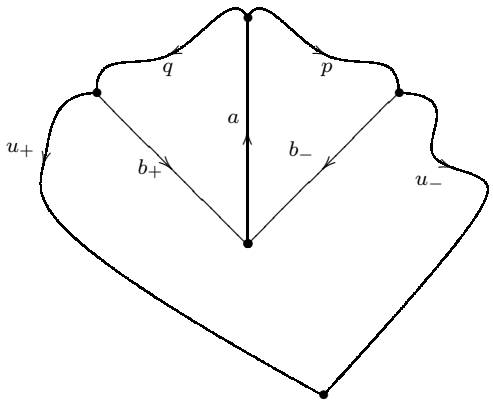

(7.4.3)

In the diagram we have drawn $u_\pm := u_{b_\pm}$ as if they were paths, however it should be remembered that they are elements in the algebra and don't necessarily correspond to actual paths in the quiver. The relation dual to a is $R_a = x_p x_{b_-} - x_q x_{b_+}$, and on substitution into (7.4.2), we get

$$x_p u_- - x_q u_+ = 0 \tag{7.4.4}$$

in A. Under the isomorphism to the toric algebra, and using the relation $[p]_M + [b_-]_M = [q]_M + [b_+]_M$ we obtain:

$$0 = z^{[p]_M}\widetilde{u_-} - z^{[q]_M}\widetilde{u_+} = z^{[p]_M+[b_-]_M} \sum_{m \in M_{vj}} (\alpha_{b_-}^{m+[b_-]_M} - \alpha_{b_+}^{m+[b_+]_M}) z^m$$

The set $\{z^{m+[p]_M+[b_-]_M} \mid m \in M_{vj}\}$ is independent, and so we can see that

$$\alpha_{b_-}^{m+[b_-]_M} = \alpha_{b_+}^{m+[b_+]_M} =: \alpha^m \text{ for all } m \in M_{vj}$$

Then

$$\widetilde{u_{b_\pm}} = z^{[b_\pm]_M} \sum_{m \in M_{vj}} \alpha^m z^m$$

We have shown that this formula holds for a pair of arrows $b_\pm$ with head at v. However, recalling that the arrows around v fit together as in 7.3.1, and considering the arrows pairwise, we observe that for any arrow $b \in H_v$.

$$\widetilde{u_b} = z^{[b]_M} \sum_{m \in M_{vj}} \alpha^m z^m$$

Furthermore $\alpha^m = 0$ unless $m + [b]_M \in M_{tb,j}^+$ for all $b \in H_v$. It follows from Lemma 7.3.1

that α^m can only be non-zero when $m \in M^+_{vj}$. Thus we see that for each $b \in H_v$,

$$\widetilde{u_b} = z^{[b]_M}\widetilde{c_v} \quad \text{where} \quad \widetilde{c_v} := \sum_{m \in M^+_{vj}} \alpha^m z^m$$

which is a well defined element of $\mathbb{C}[\underline{M}^+]$. Using algebraic consistency again, there exists element $c_v \in A$ such that $u_b = x_{b_i}c_v$, and we are done.

To show that the complex is exact at $T_3 \otimes_S A$, suppose that $\phi \in T_3 \otimes_S A$ is closed. We may write ϕ in the form $\phi = \sum_{v \in Q_0} W_v \otimes u_v$. Applying the differential we observe that $\sum_{v \in Q_0} \sum_{b \in H_v} R_b \otimes x_b u_v = 0$ and since the relations R_b are linearly independent over $\mathbb{C}$ in T_2, this implies that $x_b u_v = 0$ for all $v \in Q_0$ and $b \in H_v$. Because of algebraic consistency we can use the given isomorphism and work in the toric algebra $\mathbb{C}[\underline{M}^+]$. Let $\sum_{m \in M^+_{vj}} \beta^m z^m$ be the image of $u_v e_j$, where $\beta^m \in \mathbb{C}$. Then since $x_b u_v e_j = 0$, for each $j \in Q_0$ we see that

$$z^{[b]_M} \sum_{m \in M^+_{vj}} \beta^m z^m = 0$$

The set $\{z^{m+[b]_M} \mid m \in M_{vj}\}$ is independent, therefore $\beta^m = 0$ for all $m \in M_{vj}$. Mapping back to the quiver algebra, this implies $u_v e_j = 0$, for each $j \in Q_0$ and $v \in Q_0$, so $u_v = 0$ for any $v \in Q_0$. We conclude that $\phi = 0$. □

Appendix A

Cohomology of line bundles on a toric variety and constructible sheaves on its polytope

This is a pre-print written earlier in my PhD. We include it here for completeness.

A.1 Introduction

Let X be a toric variety (not necessarily smooth) over an algebraically closed field of characteristic zero, with T the embedded torus and let D be a torus-invariant Cartier divisor on X. It is a well known result (see [8, 12]) that the cohomology $H^p(X, \mathcal{O}(D))$ splits into a direct sum of weight spaces indexed by the character lattice $M = \mathrm{Hom}(T, \mathbb{C}^*)$,

$$H^p(X, \mathcal{O}(D)) \cong \bigoplus_{m \in M} H^p(X, \mathcal{O}(D))_m \tag{A.1.1}$$

There is a theorem of Demazure (see [8]) which says that each weight space can be written as a local cohomology group, calculated on the fan of X,

$$H^p(X, \mathcal{O}(D))_m \cong H^p_{Z(\psi,m)}(|\Delta|, \mathbb{C})$$

where $Z(\psi, m) := \{v \in |\Delta| \mid \langle m, v\rangle \geq \psi(v)\}$ and $\psi = \psi_D$ as defined in section A.2.

In this article we show that when X is projective, each weight space can also be written in terms of the cohomology of certain constructible sheaves on the polytope P_X corresponding to X.

Theorem A.1.1. For all $p \geq 0$ there are canonical isomorphisms:

$$H^p(X, \mathcal{O}(D))_m \cong H^p(P_X, j_!\underline{\mathbb{C}}_W) \tag{A.1.2}$$

where $W = W(m, D)$ is the complement of $Z(m, D)$, a union of closed maximal dimensional faces of P_X, j is the open inclusion of $W(m, D)$ into P_X and $\underline{\mathbb{C}}_W$ is the constant sheaf on W.

Furthermore there is a short exact sequence of constructible sheaves (see [18, 20]),

$$0 \longrightarrow j_!j^*\underline{\mathbb{C}}_{P_X} \longrightarrow \underline{\mathbb{C}}_{P_X} \longrightarrow i_*i^*\underline{\mathbb{C}}_{P_X} \longrightarrow 0 \tag{A.1.3}$$

where i is the inclusion of $Z(m, D)$ into P_X, which induces a long exact sequence of cohomology. Since $j^*\underline{\mathbb{C}}_{P_X} = \underline{\mathbb{C}}_W$ and $i^*\underline{\mathbb{C}}_{P_X} = \underline{\mathbb{C}}_Z$, we can see that the long exact sequence is:

$$\ldots \longrightarrow H^{p-1}(Z(m, D), \mathbb{C}) \longrightarrow H^p(P_X, j_!\underline{\mathbb{C}}_W) \longrightarrow H^p(P_X, \mathbb{C}) \longrightarrow \ldots$$

from which we can calculate $H^p(P_X, j_!\underline{\mathbb{C}}_W)$ in terms of the complex cohomology on $Z(m, D)$.

Finally we remark that although the above has been stated in the projective case, if Y is a quasi-projective toric variety with a given embedding as an open subset of some projective toric variety X, then there is a corresponding open subset P_Y of the polytope P_X and, restricting to Y and P_Y respectively, the proof works as in the projective case.

A.2 Definitions and notation

In this section we define the objects and notation used in the proof. Let $X = X(\Delta)$ be an n-dimensional projective toric variety corresponding to some complete fan Δ in a lattice $N \cong \mathbb{Z}^n$. We write $\Delta(r)$ for the set of r-dimensional cones in Δ, and label the set of generators in N of the 1-dimensional cones by $\{e_i \mid i \in I\}$. It is well known (see [12]) that there is a 1-1 correspondence between prime torus invariant divisors and the elements of $\Delta(1)$, whence we shall denote these divisors $\{E_i \mid i \in I\}$ respectively. Let $M := \mathrm{Hom}(N, \mathbb{Z}) \cong \mathbb{Z}^n$ be the dual lattice to N, with dual pairing $\langle \cdot, \cdot \rangle$, and let $M_{\mathbb{R}} := M \otimes_{\mathbb{Z}} \mathbb{R} \cong \mathbb{R}^n$. Choose a divisor $A = \sum_{i \in I} a_i E_i$ which is Cartier and ample. There is a polytope in $M_{\mathbb{R}}$ associated to A, given by:

$$\begin{aligned} P_A :&= \{u \in M_{\mathbb{R}} \mid \langle u, e_i \rangle \geq -a_i \ \forall i\} \\ &= \{u \in M_{\mathbb{R}} \mid u \geq \psi_A \text{ on } |\Delta| = N_{\mathbb{R}}\} \end{aligned}$$

where the Δ-linear support function $\psi_A : |\Delta| \to \mathbb{R}$ is determined by the property $\psi_A(e_i) = -a_i$ for all $i \in I$. For any cone $\sigma \in \Delta$ we define:

$$\begin{aligned} T_\sigma :&= \{u \in M_\mathbb{R} \mid \langle u, e_i\rangle = -a_i \ \forall e_i \in |\sigma|, \text{ and } \langle u, e_i\rangle > -a_i \text{ otherwise}\} \\ &= \{u \in M_\mathbb{R} \mid u = \psi_A \text{ on } |\sigma|,\ u > \psi_A \text{ on } |\Delta|\backslash|\sigma|\} \end{aligned}$$

This is open in its closure $\overline{T_\sigma} = \{u \in M_\mathbb{R} \mid u = \psi_A \text{ on } |\sigma|,\ u \geq \psi_A \text{ on } |\Delta|\backslash|\sigma|\}$ and is thus locally closed. It can be seen that this defines a stratification $\{T_\sigma\}_{\sigma\in\Delta}$ of P_A by locally closed sets indexed by the cones $\sigma \in \Delta$. Since A is ample, each of these T_σ is non-empty. There is a natural partial order on the strata given by:

$$T_\tau \leq T_\sigma \iff T_\sigma \subseteq \overline{T_\tau}$$

Lemma A.2.1.

$$T_\tau \leq T_\sigma \iff \tau \subseteq \sigma$$

Proof. By definition $\tau \subseteq \sigma$ trivially implies $T_\sigma \subseteq \overline{T_\tau}$. Conversely suppose $u \in T_\sigma \subseteq \overline{T_\tau}$. Then $u > \psi_A$ on $|\Delta|\backslash|\sigma|$ and also $u = \psi_A$ on $|\tau|$ whence $|\tau| \subseteq |\sigma|$. □

A very similar argument shows that $\overline{T_\sigma}$ can be written as a union of the strata:

$$\overline{T_\sigma} = \bigcup_{\tau\supseteq\sigma} T_\tau \tag{A.2.1}$$

Note: As a topological object with a stratification by locally closed subsets, P_A is actually independent of the choice of ample divisor A on X and depends only on $\Delta(X)$ (ie. on X). Thus in general we write P_X for this object when we don't want to specify a particular ample divisor and we treat the strata $\{T_\sigma\}_{\sigma\in\Delta}$ as well defined subsets of this. From equation (A.2.1) we see that any closed maximal dimensional face $\overline{T_{\langle e\rangle}}$ is a union of strata depending only on the fan and is therefore also well defined in P_X. We denote it by $F_e \subset P_X$.

Lemma A.2.2. There exists a cover of P_X by open sets of the form $V_\sigma := \bigcup_{\tau\subseteq\sigma} T_\tau$

The proof of this is straightforward and left to the reader.

Lemma A.2.3. For any $\sigma \in \Delta$, V_σ is a contractible space.

Proof. V_σ is convex: Let $a, b \in V_\sigma$ so $a \in T_\tau$ and $b \in T_\gamma$ for some $\tau, \gamma \subseteq \sigma$. Let $e \in |\Delta|$, then

$$\langle ta + (1-t)b, e\rangle = t\langle a, e\rangle + (1-t)\langle b, e\rangle \geq \psi_A(e)$$

for $t \in (0,1)$, since $\langle a, e\rangle \geq \psi_A(e)$, and $\langle b, e\rangle \geq \psi_A(e)$, with equality if and only if $e \in |\tau \cap \gamma|$. Thus $ta + (1-t)b \in T_{\tau\cap\gamma} \subseteq V_\sigma$. □

Let $D = \sum_{i\in I} d_i E_i$ be a torus invariant divisor which is Cartier and fix some $m \in M$. We define a (closed) subset of P_X by:

$$Z(m, D) := \bigcup_{\{i\in I | \langle m, e_i\rangle < -d_i\}} F_{e_i}$$

a union of closed maximal dimensional faces of P_X and we define

$$W(m, D) := P_X \backslash Z(m, D)$$

the complementary open subset of P_X. Let

$$j : W(m, D) \hookrightarrow P_X$$

be the open inclusion of $W(m, D)$ into P_X.

Lemma A.2.4. For any $\sigma \in \Delta$, $V_\sigma \cap Z(m, D)$ is either empty or it is contractible.

Proof. : Suppose $V_\sigma \cap Z(m, D) = \bigcup_{\{e\in I|\langle m,e\rangle<-d_e\}}(F_e \cap V_\sigma)$ is non-empty. Then each non-empty set $F_e \cap V_\sigma$ in the union contains T_σ, since

$$F_e \cap V_\sigma = \bigcup_{\tau \ni e} T_\tau \cap \bigcup_{\delta\subseteq\sigma} T_\delta$$

and the $\{T_\alpha\}_{\alpha\in\Delta}$ partition P_X. They are also convex as F_e and V_σ are both convex subsets. If $s \in T_\sigma$, then the constant map $f : V_\sigma \cap Z(m, D) \to \{s\}$ is a homotopy equivalence since $f \circ \iota = id_{\{s\}}$ where $\iota : \{s\} \hookrightarrow V_\sigma \cap Z(m, D)$ is the inclusion and

$$\begin{aligned} F : (V_\sigma \cap Z(m, D)) \times [0, 1] &\to (V_\sigma \cap Z(m, D)) \\ (a, t) &\mapsto tm + (1-t)a \end{aligned}$$

is a well defined continuous map such that $F(-, 0) = id_{V_\sigma\cap Z(m,D)}$ and $F(-, 1) = \iota \circ f$ so $\iota \circ f \simeq id_{V_\sigma\cap Z(m,D)}$. Thus $V_\sigma \cap Z(m, D) \simeq \{s\}$. □

A.3 Proof of Theorem A.1.1

We begin with a lemma.

Lemma A.3.1. Let $\sigma \in \Delta$ and $j_\sigma : V_\sigma \hookrightarrow P_X$ be the inclusion. Then:

$$H^i(V_\sigma, j_\sigma^* j_! \underline{\mathbb{C}}_W) = 0 \quad \forall\, i > 0$$

Proof. First note that ${j_\sigma}^{-1}(W) = W \cap V_\sigma$ and we have the commutative diagram

$$\begin{array}{ccc} W \cap V_\sigma & \xrightarrow{j^\sigma} & V_\sigma \\ {\scriptstyle j_\sigma}\downarrow & & \downarrow{\scriptstyle j_\sigma} \\ W & \xrightarrow{j} & P_X \end{array}$$

where $j^\sigma : W \cap V_\sigma \hookrightarrow V_\sigma$ is the inclusion. Then using equation 6.13 on page 111 of Iversen [20]

$$(j_\sigma)^* j_! \underline{\mathbb{C}}_W = {j^\sigma}_! (j_\sigma)^* \underline{\mathbb{C}}_W$$

We note that $(j_\sigma)^* \underline{\mathbb{C}}_W = \underline{\mathbb{C}}_{W \cap V_\sigma} = (j^\sigma)^* \underline{\mathbb{C}}_{V_\sigma}$ so we have $(j_\sigma)^* j_! \underline{\mathbb{C}}_W = {j^\sigma}_! (j^\sigma)^* \underline{\mathbb{C}}_{V_\sigma}$. Since j^σ is the inclusion of an open set in V_σ and letting $i^\sigma : V_\sigma \cap Z \hookrightarrow V_\sigma$ denote the inclusion of its complement, there is a well known short exact sequence of sheaves (see [18, 20]):

$$0 \longrightarrow {j^\sigma}_! (j^\sigma)^* \underline{\mathbb{C}}_{V_\sigma} \longrightarrow \underline{\mathbb{C}}_{V_\sigma} \longrightarrow {i^\sigma}_* (i^\sigma)^* \underline{\mathbb{C}}_{V_\sigma} \longrightarrow 0 \tag{A.3.1}$$

This induces a long exact sequence of cohomology:

$$\ldots \longrightarrow H^i(V_\sigma \cap Z, \mathbb{C}) \longrightarrow H^{i+1}(V_\sigma, {j^\sigma}_! (j^\sigma)^* \underline{\mathbb{C}}_{V_\sigma}) \longrightarrow H^{i+1}(V_\sigma, \mathbb{C}) \longrightarrow \ldots$$

Using this and applying Lemmas A.2.3 and A.2.4 the result follows. □

The rest of the proof follows the same strategy as the proof of Demazure's Theorem given in [8]. We start by considering the left hand side of equation (A.1.2). There is a natural covering of $X(\Delta)$ by affine open sets U_σ with $\sigma \in \Delta$ and intersections of such sets are of the same form. By Serre's Theorem this covering is acyclic, and thus the cohomology $H^i(X, \mathcal{O}(D))$ is the same as the i-dimensional cohomology of the Čech complex with this covering:

$$C^*(\{U_\sigma\}_{\sigma \in \Delta}, \mathcal{O}(D)) = (\cdots \xrightarrow{d} \bigoplus_\sigma H^0(U_\sigma, \mathcal{O}(D)) \xrightarrow{d} \cdots) \tag{A.3.2}$$

There is a natural M-grading on each term of the complex and this grading is preserved by the differentials. The m-th piece of the cohomology, $H^i(X, \mathcal{O}(D))_m$ equals the i-dimensional cohomology of the complex of m-th pieces.

Now we look at the right hand side of (A.1.2). From Lemma A.2.2 there is an open

covering of P_X by the sets $\{V_\sigma\}_{\sigma\in\Delta}$, and by Lemma A.3.1 this cover is acyclic. Therefore by Leray's theorem, the cohomology $H^i(P_X, j_!\underline{\mathbb{C}}_W)$ is the i-dimensional cohomology of the Čech complex

$$C^*(\{V_\sigma\}_{\sigma\in\Delta}, j_!\underline{\mathbb{C}}_W) = (\cdots \xrightarrow{d} \bigoplus_\sigma H^0(V_\sigma, j_!\underline{\mathbb{C}}_W) \xrightarrow{d} \cdots) \tag{A.3.3}$$

Finally we show that the two spaces $H^0(U_\sigma, \mathcal{O}(D))_m$ and $H^0(V_\sigma, j_!\underline{\mathbb{C}}_W)$ are both isomorphic to either $\mathbb{C}$ or 0 for given σ and m. Then since the open covers for the two Čech complexes are indexed by the same set and the differentials are defined in terms of restriction maps which in both cases correspond to the identity map on $\mathbb{C}$ or zero, it can be seen that the cohomology of the complexes is the same.

We know (from [8, 12]) that $H^0(U_\sigma, \mathcal{O}(D))_m = \mathbb{C}$ when m belongs to the set $\{u \in M_\mathbb{R} \mid u \geq \psi_D \text{ on } |\sigma|\}$ and is 0 otherwise. On the other hand consider again the first part of the long exact sequence induced by equation (A.3.1):

$$0 \longrightarrow H^0(V_\sigma, j_\sigma^* j_!\underline{\mathbb{C}}_W) \longrightarrow H^0(V_\sigma, \mathbb{C}) \longrightarrow H^0(Z(m,D)\cap V_\sigma, \mathbb{C}) \longrightarrow$$

Obviously $H^0(V_\sigma, j_!\underline{\mathbb{C}}_W)$ is isomorphic to $\mathbb{C}$ when $Z(m,D)\cap V_\sigma$ is empty and is 0 otherwise. However

$$\begin{aligned}
& Z(m,D)\cap V_\sigma = \varnothing \\
\iff & F_e \cap V_\sigma = \bigcup_{\tau\ni e} T_\tau \cap \bigcup_{\delta\subseteq\sigma} T_\delta = \varnothing \quad \forall e \in \{e_i \mid \langle m, e_i\rangle < -d_i\} \\
\iff & \langle m, e_i\rangle \geq -d_i \quad \forall e_i \in |\sigma| \\
\iff & m \in \{u \in M_\mathbb{R} \mid u \geq \psi_D \text{ on } |\sigma|\}
\end{aligned}$$

Remark A.3.1. We can extend the result to cases where the toric variety is quasi-projective. Suppose $Y = Y(\Sigma)$ is a quasi-projective toric variety embedded via a toric morphism as an open subset of a projective toric variety X. There is a natural cover of Y by affine open pieces $\{U_\sigma \mid \sigma \in \Sigma\}$. On the polytope P_X there is a corresponding open cover $\{V_\sigma \mid \sigma \in \Sigma\}$ of an open subset P_Y of P_X. Restricting to Y and P_Y, the rest of the proof follows through; these covers are both acyclic as before, there are two corresponding Čech complexes (which are sub-complexes of the graded version of (A.3.2), and (A.3.3)) and by the computation above it can be seen that they are the same.

A.4 Example

As a proof of concept we do a calculation. Any toric quiver variety comes with a natural collection of line bundles, the universal bundles. It was shown by Altmann and Hille (Theorem 3.6 of [1]) that for any smooth Fano toric quiver variety the universal bundles form a strongly exceptional collection. The example here is not Fano and was constructed so that neither the Kawamata-Viehweg vanishing theorem nor Theorem 2.4(ii) from [27] is sufficient to prove the vanishing of the Ext's between all the universal bundles. Thus these vanishing theorems can not be used to show that the collection of universal bundles is strongly exceptional. We show here by direct calculation that it is, and furthermore extend the collection to produce a full strongly exceptional collection.

A.4.1 Calculation of Cohomology

Consider the following quiver Q with weights at the vertices as labelled.

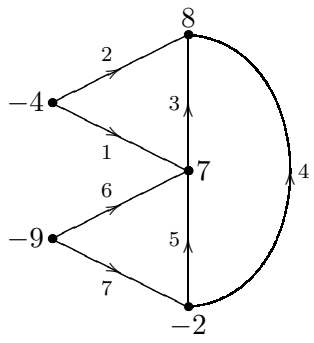

Let Q_0 be the set of vertices and Q_1 the set of arrows. There are two maps $h, t : Q_1 \to Q_0$ taking an arrow to its head and tail respectively. The corresponding toric quiver variety X (see [19]), is smooth and complete and has rays generated by $\{e_1 = (e_3 + e_4), e_2 = -(e_3 + e_4), e_3, e_4, e_5, e_6 = -(e_4 + e_5), e_7 = (e_4 + e_5)\}$. There is a correspondence between the prime torus invariant divisors on X and elements of Q_1. The universal bundles $\{\mathcal{L}_v \mid v \in Q_0\}$ satisfy the property that $\mathcal{L}_{ha} \otimes \mathcal{L}_{ta}^* \cong \mathcal{O}(E_a)$ for all $a \in Q_1$ and are unique up to a twist. Let $\{e_3^\vee, e_4^\vee, e_5^\vee\}$ be the dual basis of $\{e_3, e_4, e_5\}$ and then M is the integer lattice generated by $\{e_3^\vee, e_4^\vee, e_5^\vee\}$. The polytope P_X is three dimensional, the stereographic projection of which is shown below.

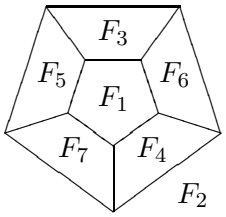

Consider again the long exact sequence of cohomology induced by the short exact sequence (A.1.3):

$$\ldots \longrightarrow H^i(Z(m,D),\mathbb{C}) \longrightarrow H^{i+1}(P_X, j_!\underline{\mathbb{C}}_W) \longrightarrow H^{i+1}(P_X,\mathbb{C}) \longrightarrow \ldots$$

where $Z(m,D)$ is some collection of closed faces of the polytope P_X. Looking at all possible unions of closed faces we see that up to homotopy equivalence, there are five possibilities. From the long exact sequence above it can be seen which of these contributes to each non-zero cohomology, and the table below lists all of these. Thus $H^i(P_X, j_!\underline{\mathbb{C}}_W) \cong \mathbb{C}$ for all Z in the row $H^i \cong \mathbb{C}$ and $H^i(P_X, j_!\underline{\mathbb{C}}_W) = 0$ for all other Z. We use the notation

$$F_J := \bigcup_{j\in J} F_j$$

and let

$$\begin{aligned}\mathbf{J} := \big\{&\{1,2\},\{3,4\},\{3,7\},\{4,5\},\{5,6\},\{6,7\},\\ &\{3,4,7\},\{3,4,5\},\{4,5,6\},\{5,6,7\},\{3,6,7\}\big\}\end{aligned}$$

contain those sets J such that F_J has two connected components. We denote the complement of J in $I := \{1,2,3,4,5,6,7\}$ by J^c and observe that F_I is the boundary of P_X.

$H^0 \cong \mathbb{C}$	$Z(m,D) \simeq \varnothing$	$Z = \varnothing$
$H^1 \cong \mathbb{C}$	$Z(m,D) \simeq \{pt\} \sqcup \{pt\}$	$Z = F_J$ for $J \in \mathbf{J}$
$H^2 \cong \mathbb{C}$	$Z(m,D) \simeq S1$	$Z = F_J$ for $J^c \in \mathbf{J}$
$H^3 \cong \mathbb{C}$	$Z(m,D) \simeq S2$	$Z = F_I$

Let $\mathcal{O}(D)$ be any invertible line bundle on X. We can choose D to be of the form $D := d_1E_1 + d_2E_2 + d_6E_6 + d_7E_7$, a torus-invariant Weil divisor which is Cartier, since $\mathrm{Pic}(X)$ is rank 4 and generated by $\{E_1, E_2, E_6, E_7\}$. Then from the table above, using the decomposition in equation (A.1.1) and applying Theorem A.1.1, it can be seen that $H^0(X,\mathcal{O}(D)) \neq 0$ if and only if there exists $m \in M$ such that $Z(m,D) = \varnothing$. This

holds if and only if

$$\begin{aligned}
&\exists m := m_3 {e_3}^\vee + m_4 {e_4}^\vee + m_5 {e_5}^\vee \in M \text{ such that } \langle m, e_i \rangle \geq -d_i \ \forall i \\
\iff &\exists m_1, m_2, m_3 \in \mathbb{Z} \text{ where } m_i \geq 0, -d_1 \leq m_3 + m_4 \leq d_2, -d_7 \leq m_4 + m_5 \leq d_6 \\
\iff &0 \leq (d_1 + d_2), 0 \leq (d_6 + d_7), d_2 \geq 0, d_6 \geq 0
\end{aligned}$$

Similarly $H^1(X, \mathcal{O}(D)) \neq 0$ if and only if there exists $m \in M$ such that $Z(m, D) = F_J$ for some $J^c \in \mathbf{J}$. Treating each case separately, we obtain a list of all the regions in $\mathrm{Pic}(X)$ where $H^1(X, \mathcal{O}(D))$ is nonzero. We can then produce a complete list of regions in $\mathrm{Pic}(X)$ where each cohomology group is nonzero either by continuing the process or applying Serre Duality. The list of these 24 regions is given in tabular form below.

$H^0 \neq 0$	1	$0 \leq (d_1 + d_2),\ 0 \leq (d_6 + d_7),\ 0 \leq d_2,\ 0 \leq d_6$
$H^1 \neq 0$	2	$-2 \geq (d_1 + d_2),\ 0 \leq (d_6 + d_7),\ -1 \geq d_1,\ 0 \leq d_6$
	3	$0 \leq (d_1 + d_2),\ 0 \leq (d_6 + d_7),\ 2 \leq d_1,\ 1 \leq (d_1 + d_6)$
	4	$0 \leq (d_1 + d_2),\ 0 \leq d_6,\ -1 \geq d_7,\ 1 \leq (d_1 + d_6),\ 2 \leq (d_1 - d_7)$
	5	$0 \leq (d_1 + d_2),\ 0 \leq (d_6 + d_7),\ 2 \leq d_7,\ 1 \leq (d_2 + d_7)$
	6	$0 \leq (d_1 + d_2),\ 1 \leq (d_2 + d_7),\ 0 \leq d_2,\ 2 \leq (d_2 - d_6)$
	7	$0 \leq (d_1 + d_2),\ -2 \geq (d_6 + d_7),\ 0 \leq d_2,\ -1 \geq d_7$
	8	$0 \leq (d_1 + d_2),\ 1 \leq (d_1 + d_6),\ 2 \leq d_1,\ 2 \leq (d_1 - d_7)$
	9	$0 \leq (d_1 + d_2),\ 0 \leq (d_6 + d_7),\ 2 \leq d_1,\ 2 \leq d_7$
	10	$0 \leq (d_1 + d_2),\ 1 \leq (d_2 + d_7),\ -3 \geq d_6,\ 2 \leq d_7,\ 2 \leq (d_2 - d_6)$
	11	$0 \leq (d_1 + d_2),\ -2 \geq (d_6 + d_7),\ 0 \leq d_2,\ 2 \leq (d_2 - d_6)$
	12	$0 \leq (d_1 + d_2),\ -2 \geq (d_6 + d_7),\ -1 \geq d_7,\ 2 \leq (d_1 - d_7)$
$H^2 \neq 0$	13	$0 \leq (d_1 + d_2),\ -2 \geq (d_6 + d_7),\ 2 \leq d_1,\ -3 \geq d_6$
	14	$-2 \geq (d_1 + d_2),\ -2 \geq (d_6 + d_7),\ -1 \geq d_1,\ -3 \geq (d_1 + d_6)$
	15	$-2 \geq (d_1 + d_2),\ -3 \geq d_6,\ 2 \leq d_7,\ -3 \geq (d_1 + d_6),\ -2 \geq (d_1 - d_7)$
	16	$-2 \geq (d_1 + d_2),\ -2 \geq (d_6 + d_7),\ -1 \geq d_7,\ -3 \geq (d_2 + d_7)$
	17	$-2 \geq (d_1 + d_2),\ -3 \geq (d_2 + d_7),\ -3 \geq d_2,\ -2 \geq (d_2 - d_6)$
	18	$-2 \geq (d_1 + d_2),\ 0 \leq (d_6 + d_7),\ -3 \geq d_2,\ 2 \leq d_7$
	19	$-2 \geq (d_1 + d_2),\ -3 \geq (d_1 + d_6),\ -1 \geq d_1,\ -2 \geq (d_1 - d_7)$
	20	$-2 \geq (d_1 + d_2),\ -2 \geq (d_6 + d_7),\ -1 \geq d_1,\ -1 \geq d_7$
	21	$-2 \geq (d_1 + d_2),\ -3 \geq (d_2 + d_7),\ 0 \leq d_6,\ -1 \geq d_7,\ -2 \geq (d_2 - d_6)$
	22	$-2 \geq (d_1 + d_2),\ 0 \leq (d_6 + d_7),\ -3 \geq d_2,\ -2 \geq (d_2 - d_6)$
	23	$-2 \geq (d_1 + d_2),\ 0 \leq (d_6 + d_7),\ 2 \leq d_7,\ -2 \geq (d_1 - d_7)$
$H^3 \neq 0$	24	$-2 \geq (d_1 + d_2),\ -2 \geq (d_6 + d_7),\ -3 \geq d_2,\ -3 \geq d_6$

Using this table it can easily be confirmed that the universal bundles form an exceptional collection. For each pair of line bundles $\mathcal{L}_p$ and $\mathcal{L}_q$ in the collection we wish to calculate the cohomology of $\mathcal{L}_q \otimes \mathcal{L}_p^* \cong \mathcal{O}(D)$, where D is chosen so that it is a linear combination of the generators $\{E_1, E_2, E_6, E_7\}$ of Pic(X). For example, if p is the vertex with weight 8 and q is the vertex with weight -2, then $\mathcal{L}_q \otimes \mathcal{L}_p^* \cong \mathcal{O}(-E_1+E_2+E_6-E_7)$. Looking at the table, the only region which contains the point $(d_1, d_2, d_6, d_7) = (-1, 1, 1, -1)$ is region 1 and so there is no higher cohomology. Similarly there is no higher cohomology for all other pairs of line bundles in the universal collection. Thus the Ext's between all pairs of line bundles in the collection are zero and the universal bundles form a strongly exceptional collection.

A.4.2 An Extended Collection

We describe a generalised Koszul complex called the Buchsbaum-Rim complex, see [28] Appendix C. We then use this in our example to construct a collection of line bundles which extends the collection of universal bundles $\{\mathcal{L}_v \mid v \in Q_0\}$ on X and which by construction spans the derived category $D^b(X)$. Finally, using the cohomology calculation above once more, we show that this collection is actually strongly exceptional.

Let V,W be vector bundles of ranks m,n over an arbitrary base, and let $f : W \to V$ be a bundle map. Then the Buchsbaum-Rim complex (K_*, d_*) is as follows: $K_0 = V$, $K_1 = W$ with $d_1 = f$ and then for $r \geq 1$

$$K_{r+1} = \Lambda^{m+r+1}(W) \otimes S^r(V^*) \otimes \det V^*$$

For $n > 2$, the maps d_n are defined to be interior product with $f : W \to V$ regarded as a section of $W^* \otimes V$ and $d_2 : \Lambda^{m+1}(W) \otimes \det V^* \to W$ is interior product with $\Lambda^m(f) : \Lambda^m(W) \to \Lambda^m(V)$ regarded as a section of $\Lambda^m(W^*) \otimes \Lambda^m(V)$. The complex (K_*, d_*) is exact away from the support of $\mathrm{coker} f$, and in particular since it has length $n - m + 1$, if the support of $\mathrm{coker} f$ is in codimension $n - m + 1$, then the complex is a resolution of $\mathrm{coker} f$ ([6]).

Any toric quiver variety X comes with a presentation of the diagonal in $X \times X$:

$$\bigoplus_{a \in Q_1} \mathcal{L}_{ta} \boxtimes \mathcal{L}_{ha}^* \longrightarrow \bigoplus_{v \in Q_0} \mathcal{L}_v \boxtimes \mathcal{L}_v^*$$

where the components of this map are $\phi_a \boxtimes 1 - 1 \boxtimes \phi_a^*$. The ranks of these bundles are $n = |Q_1|$ and $m = |Q_0|$ respectively, and the support of the cokernel of this map (i.e. the diagonal in $X \times X$) has codimension equal to the dimension of X, namely $n-m+1$. Therefore from above we can see that Buchsbaum-Rim complex for this presentation

is a resolution of the diagonal $\mathcal{O}_\Delta$ in $X \times X$. Each term of the complex consists of a product of line bundles on each side of the $\boxtimes$. Taking all the line bundles that appear on either one side or the other gives a collection which spans $D^b(X)$ ([25]). We have:

$$S^r(V^*) \otimes \det(V^*) = \bigoplus_{\substack{P:Q_0 \to \{1,2,\dots\} \\ |P|=m+r}} \left(\bigotimes_{v \in Q_0} \mathcal{L}_v^{-P(v)} \right) \boxtimes \left(\bigotimes_{v \in Q_0} \mathcal{L}_v^{P(v)} \right)$$

$$\Lambda^{m+r+1}(W) = \bigoplus_{\substack{R:Q_1 \to \{0,1\} \\ |R|=m+r+1}} \left(\bigotimes_{a \in Q_1} \mathcal{L}_{ta}^{R(a)} \right) \boxtimes \left(\bigotimes_{a \in Q_1} \mathcal{L}_{ha}^{-R(a)} \right)$$

where $|P| := \sum_{v \in Q_0} P(v)$ and $|R| := \sum_{a \in Q_1} R(a)$. Thus by considering the duals of the line bundles on the right hand side of the $\boxtimes$ we have shown:

Proposition A.4.1. Let X be a smooth toric quiver variety with associated quiver Q. The following line bundles on X extend the universal bundles $\{\mathcal{L}_v \mid v \in Q_0\}$, to a collection which spans the derived category $D^b(X)$:

$$\bigotimes_{a \in Q_1} \mathcal{L}_{ha}^{R(a)} \otimes \bigotimes_{v \in Q_0} \mathcal{L}_v^{-P(v)} \tag{A.4.1}$$

for every $P : Q_0 \to \{1, 2, \dots\}$ and $R : Q_1 \to \{0, 1\}$ such that $|Q_0| + 1 \leq |P| + 1 = |R| \leq |Q_1|$.

Note that if we replace ha by ta in (A.4.1) this gives another collection extending the universal bundles and spanning the derived category, which is the collection obtained by taking all the line bundles on the left hand side of the $\boxtimes$.

Calculating the first of these collections in the example above, we obtain ten line bundles corresponding to the vertices in the quiver below. The arrows which correspond to Hom's between the bundles are decorated with the labels of the corresponding divisors, i.e. an arrow from $\mathcal{L}_p$ to $\mathcal{L}_q$ is labelled 1+5+7 when $\mathcal{L}_q \otimes \mathcal{L}_p^* \cong \mathcal{O}(E_1 + E_5 + E_7)$.

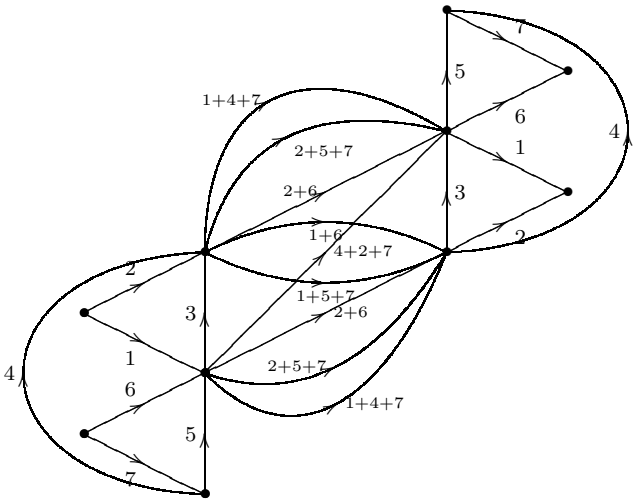

Again for each pair of line bundles $\mathcal{L}_p$ and $\mathcal{L}_q$ in the collection we wish to calculate the cohomology of $\mathcal{L}_q \otimes \mathcal{L}_p^* \cong \mathcal{O}(D)$. By looking at the table above it can be seen that for each such pair, the divisor D does not lie in any of the regions of $\mathrm{Pic}(X)$ where $H^i(\mathcal{O}(D)) \neq 0$ for $i > 0$. Hence there is no higher cohomology, so the Ext's between all pairs of line bundles in the collection are zero. Thus we have a full strongly exceptional collection of line bundles on our toric variety.

A.4.3 Bondal's Collection

Given any smooth toric variety X, Bondal has described a method to produce a candidate collection of line bundles on X, which for a certain class of Fano varieties is expected to be strongly exceptional. In this section we determine this collection in the case of our non-Fano example from section A.4, and show that it is not strongly exceptional. This is not unexpected but gives another illustration of the method.

For any toric variety X and $l \in \mathbb{N}$, there is a well-defined toric morphism

$$\pi_l : X \to X$$

which restricts, on the torus T, to the map

$$\pi_l : T \to T, \quad t \mapsto t^l$$

In the case when X is smooth then the direct image,

$$(\pi_l)_* \mathcal{O}_X = \bigoplus_{\chi} \mathcal{L}_\chi$$

is a direct sum of line bundles indexed by the characters of the l-torsion subgroup of T. This is because the map π_l is the quotient of X by this group. The set $\mathcal{B}$ of line bundles which occur as summands of this direct sum for all sufficiently large l exists and is given by

$$\begin{aligned}\mathcal{B} =&\{\mathcal{O}(D) \mid D := -\sum_{i=1}^{d}\{\langle e_i, m\rangle\}E_i,\ m \in M_{\mathbb{Q}}\}\\ =&\{\mathcal{O}(\bar{D}) \mid \bar{D} := \sum_{i=1}^{d}\lfloor\langle e_i, m\rangle\rfloor\, E_i,\ m = \sum_{i=1}^{n} m_i e_1^{\vee} \in M_{\mathbb{Q}},\ 0 \le m_i < 1\}\end{aligned}$$

where $M_{\mathbb{Q}} = M \otimes_{\mathbb{Z}} \mathbb{Q}$ and $\{\alpha\} = \alpha - \lfloor\alpha\rfloor \ge 0$ is the fractional part of α, for $\alpha \in \mathbb{Q}$. (For a more general construction one can instead consider $(\pi_l)_*\mathcal{O}_X(D)$ for some divisor D.) In the example this produces a collection of 12 line bundles corresponding to the vertices of the quiver below, where the top vertex corresponds to $\mathcal{O}_X$:

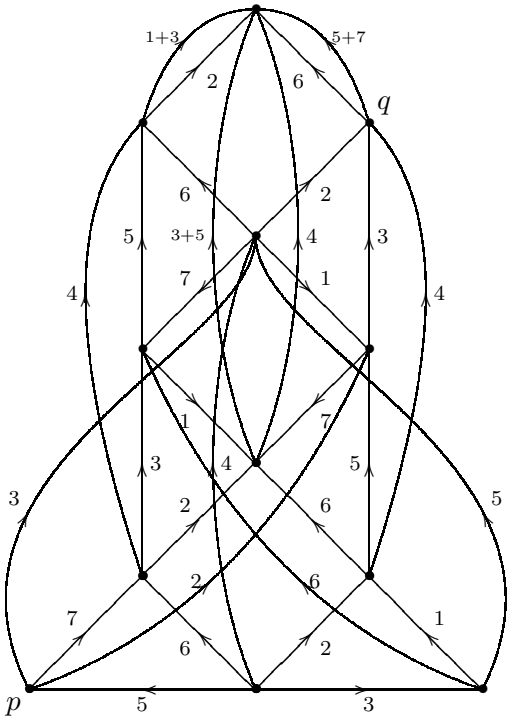

Note that the quiver:

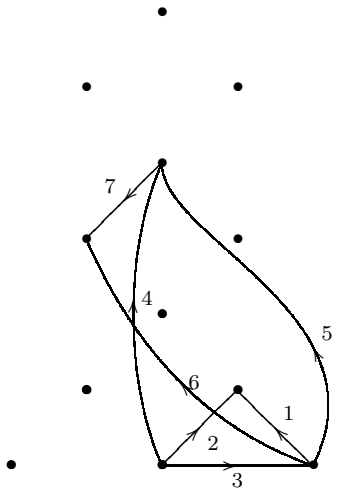

is a subquiver. This subquiver is also contained in the quiver corresponding to the full strongly exceptional collection on X which we produced above. It can be seen that, up to a twist, the duals of the universal bundles are contained in $\mathcal{B}$. There are however Ext^1's between some of the line bundles in the collection. Consider $\mathcal{L}_p$ and $\mathcal{L}_q$ where p and q are labelled on the quiver above. It can be seen from the quiver that $\mathcal{L}_q \otimes \mathcal{L}_p^* \cong \mathcal{O}(-E_1 + 2E_2)$, so $d_1 = -1, d_2 = 2, d_6 = d_7 = 0$. Then looking back at the table from the cohomology calculation, we see that these satisfy the sixth set of inequalities, so

$$\mathrm{Ext}^1(\mathcal{L}_p, \mathcal{L}_q) \cong H^1(\mathcal{L}_q \otimes \mathcal{L}_p^*) \neq 0.$$

We find that there are no Ext^2's between any of the line bundles. All the Ext^1's are shown below:

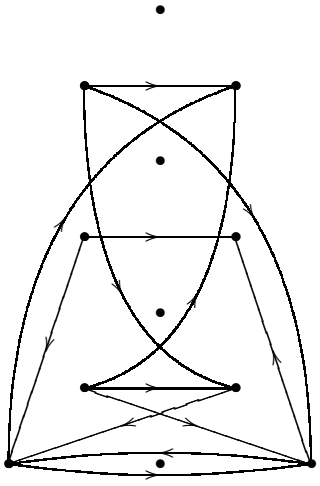

One may check that no subcollection containing any ten of these line bundles is strongly exceptional and thus there is no full strongly exceptional subcollection of $\mathcal{B}$.

Bibliography

[1] K. Altmann and L. Hille, *Strong Exceptional Sequences Provided by Quivers*, Algebras and Representation Theory, **2**: 1-17, 1999.

[2] A. Ambrosio, `http://planetmath.org/encyclopedia/ProofOfBirkoffVonNeumannTheorem.html`.

[3] G. Birkhoff, *Tres observaciones sobre el algebra lineal*, Univ. Nac. Tucumn Rev, Ser. A, no. 5, pp147-151. (1946)

[4] R. Bocklandt, *Graded Calabi Yau algebras of dimension 3*, Journal of pure and applied algebra, 212:1(2008), p. 14-32

[5] T. Bridgeland, A. King; M. Reid, *The McKay Correspondence as an Equivalence of Derived Categories*, Journal of the American Mathematical Society, Vol. 14, No. 3. (Jul., 2001), pp. 535-554.

[6] D.A. Buchsbaum and D. Eisenbud, *What makes a complex exact?*, J. Algebra **25** (1973), 259-268.

[7] D. Cox, G. Barthel, *Geometry of Toric Varieties*, Lecture Notes from 'Summer School 2000', Grenoble, 2000.

[8] V. Danilov, *The Geometry of Toric Varieties*, Russ. Math. Surveys, **33**:2 (1978), 97–154.

[9] B. Davison, *Consistency conditions for brane tilings*, preprint arXiv: 0812:4185v1

[10] G. Ewald, *Combinatorial Convexity and Algebraic Geometry*, Graduate Texts in Mathematics, Springer-Verlag, New York, 1996.

[11] S. Franco, A. Hanany, K. D. Kennaway, D. Vegh, and B. Wecht, *Brane dimers and quiver gauge theories*, preprint arXiv: hep-th/0504110 .

[12] W. Fulton, *Introduction to Toric Varieties*, Princeton University Press, Princeton, 1993.

[13] V. Ginzburg, *Calabi-Yau Algebras*, preprint arXiv:math.AG/0612139.

[14] D. R. Gulotta *Properly ordered dimers, R-charges, and an efficient inverse algorithm*, preprint arXiv:0807.3012 (July 2008)

[15] A. Hanany, C. P. Herzog, and D. Vegh, Brane tilings and exceptional collections, JHEP 07 (2006) 001.

[16] A. Hanany and K. D. Kennaway, *Dimer models and toric diagrams*, preprint arXiv: hep-th/0503149.

[17] A. Hanany and D. Vegh, *Quivers, Tilings, Branes and Rhombi*, preprint arXiv: hep-th/0511063v1

[18] R. Hartshorne, *Algebraic Geometry*, Graduate Texts in Mathematics, Springer-Verlag, New York, 1977.

[19] L. Hille, *Toric quiver varieties*, Algebras and Modules II (I.C.R.A. 8) (I. Reiten, S.O. Smalø and O. Solberg, eds.), Canadian Math. Soc. Proceedings, vol. 24, 1998, pp. 311-325.

[20] B. Iversen, *Cohomology of Sheaves*, Universitext, Springer-Verlag, Berlin, 1986.

[21] R. A. Jarvis, *On the identification of the convex hull of a finite set of points in the plane*, Information Processing Letters 2: 1821. (1973)

[22] K. D. Kennaway, *Brane Tilings*, International Journal of Modern Physics A (IJMPA), Volume:22, No:18 Year: 2007 pp. 2977-3038

[23] R. Kenyon, *An introduction to the dimer model*, preprint arXiv: math.CO/0310326

[24] R. Kenyon and J.M. Schlenker, *Rhombic embeddings of planar quad-graphs*, Transactions of the AMS, Volume 357, Number 9, Pages 3443-3458 (2004)

[25] A. King, *Tilting Bundles on some Rational Surfaces*, preprint at `http://www.maths.bath.ac.uk/~masadk/papers`, 1997.

[26] S. Mozgovoy and M. Reineke, *On the noncommutative Donaldson-Thomas invariants arising from brane tilings*, preprint arXiv: 0809:0117

[27] M. Mustaţă, *Vanishing Theorems on Toric Varieties*, Tohoku Math. J.(2), vol. 54 , 451-470, 2002.

[28] D.G. Northcott, *Finite Free Resolutions*, Cambridge Tracts in Math., vol. 71, C.U.P., Cambridge, 1976.

[29] J. Stienstra, *Hypergeometric Systems in two Variables, Quivers, Dimers and Dessins d'Enfants*, Modular Forms and String Duality, Fields Institute Communications volume 54 (2008), pp. 125-161

[30] B. Szendröi *Non-commutative Donaldson-Thomas invariants and the conifold*, Geometry and Topology 12 (2008) 1171-1202.

[31] M. Van den Bergh, *Non-commutative Crepant Resolutions*, The legacy of Niels Henrik Abel, 749–770, Springer, Berlin, 2004.